RESEARCH TECHNICAL REPORT

Flammability Characterization of Lithium-ion Batteries in Bulk Storage

FM Global®

Flammability Characterization of Lithium-ion Batteries in Bulk Storage

by

Benjamin Ditch and Jaap de Vries

March 2013

FM Global
1151 Boston-Providence Turnkpike
Norwood, MA 02062

DISCLAIMER

The research presented in this report, including any findings and conclusions, is for informational purposes only. Any references to specific products, manufacturers, or contractors do not constitute a recommendation, evaluation or endorsement by Factory Mutual Insurance Company (FM Global) of such products, manufacturers or contractors. FM Global makes no warranty, express or implied, with respect to any product or process referenced in this report. FM Global assumes no liability by or through the use of any information in this report.

EXECUTIVE SUMMARY

A project was initiated to provide a flammability characterization of Lithium-ion (Li-ion) batteries in bulk storage. This report describes a comparison of cartoned Li-ion batteries and FM Global standard commodities in a rack storage configuration. Subsequent large-scale fire tests were conducted to assess the effectiveness of ceiling-level sprinkler protection. The results provide the basis for the long-term project goal to establish protection options specific to the unique hazards associated with Li-ion batteries in storage occupancies.

This project was conducted in conjunction with the Property Insurance Research Group (PIRG) through the National Fire Protection Association's (NFPA) Fire Protection Research Foundation (FPRF). PIRG is comprised of domestic and international property insurance companies with the goal of acquiring general knowledge for issues spanning the property insurance industry. Participation is voluntary, and projects are funded by an annual fee. All projects are overseen by a technical committee including industry experts, consultants and sprinkler association members. PIRG has previously sponsored a use and hazard assessment of Li-ion batteries[i].

Li-ion battery commodities, used in the project, were selected to represent a wide range of commercially available battery formats including Li-ion battery-containing devices. The selected Li-ion battery types were: 18650 format cylindrical cells, power tool packs (comprised of 18650 format cells), and polymer cells. The selected comparison commodities were FM Global standard class 2 and cartoned unexpanded plastic (CUP)[ii].

Two independent test series were conducted by FM Global at the FM Global Research Campus in Rhode Island, USA. These tests represent a unique approach to hazard evaluation with limited commodity and were necessary due to cost and availability of Li-ion batteries and personnel safety concerns identified during the project planning phase. It is important to note that the approach does not provide the same level of information regarding protection system

[i] C. Mikolajczak, M. Kahn, K. White, and R.T. Long, "Lithium-Ion Batteries Hazard and Use Assessment" Prepared for the Fire Protection Research Foundation, June 2011.

[ii] Also referred to as cartoned Group A plastic commodity or standard plastic commodity.

performance gained through Commodity Classification[iii] or sprinklered large-scale tests using bulk-stored Li-ion batteries. Consequently, protection recommendations for Li-ion batteries are strictly limited to the conditions included in this report. The combined effects of different storage height, ceiling height, protection system design and commodity type are yet to be well understood and may not be inferred from these test results alone. The applicable storage conditions are:

- Rack storage up to 4.6 m (15 ft)
- Ceiling heights up to 9.1 m (30 ft)
- Bulk-packaged small-format Li-ion batteries in corrugated board cartons (*i.e.,* 18650-format cylindrical cells, power tool packs (comprised of 18650 format cells), and polymer cells) at 50% state-of-charge.

The first series evaluated the flammability characteristics of small format Li-ion batteries and FM Global standard cartoned commodities in a rack storage array. Due to the high cost of Li-ion batteries, a reduced-commodity approach was established where test product was only located in the portion of the rack where initial fire growth would lead to sprinkler operation. These tests, referred to as "reduced-commodity," were used to estimate the fire hazard present at the time of first sprinkler operation in a sprinklered fire scenario. Measurements focused on the fire development of each commodity and the time of battery involvement for the Li-ion products under a free-burn fire condition.

Thirteen tests were conducted using a three-tier-high, single-row, open-frame rack storage array. Ignition was achieved using an external fire located within the flue space of the array. Results suggest that sprinkler protection recommendations for Li-ion batteries may be established through testing with standard commodities. Without large-scale suppression test experience with Li-ion batteries, this assumption requires that the Li-ion batteries do not become significantly involved in the fire.

[iii] Y. Xin and F. Tamanini, "Assessment of Commodity Classification for Sprinkler Protection Using Representative Fuels," Journal of Fire Safety Science, Volume 9, pp. 527-538, 2008. DOI:10.3801/IAFSS.FSS.9-527

Based on the results of the tests presented in this report the following conclusions can be made:

- The Li-ion cylindrical and polymer cells used in this project contributed to the overall fire severity of the rack storage array within 5 minutes under free burn conditions.
- The overall agreement of the fire growth characteristics for Li-ion batteries and FM Global standard commodities supports the assumption that for three-tier-high, open-frame racks, cartoned commodities exhibit similar fire development up to first sprinkler operation.
- Plastic content and density of packed batteries are driving factors in the commodity hazard, in particular:
    - Commodity containing significant quantities of loosely packed plastics (*i.e.,* CUP and power tool packs) exhibit a similar rapid increase in the released energy due to plastics involvement early in the fire development. For the Li-ion power tool packs used in this project, the plastics dominated the fire growth and there was no observable energy release contribution from the Li-ion batteries.
    - Commodity containing densely packed Li-ion batteries and minimal plastics (*i.e.,* Li-ion cylindrical and polymer cells) exhibit a delay in the battery involvement due to heating of the batteries.
- FM Global standard cartoned unexpanded plastic (CUP) commodity exhibits a fire hazard leading to initial sprinkler operations similar or greater than the Li-ion battery products tested in the project. This result indicates that CUP commodity is a suitable surrogate for Li-ion batteries in a bulk-packed rack storage test scenario; provided the protection system design suppresses the fire within 5 min (*i.e.*, the time when the Li-ion batteries tested in this project contributed to the fire severity).
- In the absence of sprinklered large-scale test experience with Li-ion batteries, a protection system must preclude battery involvement by early extinguishment of the carton packaging fire.

The second test series evaluated the protection provided by ceiling level sprinklers with the goal of establishing protection recommendations for Li-ion batteries. Two fire tests were conducted focusing on the potential of the sprinkler system to very quickly suppress a large-scale rack

storage fire of FM Global CUP commodity. The specific test configuration investigated was a three-tier-high rack storage array that was centered among four sprinklers. This array size represents storage up to 4.6 m (15 ft) high. Protection was provided by quick-response, pendent sprinklers, having a 74°C (165°F) rated link, with either 1) a K-Factor of 360 L/min/bar$^{1/2}$ (25.2 gpm/psi$^{1/2}$) under a 9.1 m (30 ft) ceiling, or 2) a K-Factor of 200 L/min/bar$^{1/2}$ (14 gpm/psi$^{1/2}$) under a 7.6 m (25 ft) ceiling.

For protection to be considered adequate, sprinkler activation needed to occur while the fire severity was attributed to the combustion of the corrugated cartons and suppressed to the point of near extinguishment prior to time of battery involvement established for the Li-ion battery commodities in the reduced-commodity tests. In both tests, the CUP commodity cartons breached before the initial sprinkler operation. In accordance with the evaluation criteria established for this project, the adequacy of ceiling-level sprinkler protection could not be established due to persistent burning of the CUP commodity beyond the predicted time of battery involvement. These results indicate that the effectiveness of ceiling-level sprinkler protection cannot be assessed without repeating the tests using bulk-packed Li-ion batteries.

Protection recommendations for Li-ion batteries could not be directly and explicitly developed during this project; however, the test results do support analogous protection requirements for commodities with similar hazard characteristics. In consultation with the FM Global Engineering Standards group, which is responsible for the FM Global Property Loss Prevention Data Sheets, protection recommendations have been established based on current knowledge and may be amended if additional research specific to the hazard of Li-ion batteries is conducted.

The best protection recommendations based on current knowledge, for each Li-ion battery included in this project, are summarized below:

- Li-ion cylindrical cells (*i.e.,* small-format):
    - For a single unconfined pallet load of cells stored on the floor to a maximum 1.5 m (5 ft) high, protect as an HC-3 occupancy per FM Global Property Loss Prevention Data Sheet 3-26, *Fire Protection Water Demand for Nonstorage*

Sprinklered Properties, July 2011. Additionally, maintain a minimum separation of 3.0 m (10 ft) from adjacent combustibles for manufacturing occupancies; increase the separation distance to 15 m (50 ft) from areas of contiguous storage.

- For protection of cells stored on pallets greater than one high, store pallet loads in racks and protect racks with Scheme A per Section D.2.2.1 of FM Global Property Loss Prevention Data Sheet 7-29, *Ignitable Liquid Storage in Portable Containers*, April 2012.

- Li-ion polymer cells (*i.e.,* small-format):
  - For a single unconfined pallet load of cells stored on the floor to a maximum of 1.5 m (5 ft) protect as an HC-3 occupancy per FM Global Property Loss Prevention Data Sheet 3-26, *Fire Protection Water Demand for Nonstorage Sprinklered Properties*, July 2011. Additionally, maintain a minimum of 3.0 m (10 ft) separation between adjacent combustibles.
  - For protection of cells stored on pallets greater than one high, store pallet loads in racks and protect racks with Scheme A per Section D.2.2.1 of FM Global Property Loss Prevention Data Sheet 7-29, *Ignitable Liquid Storage in Portable Containers*, April 2012.
- Li-ion power tool packs (*i.e.,* small-format cylindrical cells)
  - For cells stored on pallets up to three high (*i.e.*, 4.6 m (15 ft)) under a ceiling up to 9.1 m (30 ft) high, store pallet loads in racks and protect as FM Global standard cartoned unexpanded plastic (CUP) commodity per FM Global Property Loss Prevention Data Sheet 8-9, *Storage of Class 1, 2, 3, 4 and Plastic Commodities*, FM Global, July 2011.
  - For protection of cells stored on pallets greater than three high (*i.e.*, 4.6 m (15 ft)), store pallet loads in racks and protect racks with Scheme A per Section D.2.2.1 of FM Global Property Loss Prevention Data Sheet 7-29, *Ignitable Liquid Storage in Portable Containers*, April 2012.
  - For protection of cells stored beneath a ceiling greater than 9.1 m (30 ft), regardless of storage height, store pallet loads in racks and protect racks with Scheme A per Section D.2.2.1 of FM Global Property Loss Prevention Data Sheet 7-29, *Ignitable Liquid Storage in Portable Containers*, April 2012.

ABSTRACT

A unique approach was developed to evaluate the hazard posed by bulk storage of Li-ion batteries in warehouse scenarios. This methodology incorporated two independent fire test series as a means of reducing the required quantity of Li-ion batteries. The first series evaluated the flammability characteristics of cartoned small-format Li-ion batteries and FM Global standard cartoned commodities in a three-tier-high rack storage array. These were free-burn fire tests focused on measurement of the fire development of each commodity and the time of battery involvement for the Li-ion products. For each test only the ignition flue area of the array was lined with commodity. The overall agreement of the fire growth characteristics supported the assumption that cartoned commodities, in a three-tier high open frame rack, exhibit similar fire development leading to first sprinkler operation. The second test series evaluated the ability of ceiling-level sprinkler protection to suppress a large-scale rack storage fire of CUP commodity as a surrogate for Li-ion batteries. The performance of the protection of a three-tier-high array was found to be inconclusive due to persistent flames beyond the time of battery involvement established in the free-burn fire tests. Lacking complete suppression test experience with Li-ion batteries due to inordinate costs of both materials and testing, robust sprinkler protection system design incorporating features effective for high-hazard commodities, such as Level 3 aerosols, has been recommended.

All conclusions in this report are specific to the storage configuration used in these tests. The combined effects of different storage height, ceiling height, protection system design, and commodity type are yet to be well understood and may not be inferred from these test results alone.

ACKNOWLEDGEMENTS

The authors thank Mr. R. Chmura, Mr. J. Chaffee, Mr. M. Skidmore and the entire FM Global Research Campus crew for their efforts in conducting the fire tests. There were several testing phases included in this project that utilized the talented personnel of many laboratories. In particular, Mr. J. Tucker and Mr. M. Bardol of the Calorimetry Lab were crucial to the successful completion of this project. The diligent oversight of project safety and hazardous material disposal by Mrs. J. Pitocco ensured personnel safety throughout this project.

The authors greatly acknowledge the discussion and input from the FM Global Engineering Standards group. Their expertise in loss prevention allowed for definitive protection recommendations, improving the practical application of this work.

The authors further thank Kathleen Almand, as head of the Fire Protection Research Foundation, and the members of the Property Insurance Research Group for their insightful discussions. In addition, the funding provided by PIRG members and additional sponsors for the Lithium-ion batteries was essential to the economic feasibility of this project.

In addition, the authors would like to thank Ms. Patti Barrett for processing this report.

TABLE OF CONTENTS

LIST OF FIGURES

LIST OF TABLES

1 INTRODUCTION

Since the 1990s, Lithium-ion (Li-ion) batteries have become the rechargeable power supply of choice for consumer electronics [1]. A high-energy density has driven the demand for these batteries in devices such as laptops, power tools, cameras, and cell phones. The recent influx in bulk storage of Li-ion batteries has heightened the need for sprinkler protection options that address the hazards associated with Li-ion battery fires.

Li-ion batteries present several unique fire hazard challenges compared to traditional battery types. From a fire protection standpoint, the primary concern is the presence of a flammable organic electrolyte within a Li-ion battery compared to the aqueous electrolytes found in other battery types (*i.e.,* nickel metal hydride, nickel cadmium, and lead acid). Under abnormal conditions, such as an external fire, Li-ion batteries have been known to experience thermal runaway reactions resulting in combustion of the ignitable organics and the potential rupture of the battery [2]. To date, neither FM Global Property Loss Prevention Data Sheets nor National Fire Protection Association Standard 13, "Standard for the Installation of Sprinkler Systems," [3] contain specific, research-based, sprinkler installation recommendations or requirements for Li-ion battery storage.

This project was conducted in conjunction with the Property Insurance Research Group (PIRG) through the National Fire Protection Association (NFPA). A technical panel oversight committee included industry experts, consultants, battery manufacturers, recyclers and sprinkler association members. The agreed-upon test scope included bulk-packed 18650-format cylindrical cells, polymer cells and power tool packs. A consultancy company, Exponent Inc., was retained to organize acquisition of the Li-ion batteries, provide a detailed description of the batteries, and prepare a summary report of the project findings. PIRG has previously sponsored a use and hazard assessment of Li-ion batteries [4].

FM Global donated the resources associated with conducting the research program, clean-up and disposal of Li-ion batteries, and all costs associated with the baseline tests. The balance of the costs, which included engineering and program management services and costs for Li-ion battery commodity, was supplied by PIRG.

2 BACKGROUND

The fire hazards inherent to Li-ion battery technology have been a topic of considerable discussion in the fire protection community [5,6]. As an emerging technology, there are currently no known fire protection standards that are based on real-scale testing of Li-ion batteries in a bulk-storage scenario. Consequently, the existing approach for sprinkler protection often relies on designs for high-hazard commodities, *e.g.*, automatic in-rack sprinklers. This approach seems prudent without detailed knowledge of the impact that storage conditions have on the effectiveness of sprinkler protection. As an initial effort in establishing protection options, this project addresses a common bulk-storage scenario in terms of state of charge (SOC), cell format, packaging and storage arrangement.

As indicated, limited research has focused on the hazards of Li-ion batteries in a scale relevant to actual storage scenarios. Recent work sponsored by the Federal Aviation Administration (FAA) has shown that exposure of individual Li-ion batteries to an external fire can result in violent release and ignition of the stored flammable electrolyte, further fueling the existing fire [7]. Subsequent testing with larger quantities of cartoned Li-ion batteries (5,000 cylindrical cells, 18650-format) showed that the propagation of thermal runaway can occur from cell to cell [8]. In this experiment, the initiating event was a 100-watt cartridge heater that replaced one of the cells to simulate the thermal runaway. With the cells at a 50% SOC, over an hour was required to involve all 5,000 cells indicating that cell-to-cell propagation occurs slowly without an external fire source. Cell rupture often occurred violently, resulting in substantial flaming projectiles up to 40.5 m (133 ft) [8].

Detailed investigations by Sandia National Laboratories [9,10] have used accelerating rate calorimetry (ARC) and other techniques to decipher the sequence of events leading to thermal runaway of a Li-ion battery. It was concluded that cells containing flammable electrolyte-based chemistries are prone to thermal runaway at temperatures around 180^{o}C (356^{o}F). When applied to a bulk-storage scenario this sets a maximum temperature threshold, which needs to be crossed for battery involvement in a fire. It is important to note that cell heating will occur slowly compared to the growth rate of a typical storage fire due to the thermal inertia of the batteries.

Effective fire protection system design should, therefore, quickly suppress the initial fire before the cells heat above the threshold temperature and become involved in the fire.*

The French National Institute for Industrial Environment and Risks (a.k.a., INERIS) recently conducted extensive small-scale combustion tests on Li-ion polymer cells using the Fire Propagation Apparatus (FPA) [11]. The report concluded that cell SOC impacts the reactivity of the cell during an external fire scenario. In particular, a fully charged battery has an increased propensity to undergo a thermal runaway reaction, increased initial fire growth rate and, interestingly, decreased total energy release (due to oxygen depletion within the cell) [11]. This suggests that, to reduce the hazard potential in bulk storage, Li-ion batteries should be maintained at a reduced SOC.

Current industry practices also place Li-ion batteries at a reduced SOC. A PIRG-sponsored hazard and use assessment of Li-ion batteries [4] concluded that Li-ion batteries are typically stored at an intermediate charge of 50% because,

> *"…lithium-ion cell manufacturers have determined that delivering cells at approximately 50% SOC is optimal for maximizing cell performance upon receipt by the customer; the reduced cell voltage reduces the effects of calendar aging, while the remaining capacity in the cell will prevent cell over-discharge for significant periods."*

A supplementary survey of Li-ion battery manufacturers, recyclers and others, indicated that Li-ion batteries are primarily packaged in corrugated board cartons for bulk storage. The cartoned packages are then placed on pallets in solid-pile or rack storage arrangements. This storage style is consistent with the experience of FM Global and other PIRG members.

* Significant battery involvement is qualitatively assessed based on visual observations of the fire and a simultaneous increase in the convective heat release rate. Additional details can be found in Section 4.9.

2.1 STANDARD METHOD TO EVALUATE PROTECTION REQUIREMENTS

The standard approach to classify bulk packaged materials for fire sprinkler protection is commodity classification [12,13]. This approach was not feasible, for the current project, due to excessive cost* and difficulties acquiring the necessary quantity of Li-ion batteries. Therefore, a test was desired that captures the flammability and suppression characteristics inherent in a rack storage fire while limiting the total quantity of test commodity to one pallet load.

This section presents the relevant fire growth dynamics leading up to water application in a Commodity Classification test [13]. FM Global standard class 2 and cartoned unexpanded plastic (CUP) commodities were selected to represent the expected lower and upper end of the fire hazard for cartoned products comprised of components similar to bulk storage of Li-ion cells (detailed later in Section 4.3). This analysis provides the basis for development of a comparable test using a limited quantity of product.

A primary flammability characteristic for rack storage fires is the fire growth rate leading up to water application. The chemical fire growth rate is the value typically reported by Xin for commodity classification [13] and relates to the total heat release rate of the fire. Though not reported by Xin, the convective fire growth is also useful as it relates to the conditions experienced by a sprinkler over the fire. Table 2-1 presents the chemical fire growth rates for class 2 and CUP commodities, based on the consumption rate of oxygen. The commodities exhibit similar fire growth rates at two- and three-tiers, both of which increase with storage height. This is an expected result as the corrugated board typically dominates the initial growth of a three-tier-high cartoned commodity fire†.

* The cost per pallet load of 18650-format cylindrical cells (~20,000 cells) and polymer cells (~15,000 cells) was greater than US$65,000.

† The exception is cartoned expanded plastic (CEP) commodity, which has a significantly faster fire growth rate due to the increased flammability of the expanded plastic.

Table 2-1: Fire growth rates (kW)* for Class 2 and CUP commodities at 2- and 3-tiers

Commodity	2-tier (2 x 2 x 2 array)	3-tier (2 x 4 x 3 array)
Class 2	107	168
CUP	107	152

*based on oxygen consumption

Visual observations are also a convenient means of qualitatively evaluating the fire growth, in terms of the location and progression of flaming combustion. Figure 2-1 and Figure 2-2 illustrate the fire development for rack storage arrays of Class 2 and Cartoned Unexpanded Plastic (CUP) commodities. In both cases, the fire development is shown for two- and three-tier arrays until 60 s after ignition, which coincided with activation of a hypothetical sprinkler. The following comments can be made:

- Visually, Class 2 and CUP commodity have similar fire growth before sprinkler activation for both two- and three-tier arrays. This observation agrees with the measured fire growth rates shown in Table 2-1.
- The fire development at the first tier is different than at the upper tiers. The igniters are placed at the bottom on the first tier, above the wood pallet at the corner of each commodity in the central flue. The resulting fire spread on the first tier is a 'V' pattern. At each subsequent tier, the flames from the tier below impinge on a wider portion of the commodity resulting in primarily vertical fire spread. The second tier of a 2 x 2 x 2 high array and the second and third tiers of 4 x 2 x 3 high array have similar areas of flame spread.
- Initial flame impingement on the second tier is contained to the ignition area with minimal flame spread under the pallet.
- Flames do not attach to the aisle face of the commodity before sprinkler operation.
- Flames are contained to the commodity surrounding ignition (*i.e.*, flames do not jump across transverse flues).

	Ignition + 10s	Ignition + 20s	Ignition + 40s	Ignition + 60s
2 x 2 x 2				
4 x 2 x 3			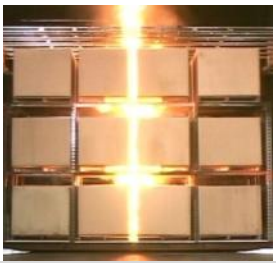	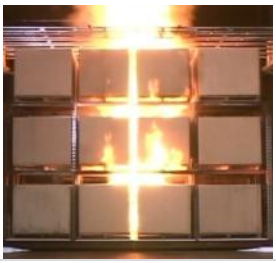

Figure 2-1: Fire development for rack storage Class 2 commodity at 2- and 3-tiers

	Ignition + 10s	Ignition + 20s	Ignition + 40s	Ignition + 60s
2 x 2 x 2		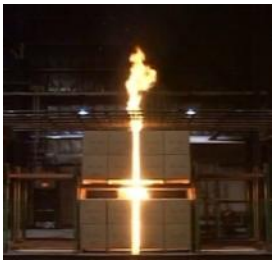		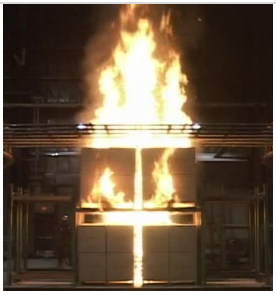
4 x 2 x 3	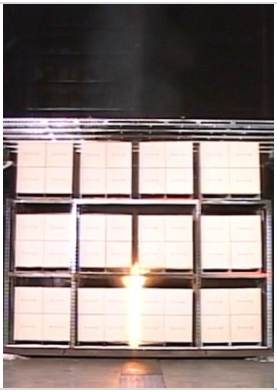	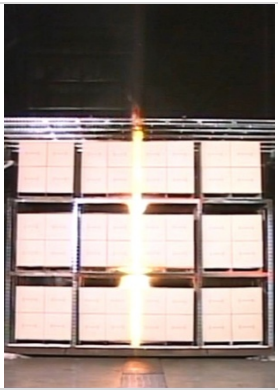	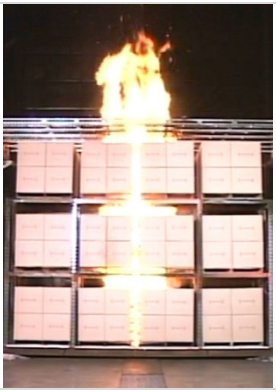	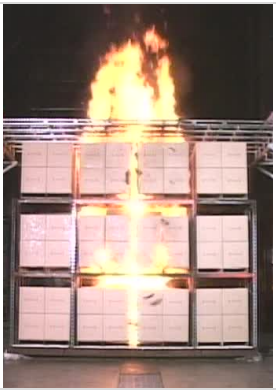

Figure 2-2: Fire development for rack storage CUP commodity at 2- and 3-tiers

2.2 COMMENTS ON HEAT RELEASE RATE CALCULATIONS

It is important to note that for this project the fire growth rate was characterized by the convective heat release. In addition to the usual sources of measurement uncertainty [14,15,16], the chemical heat release of a Li-ion battery cannot be accurately measured because the vent gases contain significant percentages of CO_2 formed from thermal degradation processes (pyrolysis rather than combustion) of the organic carbonates in the electrolyte. This form of CO_2 production (breaking of a C-C bond in a carbonate compound to release an O-C-O functional group) does not involve the same energy release as the formation of CO_2 from typical combustion processes (reaction of CO and OH). Therefore, carbon dioxide and oxygen consumption calorimetry will overpredict the chemical heat release rate [1]. Recent work at INERIS noted that the resulting uncertainty was at least 10% for a small format polymer battery [11]. The magnitude of the measurement error is difficult to generalize as it depends on the type (*e.g.*, format, chemistry, etc.) and quantity of batteries involved in a fire and can change as the fire develops. For reference, chemical heat release rate measurements for testing with FM Global standard commodities based on the generation rates of carbon dioxide and carbon monoxide (HRR-COCO2) and oxygen consumption (HRR-O2) are provided in Appendix A.

3 REPORT SCOPE AND RATIONALE

Two series of fire tests were conducted to establish protection recommendations for Li-ion batteries in bulk storage. This testing represents a unique approach to hazard evaluation with limited commodity and was necessary due to cost and availability of the commodity and personnel safety concerns. It is important to note that the approach does not provide the same level of information gained through Commodity Classification [12] or large-scale testing. Consequently, protection recommendations for Li-ion batteries are strictly limited to the conditions included in this report. All testing was conducted at the FM Global Research Campus in Rhode Island, USA.

The first test series evaluated the flammability characteristics of small format Li-ion batteries in a rack storage array compared to FM Global standard cartoned commodities. These were free-burn fire tests focused on measurement of fire development of each commodity and the time of battery involvement for the Li-ion products. The results of these tests, referred to as "reduced commodity," were used to estimate the fire hazard present at the time of first sprinkler operation in a sprinklered fire scenario. The reliance on free-burn fires allows for a reduction in test commodity; however, it does not provide the same information as Commodity Classification [12] or a sprinklered large-scale fire test. The obvious concern for Li-ion battery storage is the additional hazard posed by thermal runaway reactions occurring within the commodity initiated by an external fire scenario.[*] In a sprinklered fire test, the effectiveness of the protection system on a Li-ion battery fire due to external heating can be evaluated directly. The result is a high level of confidence that the protection system is adequate for the hazard of both the outer carton packaging and the stored Li-ion batteries. Lacking this experience, it is necessary to demonstrate that a protection system can preclude battery involvement by early extinguishment of the carton fire.

The second test series evaluated the level of protection provided by ceiling-level sprinklers to support the development of recommendations for Li-ion batteries. These tests focused on the ability of the sprinkler system to suppress a large-scale rack storage fire of CUP commodity prior

[*] Scenarios initiated by thermal runaway within the core of a pallet load of commodity are beyond the project scope.

to involvement of the contents. For protection to be considered adequate, the fire had to be nearly extinguished before the predicted time of battery involvement established for the Li-ion batteries in the reduced-commodity tests.

4 REDUCED-COMMODITY TESTS

Thirteen reduced-commodity fire tests were conducted focusing on a comparison of the flammability characteristics of FM Global standard commodities and several commercially available Li-ion battery products. These were free-burn fire tests conducted under a 5-MW Fire Products Collector (FPC) to measure the heat release rate of each commodity and the time of battery involvement for the Li-ion products. Subsequent predictions establish the theoretical time of first sprinkler operation and corresponding fire hazard present in a sprinklered fire scenario. These predictions provide the basis for protection system recommendations for bulk storage of Li-ion batteries.

4.1 CALORIMETRY LABORATORY

The tests for this program were conducted under the 5-MW fire products collector (FPC) in the Calorimetry Burn Laboratory located in the Fire Technology Laboratory at the FM Global Research Campus in West Glocester, Rhode Island, USA. The Calorimetry Lab measures 40 m x 16 m (130 ft x 52 ft) and consists of four test locations: a movable ceiling, 0.2-MW FPC, 1-MW FPC, and 5-MW FPC. A separate air emission control system (AECS) is provided for each test location. Additional extraction points are located at the lab ceiling to increase air exhaust as needed. The 5-MW FPC consists of a 6.1 m (20 ft) diameter inlet that tapers down to a 1.5 m (5 ft) diameter duct. The inlet to the FPC is at an elevation of 7.9 m (26 ft) from the floor. Gas concentration, velocity, temperature and moisture measurements are within the duct. Beyond the measurement location, the exhaust duct connects to a wet electrostatic precipitator (WESP) prior to the gases venting to the atmosphere. All tests were conducted at a nominal exhaust rate of 1,400 m^3/min (50,000 ft^3/min).

4.2 TEST CONFIGURATION OVERVIEW

The test array was designed to capture the fire growth characteristics, discussed in Section 2, using a reduced amount of commodity. As shown in Figure 4-1, the array consists of a three-tier-high, open-frame, single-row steel rack with overall dimensions of approximately 2.4 m long x 1.2 m wide x 4.3 m tall (8 ft x 3.25 ft x 14 ft). This array size is used to represent rack storage up to 4.6 m (15 ft), assuming nominally 1.5 m (5 ft) per tier. To allow for a meaningful comparison

between commodities, it is necessary to maintain a similar geometric area of commodity exposed to the fire; therefore, only the ignition flue area of the array is lined with commodity.

The bottom tier of the array consists of a noncombustible product (metal liner) supported on a wood pallet. The upper tiers are made of the same noncombustible product lined with test commodity on the flue faces. The noncombustible product is constructed to maintain the FM Global standard 1.07 m x 1.07 m x 1.07 m (42 in. x 42 in. x 42 in.) commodity dimensions and maintain representative airflow around the commodity. Specific dimensions of the test commodity and noncombustible product for each test are included in Section 4.3.

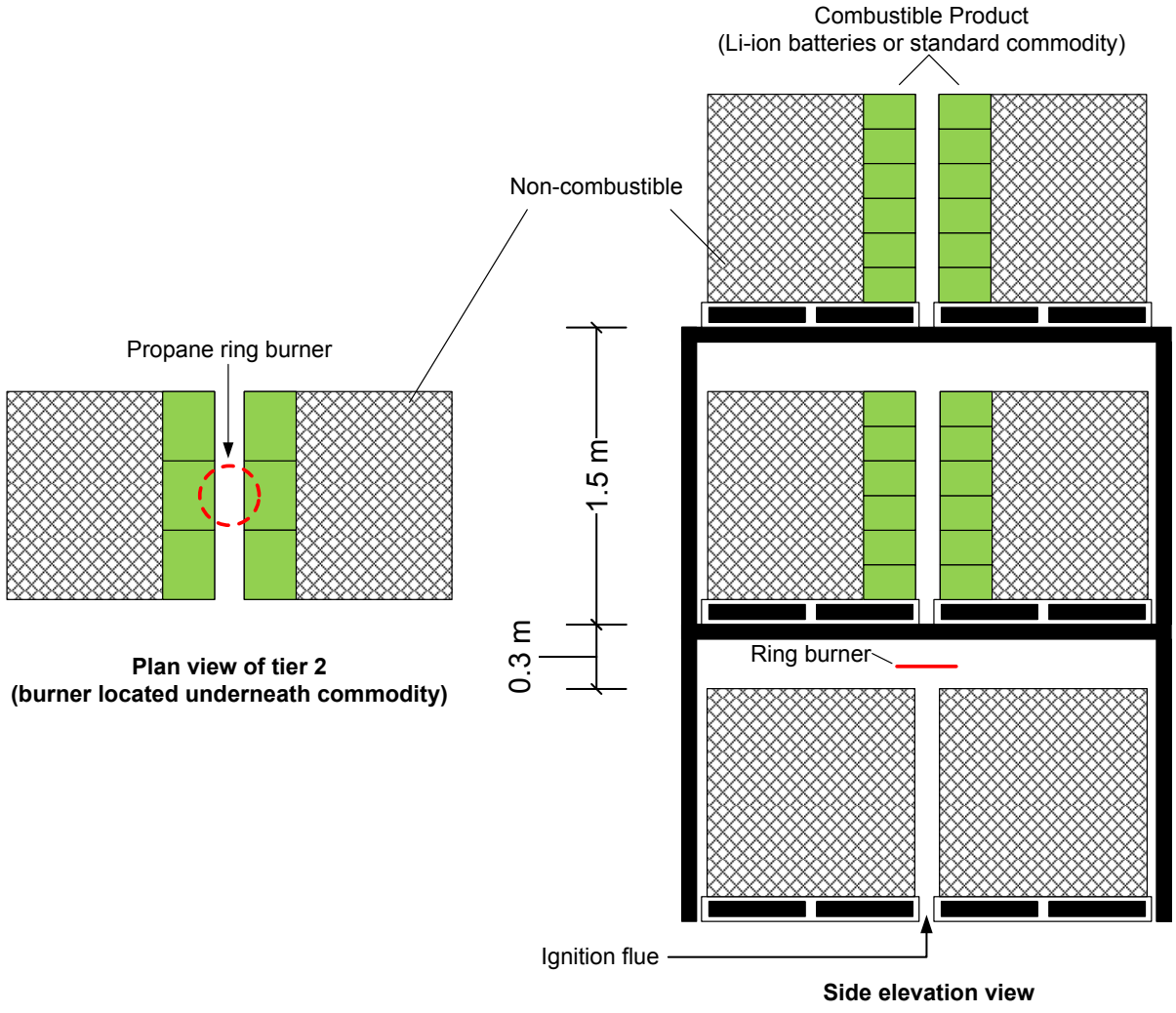

Figure 4-1: Schematics of reduced-commodity rack storage test; plan view of tier 2 (left) and side elevation view (right).

For reference, the specific modifications compared to a standard rack storage arrangement are:

1) The array was modified to a 1 x 2 x 3 pallet load tall arrangement with ignition shifted to mid-pallet.

   This allows the test commodity to span the entire pallet width and allows for horizontal fire spread. A 2 x 2 x 4 arrangement would result in test commodity on only the corner of each pallet, which is not sufficient to allow for horizontal fire spread.

2) No commodity was present on the first/bottom tier.

   The fire grows in a 'V' pattern from the igniter, which would result in reduced area of possible commodity involvement. Flame impingement from the first to the second tier can be adequately represented by adjusting the ignition scenario.

3) Commodity on the second and third tier was only located on the flue-facing sides of the pallet.

   This commodity placement coincides with the area of flame attachment at first sprinkler operation during a typical rack storage test.

4) Ignition was accomplished with a 0.4 m (16 in.) diameter propane ring burner located on top of the first tier commodity, centered within the flue. Propane was supplied at a rate of 1.1 ft^3/min (30 L/min).

   The modified ignition location replicates the flame impingement on the bottom of the second tier resulting from the fire on the first tier.

4.3 TEST COMMODITY

Two FM Global standard commodities were selected for this project: class 2 and cartoned unexpanded plastic (CUP). Three Li-ion battery types were identified to represent the broad spectrum of commercially available products: 18650 format cylindrical cells, polymer cells, and high capacity power tool battery packs. Specifications for each battery used in this project are shown in Table 4-1.

Table 4-1: Li-ion battery specifications [*courtesy of Exponent, Inc.]*

Cell Type	18650-Format Cylindrical	Power Tool Pack (individual cell)*	Polymer
Chemistry	Lithium Cobalt Oxide	Lithium Nickel Manganese Cobalt Oxide	Lithium Cobalt Oxide
Nominal Voltage	3.7 V	18.5 V (3.7 V)	3.7 V
Nominal Capacity	2600 mAh	2600 mAh (1300 mAh)	2700 mAh
Approximate State-of-Charge (SOC)	40%	50%	60%
Nominal Weight	47.2 g	768.5 g (42.9 g)	50.0 g

* The power tool battery packs each contain ten 18650-format cylindrical cells with a nominal voltage of 3.7 V and nominal capacity of 1300 mAh. The resulting specifications of the power tool pack are a nominal voltage of 18.5 V and a nominal capacity of 2600 mAh.

4.3.1 FM Global Standard Commodities

FM Global standard class 2 commodity consists of three double-wall corrugated paper cartons, Figure 4-2. The dimensions for the inner, middle and outer box are 1.02 m x 1.02 m x 0.96 m (40.3 in. x 40.3 in. x 37.8 in.), 1.04 m x 1.04 m x 0.99 m (41.0 in. x 41.0 in. x 39.1 in.), and 1.06 m x 1.06 m x 1.05 m (41.8 in. x 41.8 in. x 41.5 in.), respectively. Inside the cartons is a five-sided sheet metal liner, representing noncombustible content. The cartoned liner is supported on an ordinary, two-way, slatted-deck hardwood pallet, measuring 1.07 m x 1.07 m x 127 mm (42 in. x 42 in. x 5 in.).

The modified pallet design for the FM Global standard class 2 commodity, for the reduced-commodity tests, was constructed by covering a portion of the corrugated board carton with thick aluminum foil, securely affixed at the exposed carton edge with metal bands, to leave an exposed area of 0.27 m x 1.07 m x 1.07 m (10.5 in. x 42 in. x 42 in.), Figure 4-2. The total combustible weight of the commodity is 33.9 kg (74.7 lb); the exposed portion of the corrugated containerboard weighs 11.5 kg (25.4 lb)* and the pallet weighs 22.4 kg (49.4 lb). The total chemical energy for a pallet of the modified class 2 commodity was nominally 443 ± 11 MJ, based on the above masses and the heat of combustion for each material, Section 4.3.5. The total chemical energy of the entire array is 2,328 ± 58 MJ, *i.e.,* four pallets loads of commodity plus two additional pallets under the first tier noncombustible (443 x 4 + 278 x 2 = 2,328 MJ).

Figure 4-2: FM Global standard Class 2 commodity (left) and modified pallet design for reduced-commodity tests (right)

The FM Global standard CUP commodity consists of group A unexpanded rigid crystalline polystyrene cups (empty, 0.47 L, 16 oz.) packaged in single-wall, corrugated paper cartons. Cups are individually compartmentalized with corrugated paper partitions, and are arranged in five layers, with 25 cups per layer, to result in 125 cups per carton. Eight 0.53-m (21-in.) cube cartons, arranged 2 x 2 x 2, form a pallet load. Overall, the cube unit measures 1.07 m (42 in.) on

* The exposed portion of the corrugated containerboard (*i.e.*, portion not covered with foil) weighs 11.5 kg, which represents 32.5% of the total 35.4 kg (78.0 lb) mass of corrugated board of a Class 2 commodity.

the outside, and is supported on an ordinary, two-way, slatted-deck hardwood pallet, measuring 1.07 m x 1.07 m x 127 mm (42 in. x 42 in. x 5 in.).

The modified pallet design for the FM Global standard CUP commodity, for the reduced-commodity tests, consisted of four 0.53 m x 0.53 m x 0.53 m (21 in. x 21 in. x 21 in.) plastic cup filled corrugated cartons stacked 1 x 2 x 2 cartons high. The remaining pallet area consisted of a metal liner with dimensions of 1.07 m x 0.53 m x 1.07 m (42 in x 21 in. x 42 in.), Figure 4-3. The total combustible weight of the modified commodity is 48.1 kg (106.0 lb); the corrugated carton and paper partitions weigh 9.9 kg (21.8 lb)[*], the plastic cups weigh 15.8 kg (34.8 lb), and the pallet weighs 22.4 kg (49.4 lb). The total chemical energy for a pallet of the modified CUP commodity was nominally 855 ± 21 MJ, based on the above masses and the heat of combustion for each material, Section 4.3.5. The total chemical energy of the entire array is 3,976 ± 100 MJ, *i.e.,* four pallets loads of commodity plus two additional pallets under the first tier non-combustible (855 x 4 + 278 x 2 = 3,976 MJ).

Figure 4-3: FM Global standard CUP commodity (left) and modified pallet design for reduced-commodity tests (right)

[*] Based on four plastic cup filled corrugated cartons per pallet (a full FM Global standard CUP commodity contains eight plastic cup filled corrugated cartons).

4.3.2 Li-ion 18650 Format Cylindrical Cells

The 18650-format cylindrical cell is currently the most widely used battery type and has dimensions of 18 mm diameter x 65 mm long (0.7 in. x 2.6 in.). The cell is constructed by winding long strips of electrodes into a "jelly roll" configuration, which is then inserted into a hard metal case and sealed with gaskets, Figure 4-4 and Figure 4-5.

The packaging, as received from the manufacturer, consisted of two 220 mm × 213 mm × 74 mm (8.7 in. x 8.4 in. x 2.9 in.) inner corrugated board cartons within a 444 mm × 237 mm × 93 mm (17.5 in. x 9.3 in. x 3.7 in.) outer corrugated board carton, Figure 4-6. Each inner carton contained 100 cylindrical cells separated by paperboard partitions.

The pallet design for the cylindrical cells consisted of manufacturer cartons received from the manufacturer stacked 12 levels high resulting in dimensions of 1.0 m x 0.22 m x 1.07 m (38 in. x 8.75 in x 42 in.), Figure 4-7. To maximize the width of the palletized product, the outer corrugated board cartons were cut in half crosswise and placed 4 wide per level, resulting in a total of 24 full cartons (48 half cartons) of commodity per pallet (4,800 cylindrical cells). Metal liners were fabricated to fill the remaining portion of the pallet with dimensions of 1.0 m x 0.84 m x 1.07 m (38 in. x 33.25 in. x 42 in.). The backside of the cartons was metal banded to the metal liner at the fourth and eighth level for additional stability.

As shown in Table 4-2, the combustible loading per outer carton of cylindrical cells is 22.1 ± 1.4 MJ and each pallet load contained the equivalent of 24 full cartons of cylindrical cells. When supported on an FM Global standard wood pallet, the combustible weight of the commodity is 53.7 kg (118.4 lb); of this total the cartoned Li-ion cylindrical cell commodity is 31.3 kg (69.0 lb) and the pallet 22.4 kg (49.4 lb). The total chemical energy for a pallet of the 18650-format cylindrical cells used in this project is nominally 809 ± 33 MJ, based on the above masses and the heat of combustion for each material listed in Section 4.3.5. The total chemical energy of the entire array is 3,789 ± 147 MJ, *i.e.,* four pallets loads of commodity plus two additional pallets under the first-tier noncombustible (809 x 4 + 278 x 2 = 3,789 MJ).

Figure 4-4: Li-ion cylindrical cell; external case side (left) and end view (right).

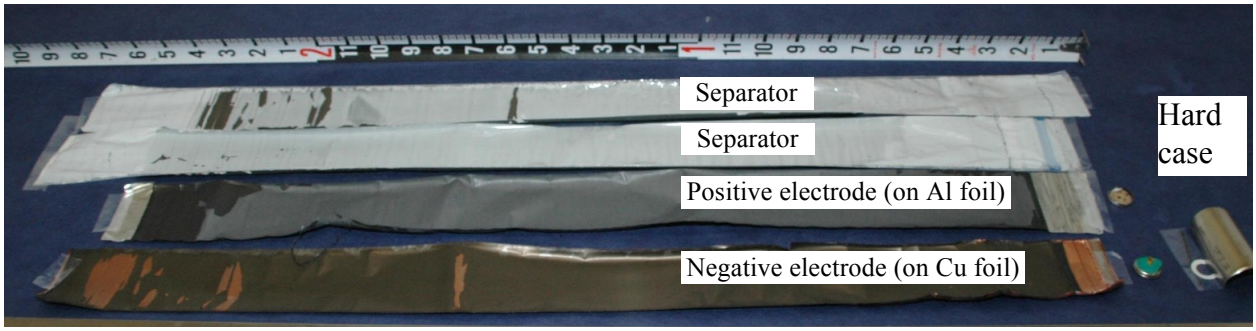

Figure 4-5: Li-ion cylindrical cell internal components *(image courtesy of Exponent, Inc.)*

Figure 4-6: Li-ion cylindrical cell packaging as received from manufacturer

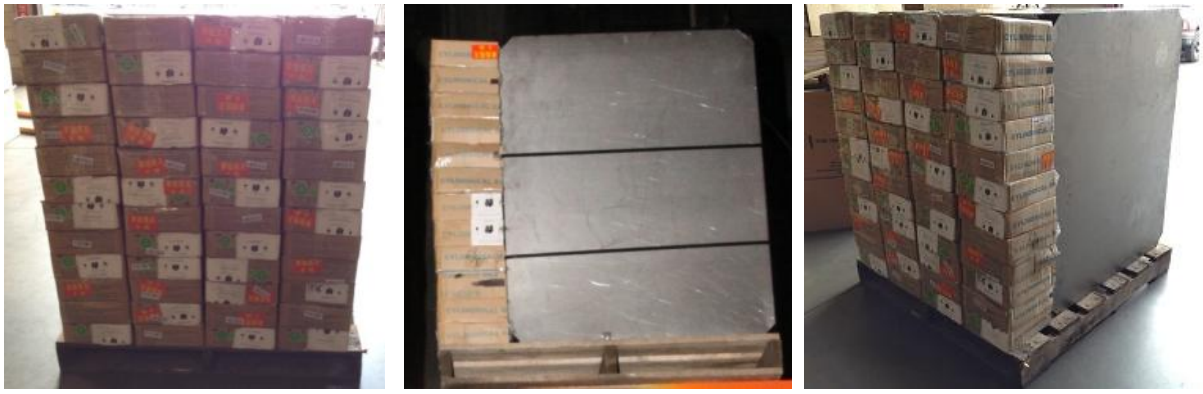

Figure 4-7: Pallet design for Li-ion cylindrical cells

Table 4-2: Combustible load per carton of Li-ion cylindrical cells

Component	Individual Weight (g)	Quantity per Carton (ea)	Weight per Carton (g)	Energy* (MJ)
Outer corrugated carton	330	1	330	4.7 ± 0.12
Inner corrugated carton	97.0	2	194	2.8 ± 0.07
Linerboard partition	111	2	222	3.2 ± 0.08
Corrugated board cover	18.7	2	37.4	0.5 ± 0.01
Cell electrolyte	2.6	200	520	10.9 ± 1.1
		Total:	**1,303**	**22.1 ± 1.4**

* Uncertainty values listed in Section 4.3.5

4.3.3 Li-ion 18 V Power Tool Packs

The power tool packs are comprised of cylindrical cells encased in a rugged plastic case that measures 140 mm x 82.5 mm x 108 mm (5.5 in. x 3.25 in. x 4.25 in.). The battery packs are encased in plastic blister packs for display, Figure 4-8. Each power tool pack contains ten 18650-format cylindrical cells; five cells are connected in series to produce a nominal voltage of 18.5 V (3.7 V per cell x 5 cells in series) and the two sets are then connected in parallel to produce a nominal capacity of 2600 mAh (1300 mAh per set of 5 cells x 2 in parallel), Figure 4-9. For simplicity, this pack design is often listed as 48 Wh (18.5 V x 2.6 Ah = 48.1 Wh).

The packaging, as received from the manufacturer, consisted of an outer corrugated board carton with dimensions of 203 mm x 203 mm x 210 mm (8 in. x 8 in. x 8.25 in). Each carton contained four power tool packs which were tessellated (staggered) top-to-bottom and separated by corrugated board dividers, Figure 4-10.

The pallet design for the Li-ion power tool packs consisted of manufacturer cartons stacked 5 wide by 5 tall, resulting in dimensions of 1.0 m x 0.15 m x 1.07 m (38.75 in. x 6 in. x 42 in.). As received, each carton contained four power tool packs. Each carton was cut in half and fitted with a corrugated board end cap to reduce the number of packs to two per carton. A metal liner was fabricated to fill the remaining portion of the pallet with dimensions of 1.0 m x 0.9 m x 1.07 m (38.75 in. x 36 in. x 42 in.). The backside of the cartons was metal banded to the metal liner at three elevations for additional stability. This pallet design resulted in 25 half cartons (50 power tool packs) per pallet, containing a total of 500 Li-ion cylindrical cells per pallet.

The combustible loading per carton of power tool packs is 33.3 ± 1.1 MJ; each pallet load contained the equivalent of 12.5 cartons of power tool packs. When supported on an FM Global standard wood pallet, the total combustible weight of a pallet of commodity is 41.0 kg (90.4 lb); the cartoned power packs weigh 18.6 kg (41.0 lb) and the pallet weighs 22.4 kg (49.4 lb). The total chemical energy for the pallet design of the power tool packs used in this project is nominally 694 ± 21 MJ, based on the above masses and the heat of combustion for each material listed in Section 4.3.5. The total chemical energy of the entire array is 3,332 ± 125 MJ, *i.e.,* four pallet loads of commodity plus two additional pallets under the first-tier noncombustible (694 x 4 + 278 x 2 = 3,332 MJ).

Figure 4-8: Li-ion power tool pack shown with blister case (left) without blister case (right)

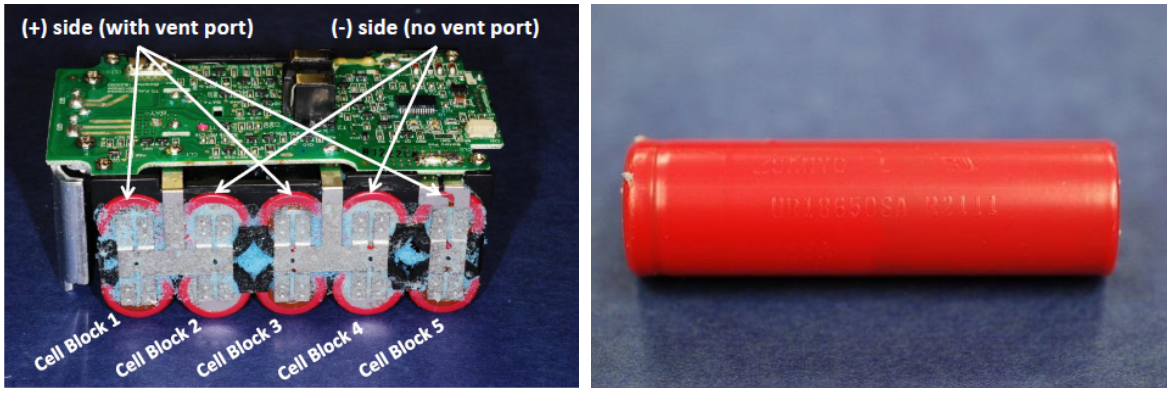

Figure 4-9: Li-ion power tool pack internal components (left) and individual 18650-format cylindrical cell (right) *(images courtesy of Exponent, Inc.)*

Figure 4-10: Li-ion power tool pack packaging as received from manufacturer

Figure 4-11: Pallet design for Li-ion power tool packs

Table 4-3: Combustible load per carton of Li-ion power tool packs

Component	Individual Weight (g)	Quantity per Carton (ea)	Weight per Carton (g)	Energy* (MJ)
Outer corrugated carton	213	1	213	3.1 ± 0.08
Corrugated board end cap	71.0	2	142	2.0 ± 0.05
Cardboard dividers	40.8	4	163	2.4 ± 0.06
Unexpanded plastic blister pack	8.2	4	32.8	0.9 ± 0.02
Unexpanded plastic cell casing (ABS)	201	4	803	22.1 ± 0.55
Cell electrolyte	3.3	40	132	2.8 ± 0.3
		Total:	**1,486**	**33.3 ± 1.1**

* Uncertainty values listed in Section 4.3.5

4.3.4 Li-ion Polymer Cells

Li-ion polymer cells are commonly found in mobile phones and tablet computers and have a soft-case enclosure to reduce the overall size and weight. The polymer cell selected for this project had dimensions of 99 mm x 41 mm x 6 mm (3.9 in. x 1.6 in. x 0.23 in.). The cells are constructed by winding long strips of electrodes into a "jelly roll" configuration*, which is then enclosed in a polymer-coated aluminum pouch with heat-sealed seams, Figure 4-12 and Figure 4-13. The packaging, as received by the manufacturer, consisted of two 350 mm x 160 mm x 110 mm (13.8 in. x 6.3 in. x 4.3 in.) inner corrugated board cartons within a 366 mm x 355 mm x 120 mm (14.4 in. x 14.0 in. x 4.7 in.) outer corrugated board carton, Figure 4-6. Each inner carton contained 72 cylindrical cells separated by nested clear unexpanded plastic dividers.

The pallet design for the Li-ion polymer cells consisted of manufacturer cartons stacked 3 wide by 9 tall, resulting in dimensions of 1.10 m x 0.36 m x 1.07 m (43.2 in. x 14 in. 42 in.). Metal liners were fabricated to fill the remaining portion of the pallet 1.07 m x 0.7 m x 1.07 m deep (42 in. x 28 x 42 in.). This pallet design resulted in 27 cartons per pallet containing a total of 3,888 polymer cells per pallet.

As shown in Table 4-4, the combustible loading per outer carton of polymer cells is 43.9 ± 2 MJ and there were 27 cartons per pallet. When supported on an FM Global standard wood pallet, the total combustible weight of the commodity is 79.1 kg (174.4 lb); the cartoned Li-ion polymer cell commodity contributing 56.7 kg (125.0 lb) and the pallet 22.4 kg (49.4 lb). The total chemical energy for a pallet of the polymer cells is nominally 1,463 ± 61 MJ, based on the above masses and the heat of combustion for each material listed in Section 4.3.5. The total chemical energy of the entire array is 6,409 ± 258 MJ, *i.e.,* four pallet loads of commodity plus two additional pallets under the first-tier noncombustible (1,463 x 4 + 278 x 2 = 6,409 MJ).

* As opposed to a stacked electrode configuration that is also common for polymer cells.

Figure 4-12: Li-ion polymer cell; complete cell (left) and partially disassembled cell (right)

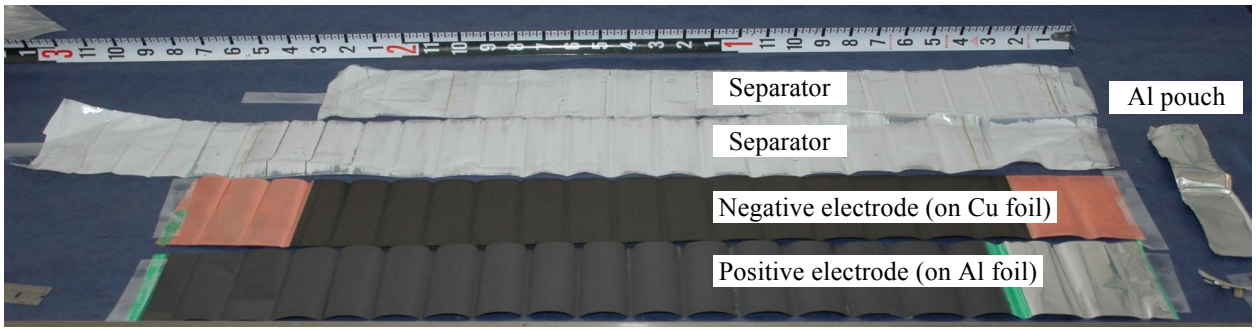

Figure 4-13: Li-ion polymer cell internal components *(image courtesy of Exponent, Inc.)*

Figure 4-14: Li-ion polymer cell packaging as received from manufacturer

Figure 4-15: Pallet design for Li-ion polymer cells

Table 4-4: Combustible load per carton of Li-ion polymer cells

Component	Individual Weight (g)	Quantity per Carton (ea)	Weight per Carton (g)	Energy* (MJ)
Outer corrugated carton	470	1	470	6.8 ± 0.2
Inner corrugated carton	147	2	294	4.2 ± 0.1
Expanded foam insert	1.7	2	3.4	0.1 ± 0.0
Unexpanded plastic divider	28.5	26	741	20.4 ± 0.5
Shrink wrap	7.2	2	14.4	0.4 ± 0.01
Cell electrolyte	4.0	144	576	12.0 ± 1.2
		Total:	**2,099**	**43.9 ± 2.0**

***** Uncertainty values listed in Section 4.3.5

4.3.5 Heats of Combustion

Table 4-5 contains average chemical heat of combustion values for each component of the test commodities. These are average values for each material type and up to 5% variance can be expected with the exception of the Li-ion battery electrolyte. The heat of combustion value for diethyl carbonate (DEC) was used as a representative estimate for electrolyte as it has been shown to be similar to other organic carbonate solvents typically found in Li-ion battery electrolyte [17]. The exact composition of the Li-ion battery electrolytes is unknown, therefore a variance of 20% was assumed.

Table 4-5: Heat of combustions for test commodities

Material	Chemical Heat of Combustion (kJ/g)	Representative Material [Reference]	Reference
Wood pallet	12.4 ± 0.3	Red oak	[18]
Corrugated and paper board	14.4 ± 0.4	Newspaper	[18]
Unexpanded plastic	27.5 ± 0.7	Polystyrene	[18]
Expanded plastic	28.0 ± 0.7	Expanded polystyrene	[18]
Electrolyte*	20.9 ± 2	Diethyl carbonate	[17]

4.3.6 Carton Moisture Content

For each test, the commodity moisture content of the outer corrugated board cartons was controlled to within 4.0% to 8.0% on a dry basis.

4.3.7 Carton Combustion Parameters

FM Global carefully controls the material properties of the corrugated board cartons used for construction of all standard cartoned commodities. Testing of the flammability characteristics is conducted with the fire propagation apparatus (FPA) [19]. Among the measurements are the thermal response parameter (TRP)* and time to ignition under different heat flux exposures [20]. Measurements for the carton material from the three Li-ion commodities were within acceptable benchmark values for class 2 commodities. The class 2 and CUP commodities exhibit comparable fire growths rates in rack storage up to three-tier-high, as shown in Table 2-1. Therefore, all commodities included in this project should have a similar initial fire growth rate, before involvement of material contained within the cartons.

4.3.8 Ignition

Ignition was achieved with a 0.4 m (16 in.) diameter propane ring burner centered in the transverse flue 0.15 m (6 in.) below the second-tier test commodity, Figure 4-1 and Figure 4-16. Propane was supplied at a rate of 30 L/min (1.06 ft^3/min) for the entire test, resulting in a nominal 45 kW heat release rate, calculated as

$$\dot{q}_{C3H8} = \dot{m} \times \rho \times \Delta H_c.$$

Here $\dot{m}$ is the mass flow in g/s, ρ is the density of propane at 0°C (32°F) and 101.3 kPa (1 atm) with a value of 1.97 kg/m^3 (0.12 lb/ft^3), and ΔH_c is the net heat of complete combustion of propane with a value of 46.0 kJ/g.

* TRP is a quantification of the ignition resistance of a material and relates the time to ignition to the net heat flux.

Figure 4-16: Propane ring burner (left) within the rack and fire size within rack (right)

4.4 DOCUMENTATION AND INSTRUMENTATION

Documentation for each test included video, still photography, and pertinent measurements necessary to evaluate product performance. All instrumentation was calibrated in accordance with ISO 17025 [21]. The following standard instrumentation was installed within the laboratory space and the exhaust duct for the 5-MW FPC:

- Ambient conditions in the lab were monitored with a Type K, bare-bead, 6.4 mm (0.25 in.) sheathed, chromel-alumel thermocouple (Pyromation Inc. K43EM-012-00-4) for temperature, a barometric pressure transducer (Setra 270) for lab pressure, and a humidity meter for lab humidity (Davis Weather Monitor II).
- Gas analyzers to measure the generation of carbon dioxide (CO_2), carbon monoxide (CO), total hydrocarbons (THC), and depletion of oxygen (O_2) captured in the exhaust. Except for THC, these measurements were only acquired for testing with FM Global standard commodities, as discussed in Section 2.2.
- A flow meter (Hasting HMF 301) and manual metering valves to monitor and control the propane flow to the ring burner.

- Mass loss during the test was monitored with a load cell (Vishay BLH Kis II beams with a LCP-104-VR3-20 controller) located under a platform supporting the entire rack structure.

In addition, several thermocouples were used to monitor internal heating of the commodity during the fire tests. Each thermocouple was a Type K, bare-bead, 6.4 mm (0.25 in.) sheathed, chromel-alumel thermocouple (Omega KQXL300E). The thermocouple locations were as follows:

- Thermocouples were located along the horizontal centerline of each commodity at the interface between the combustible product and the metal liner, Figure 4-17. These thermocouples were not present for testing with class 2 commodity because there was no interface point. The thermocouples were mechanically fastened to the metal liner, at elevations of 0.36 m (14 in.) and 0.72 m (28 in.) above the wood pallet. These thermocouples are referenced by their location within the array based on tier (T2 for tier 2 or T3 for tier 3), pallet location within the array (east or west) and elevation (low = 0.36 m above pallet or high = 0.72 m above pallet). For example, T2EL references the thermocouple located at tier 2, east pallet, low elevation.
- For test 13, an additional thermocouple was located 0.18 m (7 in.) in from the face of each commodity at the horizontal and vertical midpoint of the commodity, Figure 4-17. These thermocouples were placed between commodity cartons and are referenced based on tier (T2 for tier 2 or T3 for tier 3), pallet location within the array (east or west), and elevation on the commodity. For example, T3EC references the thermocouple located at tier 3, east pallet, at the center height of the commodity.

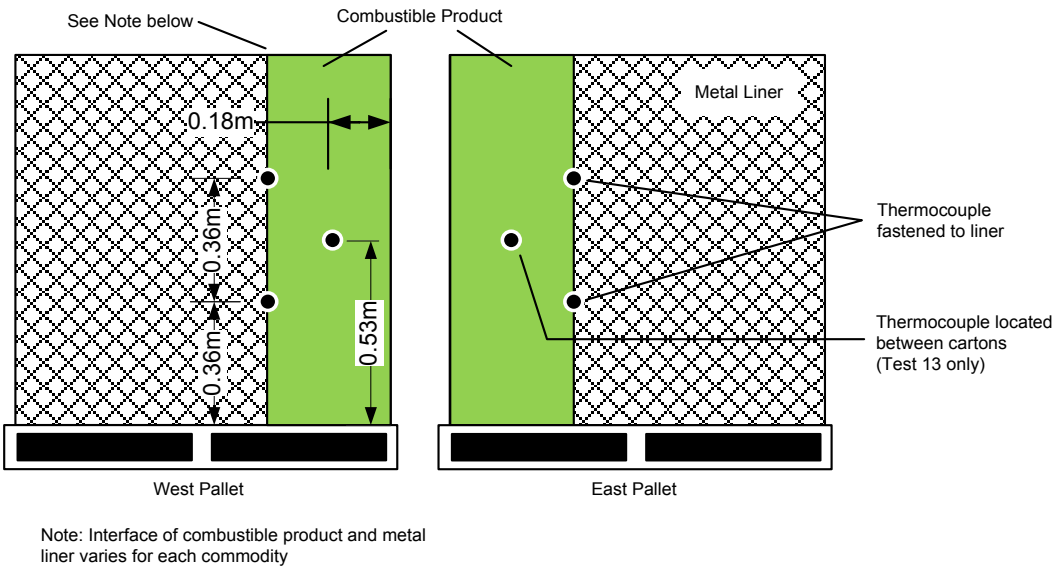

Figure 4-17: Thermocouple locations for test pallets

The video documentation included two standard definition digital video cameras, one high definition video camera, and three infrared (IR) cameras for qualitative assessments of the fire. The two standard definition digital video cameras provided a view of the test from the north (main camera) and west (remote camera). The high definition digital video camera was adjacent to the main camera. The following infrared cameras were used in this study:

- FLIR® SC655 long-wave IR (LWIR)
- FLIR® SC7600 ORION mid-wave IR (MWIR)
- THERMACAM® X90 SERIES Model PM390.

An image showing the SC7600 ORION MWIR inside its metal enclosure and the SC655 LWIR protected by aluminum foil is shown in Figure 4-18. The SC7600 camera has a rotating filter wheel in front of the indium-antimonide photodetector with a 640 x 512 pixel resolution. The filters used were a broadband (1 μm -5 μm) sapphire window, a narrowband (3.88 mm - 3.92 mm) filter (to see through flames), and a neutral density (ND = 2) filter. This camera is capable of recording at 400 frames per second (100 fps/filter). Due to proximity of this camera to large-scale fires, smoke, steam, and suppression water; the camera was placed inside a stainless steel cylindrical enclosure.

The SC655 LWIR camera has an uncooled microbolometer thermal detector with a 640 x 480 (17 μm) pixel resolution sensitive at wavelengths between 7.5 - 13 μm. The maximum full frame rate of this camera is 50 Hz. The LWIR camera has a reduced aperture placed in front of the lens, reducing the incoming IR radiation intensities and raising the usable blackbody temperature range of the camera from 650ºC (1,200ºF) to 1200ºC (2,190ºF). A separate calibration of the LWIR camera with the aperture placed in front was performed using a blackbody calibration source (Infrared Systems model 564/301, 20 - 1200ºC [68 - 2,190ºF]) powered by an IR-301 blackbody controller. The noise equivalent temperature difference (NETD) increases from 0.46 to 1.0ºC (@ 25ºC) due to this recalibration. The calibrated microbolometer camera allows capturing a full 0 - 1,200ºC temperature range on a single image.

The X90 camera has limited spatial resolution (320 x 240 pixels) and temperature range and is mainly used to allow real-time assessment during a fire test. Images taken by this camera were not further analyzed.

Figure 4-18: The SC7600 MWIR inside protective enclosure (center) and the SC655 LWIR camera protected by aluminum foil (lower right hand corner)

A schematic of each camera location is shown in Figure 4-19. The SC655 and SC7600 infrared imaging cameras provided a view of the test from a slightly northwest angle and the X90 camera provided a view of the test from the south. Standard definition video cameras provided a view of

the array from the north and west; the high definition camera provided an additional view from the north.

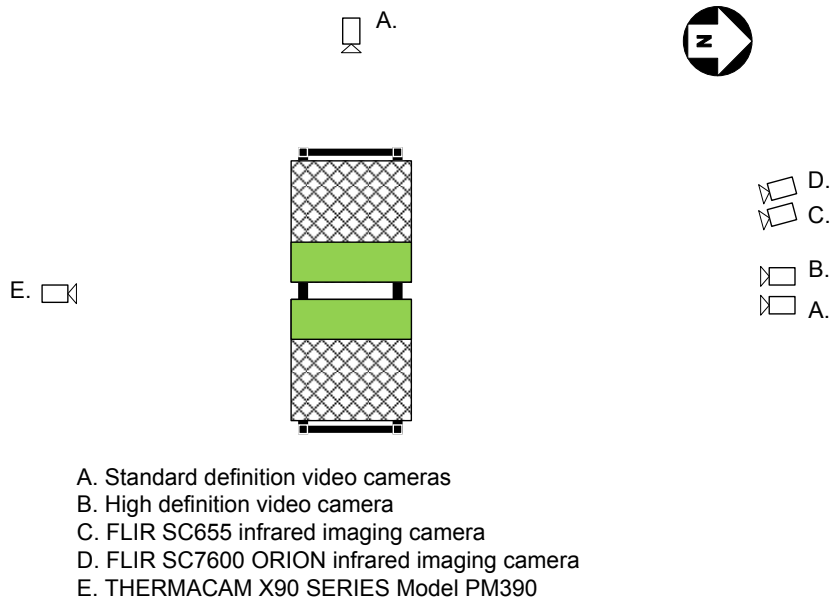

Figure 4-19: Plan view schematic of camera locations (not to scale)

4.4.1 Additional Contracted Measurements

Standard FM Global measurements within the exhaust duct were supplemented by an outside contractor, Air Pollution Characterization and Control, Ltd. (APCC), retained by Woodard and Curran. Full details of the measurements and instrumentation are reported in Reference 22.
Real-time measurements included the following species categories:

- Criteria Pollutants
- Hazardous Air Pollutants (HAPs)
- Volatile organic compound (VOC)
- Exhaust temperature and volumetric flow rates

APCC listed the primary target compounds included in the above species categories as methane, ketones, alcohols (C_xH_xOH), toluene (C_7H_8), benzene (C_6H_6), carbon monoxide (CO), carbon dioxide (CO_2), acrolein (C_3H_4O), formaldehyde (HCHO), other volatile organic compounds

(VOC), ammonia (NH_3), hydrogen chloride (CHl), hydrogen fluoride (HF), hydrogen bromide (HBr), nitrogen oxide (NO), nitrogen dioxide (NO_2) and total hydrocarbons (THC).

4.5 PREDICTION OF SPRINKLER OPERATION TIME

The primary evaluation for this project is a comparison of the predicted sprinkler operation time during a free-burn fire test to the time of battery involvement in the fire. A theoretical method to calculate the response time of sprinkler links to rack storage fires was developed by Kung, Spaulding, and You [23]. This method is used to predict sprinkler operation time for fire testing under a FPC. A brief outline of the method is given below.

The thermal response of sprinkler links can be found from a simple balance between convective heat transfer to the link and heat stored in the link for cases when thermal radiation can be neglected. The governing equation can be expressed as [24,25]

$$\frac{dT_s}{dt} = \frac{v^{1/2}(T - T_s)}{RTI}$$

where T_s is the temperature of the simulated link, T is the ceiling gas temperature, v is the gas velocity, and RTI is the thermal response index of the simulated link. To determine the link temperature, both the gas temperature and velocity under the ceiling are required. For testing under the 5-MW FPC, where no ceiling is present, these values can be estimated using well-known plume laws for plume centerline excess gas temperature [26,27], ΔT_c, and centerline velocity, v_c:

$$\frac{\Delta T_c}{T_a} = A g^{-1/3}\left(c_p \rho_a T_a\right)^{-2/3} Q_c^{2/3}(z - z_o)^{-5/3}$$

$$v_c = B g^{1/3}\left(c_p \rho_a T_a\right)^{-1/3} Q_c^{1/3}(z - z_o)^{-1/3}$$

Here, c_p is the specific heat of the plume gases, T_a and ρ_a are ambient temperature and density, z is the plume height above the top surface of the fuel array, and z_o is the virtual origin location relative to the top surface. The constants A and B have values of 11 and 4.25, respectively. The

convective heat release rate, $Q_{c,}$ is calculated from the gas temperature and mass flow through the 5-MW FPC as

$$\dot{Q}_c = \frac{\dot{m}_{gas}\left[(1.0008 + 2.3y_w)(T - T_\infty) + 6.674^{-5}(T^2 - T_\infty^2) + 2589.9\left(\frac{1}{T} - \frac{1}{T_\infty}\right)\right]}{1 + y_w}$$

where, $\dot{m}_{gas}$ is the mass flow entering the duct in kg/s. y_w is the humidity ratio, *i.e.*, mass of water / mass of air, and all temperatures are entered in K. The convective heat release rate, $Q_{c,}$ is given in kW.

For a three- and four-tier-high storage array, the virtual origin correlates with the convective heat release as [23]

$$z_o = -2.4 + 0.095\dot{Q}_c^{2/5},$$

where z_o is in m and Q_c must be entered in kW.

Using the above equations, the link temperature during a fire test under the 5-MW FPC was calculated for two generic sprinkler types: quick-response {RTI = 50 (ft-s)$^{1/2}$ [28 (m·s)½]}, and standard-response {RTI = 300 (ft-s)$^{1/2}$ [170 (m·s)½]}. Link operation is then predicted as the time after ignition at which the link reaches a specified value, *i.e.,* 74^{o}C (165^{o}F) for this project.

It should be noted that this method does not account for the contribution to the initial fire growth from the ignition source. The ignition source used in this project was detailed in Section 4.3.8. Different ignition parameters, such as fire size and location, can impact the incipient fire growth phase and thus the sprinkler operation time predictions. Therefore, the sprinkler predictions solely provide a comparative analysis and should not be applied to different test configurations.

4.6 TEST RESULTS AND DATA ANALYSIS

This section presents the results of the reduced-commodity fire tests conducted to compare the flammability characteristics of FM Global standard commodities and representative Li-ion batteries. A summary of the test setup for each commodity has been shown in Section 4.3. Each

test was conducted in a 2 x 1 x 3 high pallet load rack storage arrangement under the 5-MW FPC. A complete analysis of each test can be found in Appendix A.

Tests 1 – 3 were conducted to validate the instrumentation setup and the results are not included in this report. Tests 4 – 6 and Test 10 were conducted with FM Global standard class 2 commodity, detailed in Section 4.3.1. Tests 7 – 9 were conducted with FM Global standard cartoned unexpanded plastic (CUP) commodity, detailed in Section 4.3.1. Tests 11 – 13 were conducted with Li-ion battery commodities, detailed in Sections 4.3.2 through 4.3.4.

Table 4-6: Overview of reduced-commodity test setup

Test [#]	Commodity
1 – 3	Instrumentation setup
4 – 6; 10	Class 2
7 - 9	CUP
11	Li-ion Cylindrical Cells
12	Li-ion Power Tool Packs
13	Li-ion Polymer Cells

4.7 PERIOD OF FLAMMABILITY CHARACTERIZATION

The test design for this project consisted of a reduced amount of commodity on each pallet of a rack storage array, as discussed in Section 4.3. Comparison of the flammability characteristics between commodities should only occur during the period where fire damage was contained within the commodity of interest. Once the fire reaches the extent of the combustible commodity the results can no longer be used to evaluate sprinkler response, since further fire propagation is not possible.

It is important to note that additional information regarding the overall fire hazard of each commodity can be obtained after the period of flammability characterization. Evaluation of the time of significant battery involvement in the fire and the overall fire hazard from the quantity of commodity in each test are discussed in Section 4.8.

The four monitoring techniques for fire propagation are:

- Standard video cameras to monitor the location of flame attachment (Section 4.7.1).
- Infrared imaging cameras to monitor external heating of the commodity (Section 4.7.2).
- Thermocouples attached to the commodity-metal liner interface to monitor internal heating of the commodity (Section 4.7.3).
- Product collapse due to fire damage (Section 4.7.4).

Table 4-7 presents an overview of the period of flammability characterization based on the monitoring techniques. The analysis method for each technique is described in Sections 4.7.1 through 4.7.4, using the Li-ion polymer cell test as an example. Based on the compiled techniques, the period of flammability characterization for each test should extend to nominally 75 ± 5 s after ignition, *i.e.,* the midpoint between 60 s and 90 s after ignition.

Table 4-7: Period of flammability characterization using all indicators. Data presented as time (s) after ignition.

Commodity	Flame Attachment	External Heating	Internal Heating	Product Collapse
Class 2	60 - 90	60 - 90	n/a	none
CUP	60 - 90	60 - 90	160	none
Li-ion Cylindrical Cells	60 - 90	60 - 90	310	497
Li-ion Power Tool Packs	60 - 90	60 - 90	120	94
Li-ion Polymer Cells	60 - 90	60 - 90	315	540

4.7.1 Flame Attachment (Standard Video Recording)

Video cameras provided a convenient means of establishing the location of attached flames on the combustible surfaces of the test array. Each test was recorded with video cameras angled perpendicular and parallel to the face of the array, as detailed in Section 4.4.

Figure 4-20 presents an example of images from the video camera angled perpendicular to the commodity face at 30, 60, and 90 s after ignition of the Li-ion polymer cell test. Here it can be seen that at 30 s the fire is contained within the ignition flue, with flames extending approximately 1.0 m (3 ft) above the array. At 60 s the flames have spread underneath about one-third of the pallet width on the third tier and flames have attached to the outer face of the product cartons. By 90 s the cartoned material on the third tier is fully involved in the fire, indicating additional flame propagation would have occurred if more combustible material was present. Based on this visual observation, the period of flammability characterization for this test should extend to 75 ± 5 s after ignition, *i.e.,* the midpoint between 60 and 90 s after ignition. Similar images for all tests can be found in Appendix A.

30 s **60 s** **90 s**

Figure 4-20: Images of Li-ion polymer cells test (Test 13) in 30 s increments from ignition

4.7.2 External Heating of Commodity (Infrared Imaging)

External heating of the commodity during each test was monitored via infrared thermography. Infrared images were acquired using an FLIR® SC655 long-wave infrared (LWIR) camera; a FLIR® SC7600 ORION mid-wave infrared (MWIR) camera; and a THERMACAM X90 SERIES model PM390 camera. Each camera is described in more detail in Section 4.4. All IR images presented in this report were taken by the SC655 LWIR camera. This work is also the subject of a paper by de Vries and Ditch discussing the potential for increased utilization of IR imaging during large fire tests [28].

Each IR image taken by the SC655 LWIR camera and visual image taken by the HD camera was corrected for perspective distortion. An example of a perspective corrected image is shown in Figure 4-21. In addition, each IR frame was registered onto a visible frame taken by the HD camera. Image registration seeks to align (fuse) two images taken of the same scene, *i.e.*, registration is the determination of a geometrical transformation that aligns points in one view of an object with corresponding points in another view of that object or another object. In this way, the infrared information can enhance the visual images, adding contrast and temperature information; an example of this is shown in Figure 4-21. The ability of the LWIR camera to see through dense layers of smoke and steam is shown in Figure 4-22.

Selected perspective corrected and registered IR images taken from Tests 5, 9, 11, 12, and 13 are shown in Figure 4-24 through Figure 4-28 A color legend showing the corresponding temperatures is shown to the right of each image. Flue temperatures in excess of 1,000ºC (1,832ºF) were measured for all Li-ion tests as well as the CUP test. For the standard class 2 commodity, the maximum flue temperatures did not exceed 875ºC (1,607ºF). Temperatures shown are only valid for the corrugated material, which has an emissivity of approximately 0.9 for a typical fire radiation spectral range.

Figure 4-24 shows registered IR images taken with the SC655 camera without the aperture in front of the lens. Some saturation of the focal plane array (FPA) is clearly visible in Fig. 4.24(b), depicted in purple color inside the central flue. After placing the aperture in front of the lens, the temperature range was increased, allowing temperatures up to 1,200ºC (2,192ºF). All other tests

were performed with the aperture placed in front of the lens at the time of ignition. The IR images show clearly how the fire spreads from the flue outwards. During each test the fire would spread over the third tier first, after which the commodity in the second tier would follow.

The IR images are a useful tool to approximate the potential for lateral flame spread along the face of the corrugated cartons. For the purpose of this analysis, flame propagation is assumed at temperatures exceeding 400°C (750°F), which relates to the critical heat flux for corrugated paper of 10 kW/m^2 [20] as:

$$\dot{q}'' = \varepsilon\sigma\left(T_f^4 - T_\infty^4\right)$$

where, *q"* is the heat flux in kW/m^2, σ is the Stefan-Boltzmann constant with the value of 5.67 x 10^{-11} kW/m^2 K^4, T_f is the steady-state temperature of the emitting surface in K, T_∞ is the ambient room temperature in K, and the emissivity (ε) should be set to 0.9 for consistency with the corrugated material.

Figure 4-28 shows registered IR images for the Li-ion polymer cell test; at 60 s the corrugated cartons have an average temperature of 300°C (570°F) indicating the cartons are not burning, while at 90 s temperatures exceeding 400°C (750°F) were recorded. Based on these measurements, the period of flammability characterization for this test should extend to nominally 75 s after ignition, *i.e.,* the midpoint between 60 and 90 s after ignition. Similar results were seen for the FM Global standard commodities and remaining Li-ion battery products.

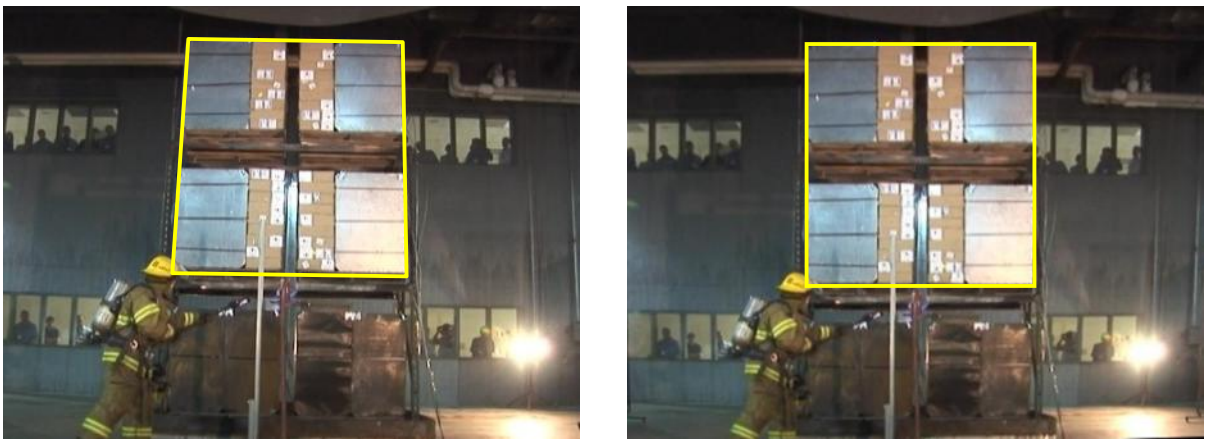

(a) (b)

Figure 4-21: Example of perspective correction. (a) Uncorrected image and (b) image after correction

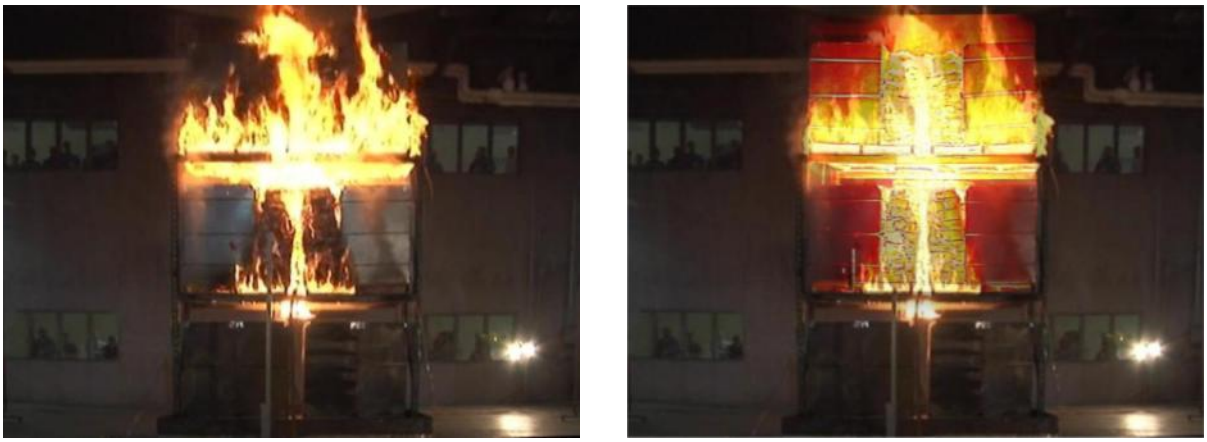

(a) (b)

Figure 4-22: Example of IR image registration. (a) Visual image and (b) IR image registered on the top two tiers

(a) (b)

Figure 4-23: Example of the LWIR camera's ability to see through smoke and steam. (a) Visual image and (b) IR image registered on the top two tiers

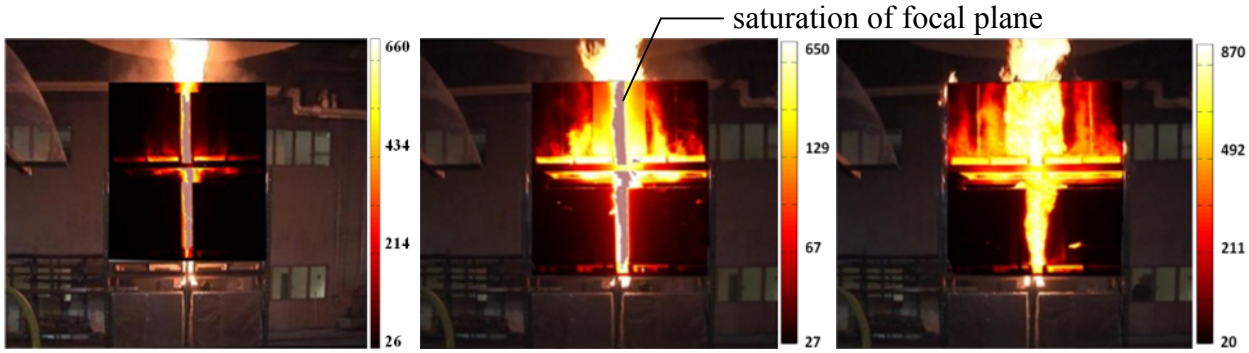

Figure 4-24: Registered images for Class 2 commodity - Test 5

Figure 4-25: Registered images from CUP commodity - Test 9

Figure 4-26: Registered images from Li-ion cylindrical cells - Test 11

60 s **90 s** **480 s**

Figure 4-27: Registered images from Li-ion power tool packs - Test 12

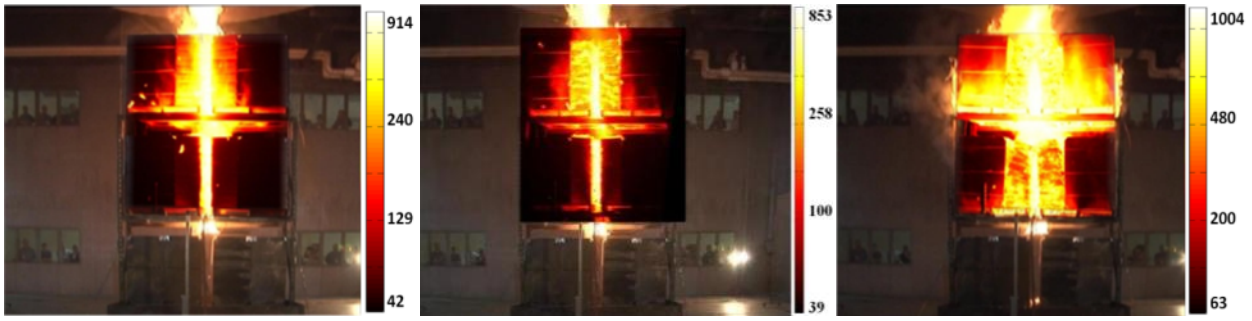

60 s **90 s** **480**

Figure 4-28: Registered images from Li-ion polymer cells - Test 13

4.7.3 Internal Heating of Commodity (Thermocouples)

Internal heating of the commodity was measured with thermocouples located at the interface between the metal liners and the test commodity. As detailed in Section 4.4, these thermocouples are referenced by their location within the array based on tier (T2 for tier 2 or T3 for tier 3), pallet location within the array (east or west) and elevation (low = 0.36 m above pallet or high = 0.72 m above pallet). It is important to note that the backside of the thermocouples was not insulated; therefore, the measurements reflect both conduction through the test commodity and heating from the air within the metal liners.

Figure 4-29 presents an example of the temperature measurements acquired during the Li-ion polymer cell test. The convective heat release rate is included for reference to the time evolvement of the fire. The threshold temperature of 180°C (356°F) was added based on the oxidation temperature of electrolyte that results in a high-rate runaway reaction (peak rates >

100°C/min) [29]. For this test, the threshold temperature was first exceeded by the thermocouple located on tier 3, east commodity, high elevation (T3EH) at 315 s after ignition.

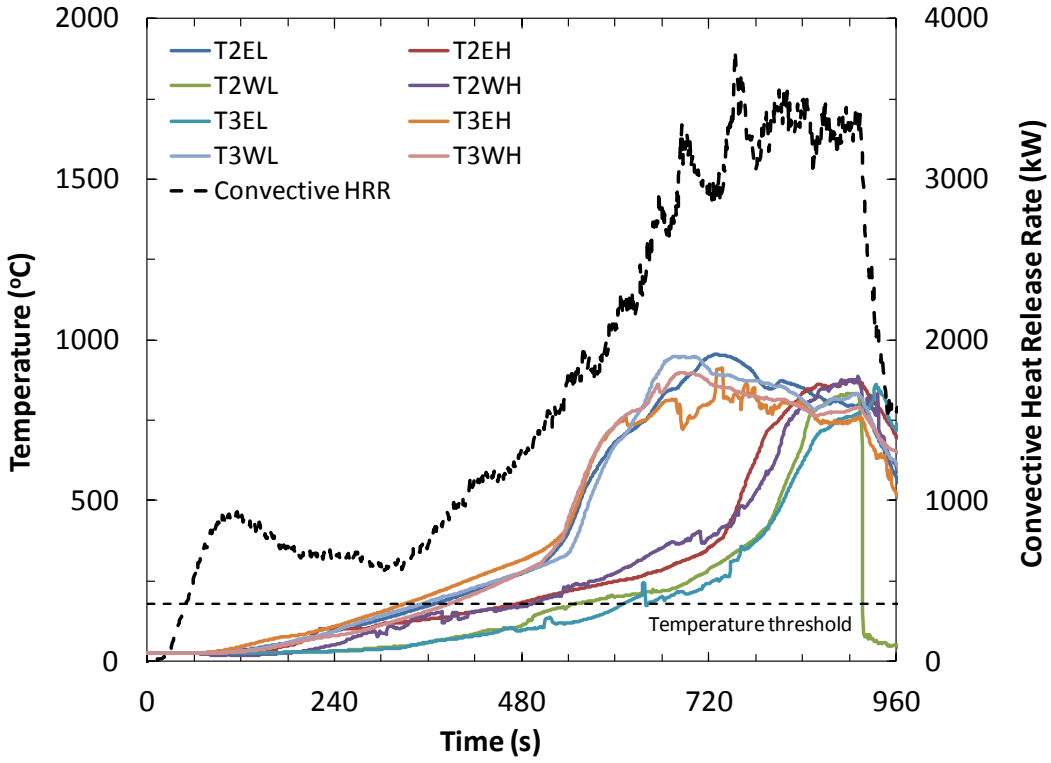

Figure 4-29: Internal heating of commodity using thermocouples at the interface of the metal liner and test commodity during Li-ion polymer cell test (Test 13)

4.7.4 Commodity Collapse

Collapse of commodity due to fire damage is common in all rack storage tests and does not impact the validity of the test. However, for the reduced-commodity array design used in this project, collapse can significantly impact the fire development because the non-combustible portion of the commodity may be exposed. It was assumed that major collapse, visually estimated as greater than 10% of the overall quantity of Li-ion batteries, in a test was sufficient to impact the fire development. All other commodity collapse was considered minor.

The time of product collapse for each Li-ion battery was as follows:

- Li-ion cylindrical cells: Minor collapse of commodity on the third tier occurred at 248 s after ignition followed by a major collapse at 497 s. Based on these observations, collapse impacting the fire development occurred by 497 s after ignition.
- Li-ion power tool packs: Sporadic collapse of individual power packs occurred from 64 s to 94 s after ignition. In total, 19 power tool packs were observed to collapse during this timeframe. A more significant collapse occurred at 105 s. Based on these observations, collapse impacting the fire development occurred by 94 s after ignition.
- Li-ion polymer cells: Minor collapse of commodity on the third tier occurred at 515 s after ignition followed by a major collapse at 540 s. Based on these observations, collapse impacting the fire development occurred by 540 s after ignition.

The FM Global standard commodities did not exhibit collapse before termination of the fire test and are therefore not discussed here. Complete chronologies for each test based on visual and audible observations can be found in Appendix A.4.

4.8 HEAT RELEASE RATE (HRR)

The convective heat release rates for each commodity are shown in Figure 4-30. To simplify the comparison, the time of each test has been slightly offset to align the initial fire growth period. Each commodity exhibits a similar initial fire growth as the flames spread vertically along the corrugated board cartons that line the fuel space above ignition. A close-up of the convective heat release rates is provided in Figure 4-31 to highlight the change in fire development that occurs once the cartons are breached and the contents become involved. The commodities are grouped based on their composition where the left figure shows CUP and power tool packs and the right figure shows class 2, cylindrical cells, and polymer cells. The former commodities are comprised of significant quantities of plastics, while the latter are comprised of minimal plastics. Appendix A contains a photographic time evolution of each test.

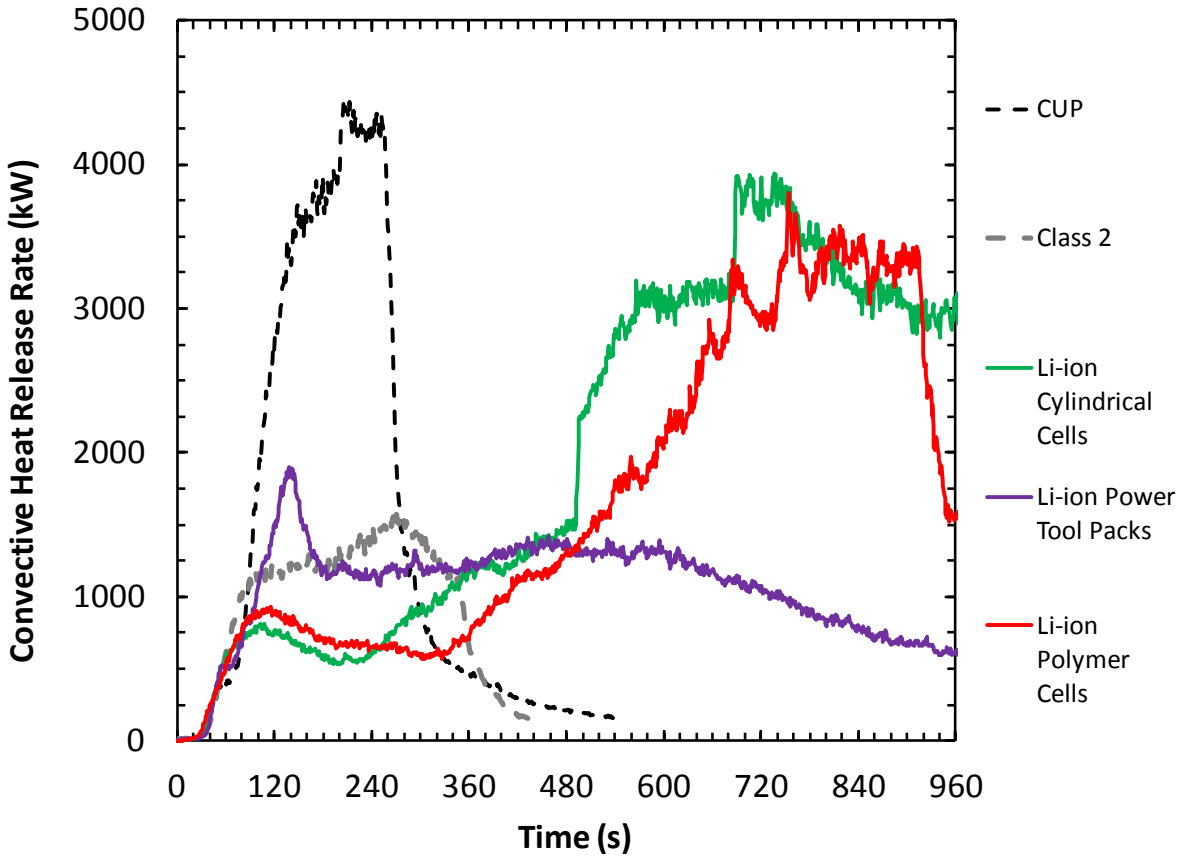

Figure 4-30: Convective heat release rates for FM Global standard commodities and Li-ion battery commodities

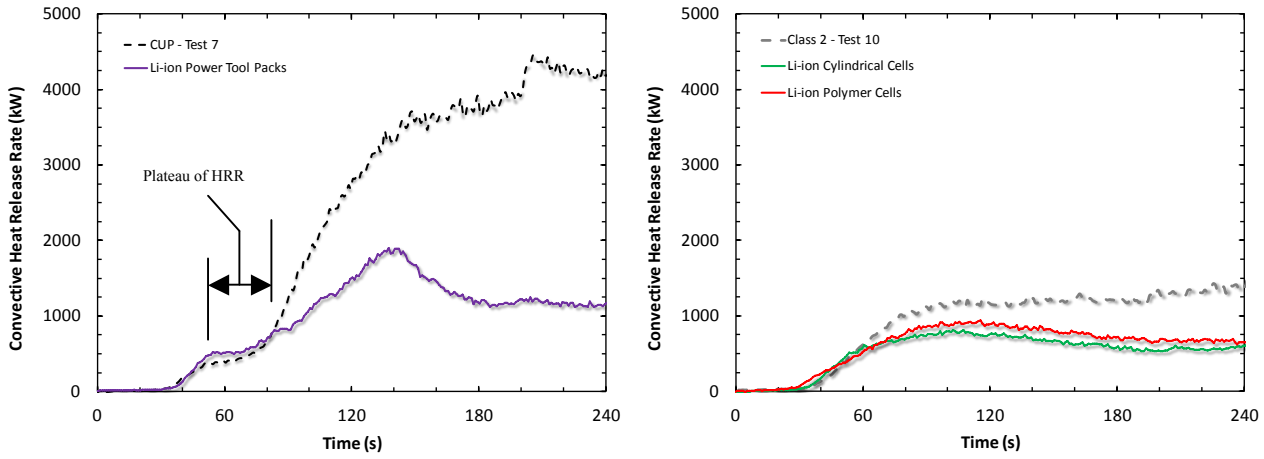

Figure 4-31: Close-up of convective heat release rates for FM Global standard commodities and Li-ion battery commodities; grouping based on similarity in growth curve

The fire development for each commodity after the initial vertical fire spread along the cartons is as follows:

In the case of class 2 commodity*, the fire reached a nominal steady-state value of 1,250 kW at 120 s as the majority of combustible surfaces, *i.e.*, corrugated board cartons and wood pallets, became involved in the fire. The corrugated cartons were then consumed leaving only the wood pallets, which continued to burn until the test was manually terminated at 360 s.

For CUP commodity*, a delay in the fire growth occurred at 50 s as the flames penetrated the cartons and the plastic cups stored within became involved in the fire. This delay was observed as a temporary plateau in the heat release curve from 50 s to 75 s. The plastics then became significantly involved starting at 75 s, and the fire grew to a nominal steady-state value of about 4,000 kW at 190 s. The fire was manually terminated at 250 s.

Li-ion cylindrical cells exhibited an initial fire development similar to that of the class 2 commodity until 110 s when the fire size began to decline due to consumption of the cartoned material. The fire size steadily declined until 200 s when the wood pallets and Li-ion cells became significantly involved and the fire reached a maximum of about 3,900 kW at 690 s. The jumps in fire size at 490 s and 685 s were a result of product collapse. Manual fire suppression began at 1,019 s and was not included in the graph.

Li-ion power tool packs exhibited a fire development trend similar to the CUP commodity. A delay in fire growth occurred at 55 s as the flames penetrated the cartons and the plastic components of the battery packs became involved in the fire. This delay was observed as a temporary plateau in the heat release curve from 55 s to 75 s. The fire then grew steadily from 75 s to 137 s until a maximum value of 1,900 kW was reached. The fire then decreased to nominal steady-state value of 1,250 kW at 180 s as the power tool packs were consumed, leaving only the wood pallets. The fire then remained steady

* Here class 2 commodity is represented by Test 10 and CUP commodity is represented by Test 7.

until 600 s when the fire size slowly tapered off as the combustibles were consumed. It is important to note that the power packs began sporadically falling off the array at 64 s, with an estimated 20 packs falling over a 30 s period, and a larger collapse occurring at 105 s. It is not expected that these collapses significantly affected the fire growth before about 90 s after ignition due to the small percentage of the overall packs having collapsed. Manual fire suppression began at 2,750 s and was not included in the graph.

The Li-ion polymer cells exhibited an initial fire development similar to that of the class 2 commodity until 110 s when the fire size began to decline due to consumption of the cartoned material. The fire size steadily declined until 305 s when the wood pallets and Li-ion cells became significantly involved and the fire reached a maximum of 3,800 kW at 750 s. A minor product collapse occurred at 515 s followed by a major collapse at 540 s. Manual fire suppression began at 910 s.

These data provide several key comparison points relative to the hazard posed by each commodity. First, the agreement of the heat release rates resulting from the initial vertical fire spread supports the assumption that cartoned commodities exhibit similar fire development for three-tier high rack storage. Subsequent breach of the cartons highlights the impact of the stored contents. For cartons containing significant quantities of loosely packed plastics (*i.e.,* CUP and power tool packs), involvement of the plastic results in a rapid increase in the released energy early in the fire development. For cartons containing densely packed Li-ion batteries and minimal plastics (*i.e.,* Li-ion cylindrical and polymer cells), the fire growth is delayed several minutes until the batteries become significantly involved. Cartons containing noncombustibles (*i.e.*, class 2) exhibit no rapid increase in fire size after the initial vertical fire growth along the cartoned packaging.

4.9 TIME OF BATTERY INVOLVEMENT

For the purposes of this report, significant battery involvement was qualitatively assessed based on visual observations of the fire and a simultaneous increase in the convective heat release rate beyond a threshold value. Specific details of the fire development used for this analysis are discussed in Section 4.8 and photographs are included in Appendix A.

Each rack storage test was conducted with a reduced quantity of commodity supported on a standard-sized wood pallet. During the class 2 commodity and Li-ion power tool pack tests, the majority of the test commodity was consumed during the initial fire growth. The subsequent nominal steady-state HRR of 1,250 kW was a result of combustion of the wood pallets on the second and third tier (1,250 kW / 4 pallets = 312.5 kW/pallet)*. Since the contribution from the wood pallets should be the same for all tests, it is reasonable to attribute any increase in the heat release rate to combustion of the Li-ion batteries. Therefore, 1,250 kW represents the upper threshold value (after the initial fire growth) corresponding to the latest time in the fire development where the batteries are not contributing to the overall fire severity. As shown in Figure 4-32, the convective HRR for Li-ion cylindrical cells and polymer cells exceeded 1,250 kW (upper horizontal dashed line) at 385 s and 470 s, respectively. No estimate can be made for the power tool packs due to the added combustible load related to the plastic components.

The time of battery involvement can also be estimated at an earlier stage in the fire development. During the Li-ion cylindrical cell and polymer cell tests, after the initial vertical flame spread along the cartoned packaging, the convective HRR steadily decreased to a nominal minimum value of 600 kW at 200 s and 305 s, respectively. Visual observations show the wood pallets on the 3rd tier (*i.e.,* two pallets) were the predominant combustible involved in the fire, which is consistent with the 312.5 kW per pallet estimate established from the class 2 commodity and Li-ion power tool pack tests. The fire size then steadily increased to the upper threshold value of 1,250 kW; however, in both tests, the wood pallets on the second tier were only partially involved in the fire, suggesting involvement of the Li-ion batteries. The exact contribution from the wood pallets and batteries to the fire severity cannot be further differentiated. Therefore, 625 kW represents the lower threshold HRR (after the initial fire growth) corresponding to the earliest time in the fire development where the batteries are contributing to the overall fire severity.

* The energy released per pallet is consistent with a previous internal study that indicated the steady-state convective heat release rate for a wood pallet ranges between 250 kW to 300 kW in a rack storage array.

Using the upper and lower threshold values, involvement of the Li-ion cylindrical cells occurred between 240 s and 385 s and involvement of the Li-ion polymer cells occurred between 305 s and 470 s. Taking the average of these values and rounding down to the nearest minute results in a nominal time of battery involvement of 300 s after ignition, under free-burn fire conditions.

The upper and lower threshold values indicating Li-ion battery contribution to the fire severity are applicable only to the tests configuration used in this project. A more quantitative analysis was not conducted because the flammable components of Li-ion batteries, *i.e.*, electrolyte and plastics, are organic and not easily distinguishable from other combustible materials present in the packaging in a bulk storage fire scenario, through diagnostics of the product stream. Several possible analysis methods included review of the THC generation rates and the ratio of CO_2 generation to O_2 depletion rate, and the time evolution of flame temperatures recorded by the SC655 infrared imaging camera.

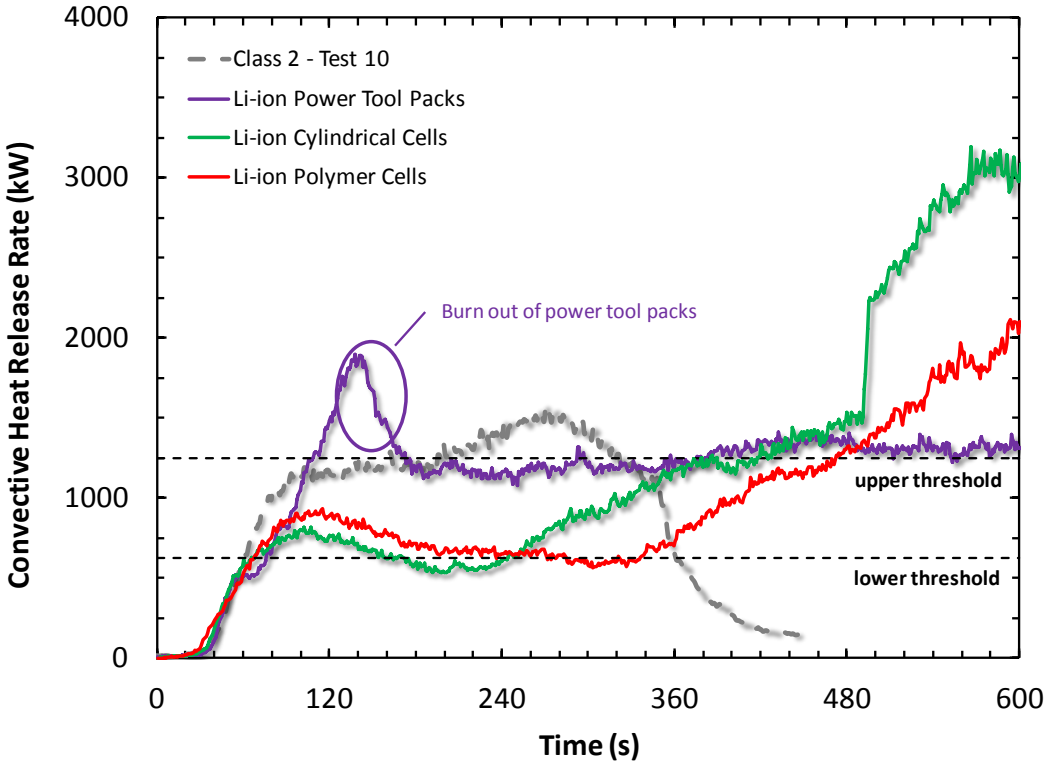

Figure 4-32: Convective HRR for Class 2 commodity and Li-ion battery commodities (subset of data presented in Section 4.8)

4.10 PREDICTED SPRINKLER RESPONSE

All sprinkler responses were calculated using the method described in Section 4.5. Figure 4-33 presents an example of the predicted response of a quick-response sprinkler link during the Li-ion polymer cell test. In this example the ceiling height is set to 3.0 m (10 ft) above the array (*i.e.,* 4.6 m (25 ft) above the floor), which results in a predicted operation time of 41 s after ignition for a 74°C (165°F) rated link. The corresponding convective fire size at link operation, $\dot{Q}_{be}$, was 256 kW and the fire was growing at a rate of 16 kW/s. As previously discussed, the fire growth rate is calculated as a 10 s linear trend of the convective fire size just before link operation.

The reader is reminded that all fire size estimates included in this report include the contribution from the propane ring burner ignition source, which was constant for the test duration.

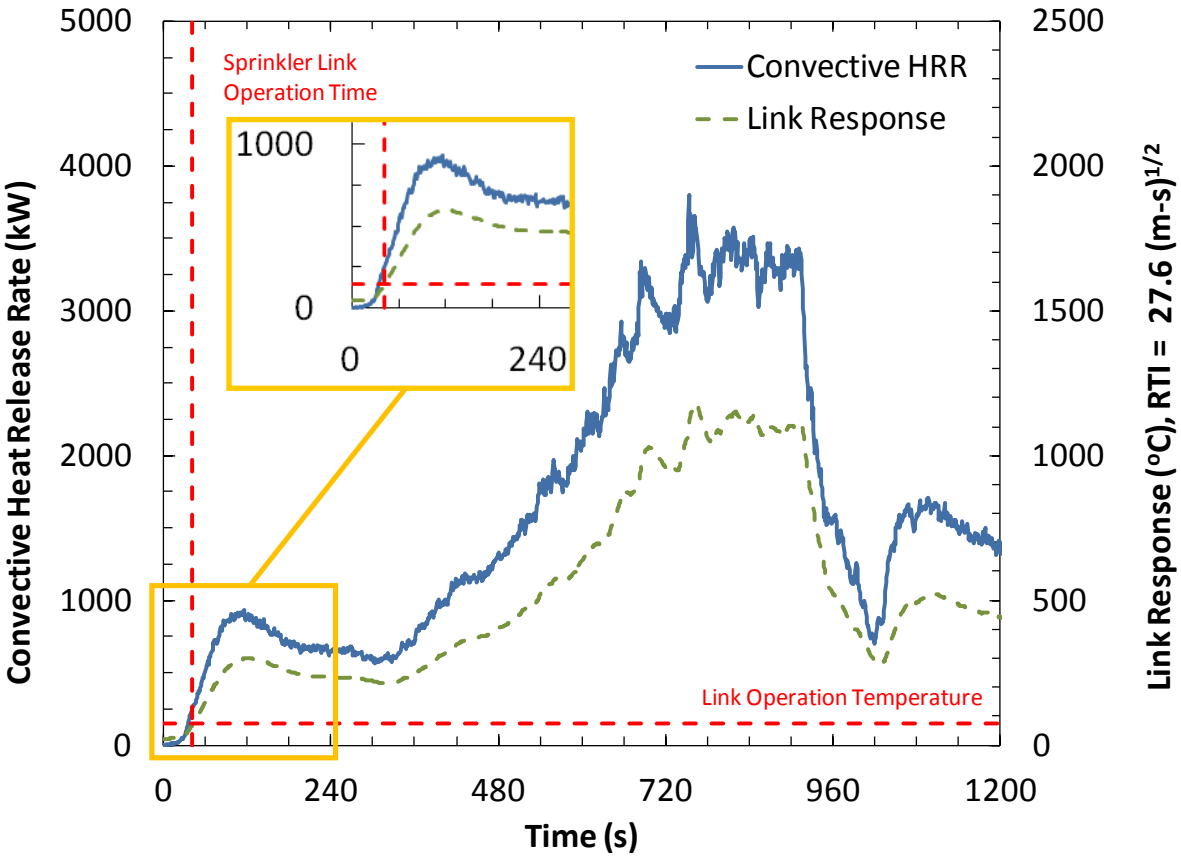

Figure 4-33: Example of sprinkler link response during Li-ion polymer cell test; quick-response sprinkler with a 74°C temperature rating below a 3.0 m ceiling

Table 4-8 and Table 4-9 contain complete sprinkler response calculations for quick-response and standard-response sprinklers, respectively. Calculations were made for ceiling heights of 7.6 m and 9.1 m (25 ft and 30 ft). For reference, Figure 4-34 also illustrates the link operation time versus corresponding fire size for each test condition. Testing with class 2 and CUP commodity were conducted several times to assess repeatability with overall excellent agreement. Additional discussion can be found in Section 6.1.

Table 4-8 presents the predicted quick-response link operation times for all commodities included in this project, assuming a 7.6 m and 9.1 m (25 ft and 30 ft) ceiling height. For a 7.6 m (25 ft) ceiling, the link reached the predetermined operation temperature of 74°C (165°F) between 41 s and 59 s after ignition. It is reasonable to assume that the difference in link operation time is a result of a delay in the incipient phase of the fire as the cartoned commodity becomes involved. The corresponding convective fire sizes at link operation, $\dot{Q}_{be}$, show good agreement for all commodities with a range of 209 kW to 284 kW. The fire growth rates at link operation also agree well with a range of 15 kW/s to 25 kW/s. Similar agreement in the predicted link operation time and fire growth characteristics was seen for a 9.1 m (30 ft) ceiling, except for the Li-ion power tool packs. For this ceiling height, not including the Li-ion power tool packs, the link operation time ranged from 52 s to 77 s, $\dot{Q}_{be}$ ranged from 321 kW to 405 kW, and the fire growth rates ranged from 11 kW/s to 24 kW/s. The general agreement of the fire growth characteristics supports the assumption that cartoned commodities exhibit similar fire development leading to first sprinkler operation for a three-tier-high open-frame rack storage arrangement[*].

The predicted link operation time of 87 s for Li-ion power tool packs assuming a quick-response sprinkler under a 9.1 m (30 ft) ceiling occurred after the flammability characterization period of 75 ± 5 s. Therefore, the array did not contain sufficient test commodity for this evaluation.

Table 4-9 presents the predicted standard-response link operation times for all commodities included in this project, assuming a 7.6 m and 9.1 m (25 ft and 30 ft) ceiling height. For a 7.6 m

[*] Provided the carton material has similar flammability characteristics, *e.g.*, TRP and ignition propensity

(25 ft) ceiling, the link operation times and corresponding convective fire sizes, $\dot{Q}_{be}$, agree well with ranges of 62 s to 77 s and 431 kW to 603 kW, respectively. The fire growth rates exhibit larger variation with a range of -1 kW/s to 22 kW/s; however, the lower growth rates of CUP and Li-ion power tool packs, 7 kW/s and -1 kW/s, respectively, can be explained by review of Figure 4-31. The link operations occur as the fire transitions from the outer carton to the stored plastic, which was observed as a temporary plateau in the heat release curve. The impact of the fire growth rate variation is expected to be minimal due to the agreement of the $\dot{Q}_{be}$ values, indicating a similar fire hazard present at link operation for all commodities in these tests. For a 9.1 m (30 ft) ceiling, the standard-response sprinkler link operations range from 86 s to 256 s, which are beyond the flammability characterization period of the test, *i.e.*, the fire reached the extent of the commodity. Therefore, the array did not contain a sufficient quantity of test commodity to evaluate the performance of standard-response sprinklers under a 9.1 m (30 ft) ceiling.

Table 4-8: Predicted quick-response sprinkler link operation time and corresponding fire growth characteristics for a 7.6 and 9.1 m ceiling. Link temperature rating of 74°C (165°F).

Ceiling Height	7.6 m (25 ft)			9.1 m (30 ft)		
Commodity	Link Operation (s)	Q_{be} (kW)	Fire Growth (kW/s)	Link Operation (s)	Q_{be} (kW)	Fire Growth (kW/s)
Class 2*	59	209	15	65	367	24
CUP+	43	232	16	52	321	11
Li-ion Cylindrical Cells	44	284	23	76	405	23
Li-ion Power Tool Packs	51	282	25	87	426	29
Li-ion Polymer Cells	41	256	16	77	370	13

*Average values for Tests 4 – 6, 10
+Average values for Tests 7 – 9

Table 4-9: Predicted standard-response sprinkler link operation time and corresponding fire growth characteristics for a 7.6 and 9.1 m ceiling. Link temperature rating of 74°C (165°F).

Ceiling Height	7.6 m (25 ft)			9.1 m (30 ft)		
Commodity	Link Operation (s)	Q_{be} (kW)	Fire Growth (kW/s)	Link Operation (s)	Q_{be} (kW)	Fire Growth (kW/s)
Class 2*	77	603	22	90	799	14
CUP+	70	431	7	86	818	30
Li-ion Cylindrical Cells	62	577	12	256	699	4
Li-ion Power Tool Packs	70	497	-1	125	719	16
Li-ion Polymer Cells	64	553	11	144	782	9

*Average values for Tests 4 - 6, 10
+Average values for Tests 7 - 9

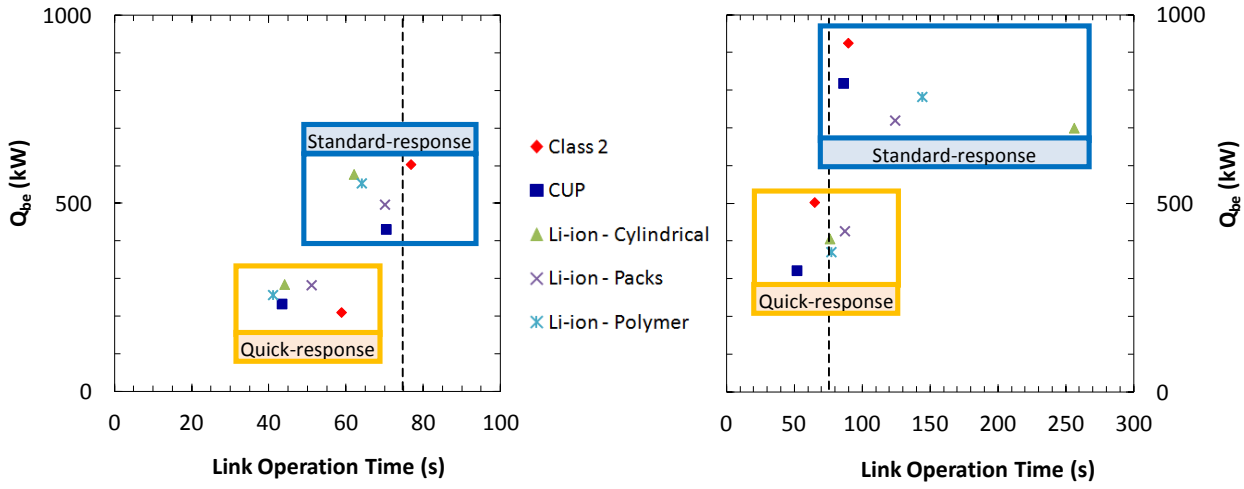

7.6 m (25 ft) ceiling **9.1 m (30 ft) ceiling**

Figure 4-34: Summary of predicted link operation times versus fire size, $\dot{Q}_{be}$, for all test conditions; vertical dashed line indicates the upper limit for the period of flammability characterization (*i.e.*, 75 ± 5 s)

4.11 AIR EMISSION RESULTS

A limited number of combustion by-products were measured by both FM Global and an outside contractor, Woodard and Curran (WC), as described in Section 4.4.1. WC data are taken directly from Reference 22. Time-resolved exhaust gas temperature and standard flow rate within the

5-MW calorimeter for the Li-ion cylindrical cell (Test 11) and power tool packs (Test 12) are shown in Figure 4-35 and Figure 4-36, respectively. Similar time-resolved concentrations of carbon dioxide and carbon monoxide are shown in Figure 4-37 and Figure 4-38. For all measurements, excellent agreement is seen between the two independent data sets. The slight deviation in the peak values between FM Global data and the WC data is attributed to differences in the measurement interval; FM Global data are one-second samples and WC data are 30-s grab samples.

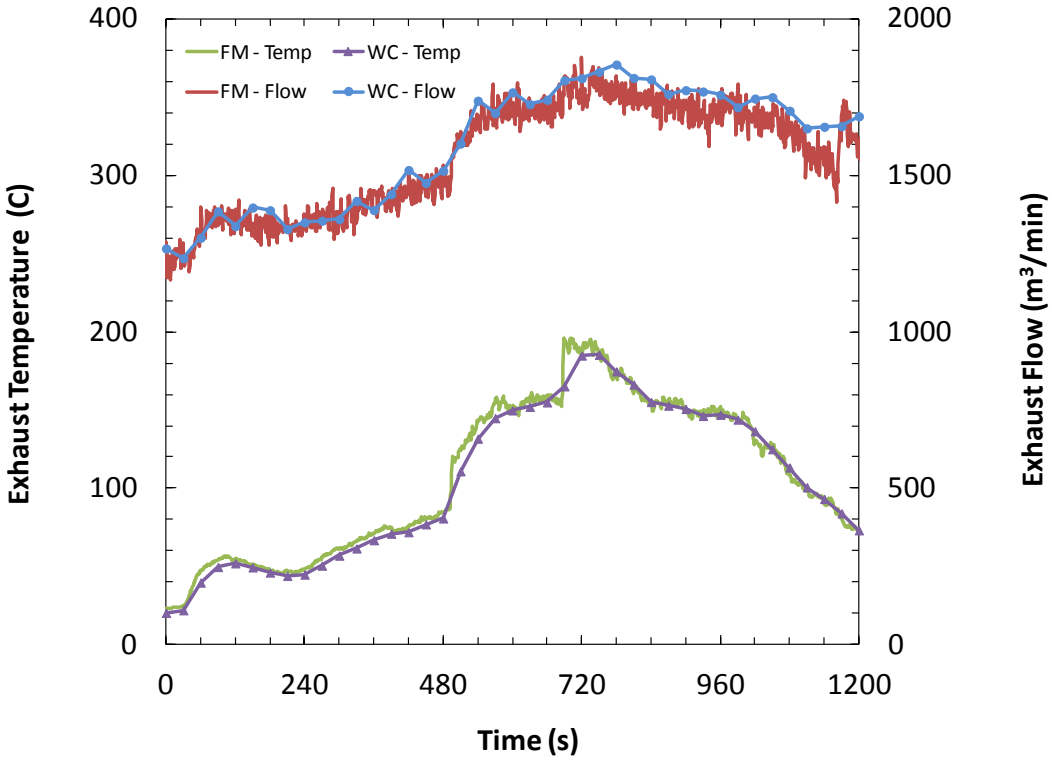

Figure 4-35: Exhaust temperature and flow for Li-ion cylindrical cells - Test 11

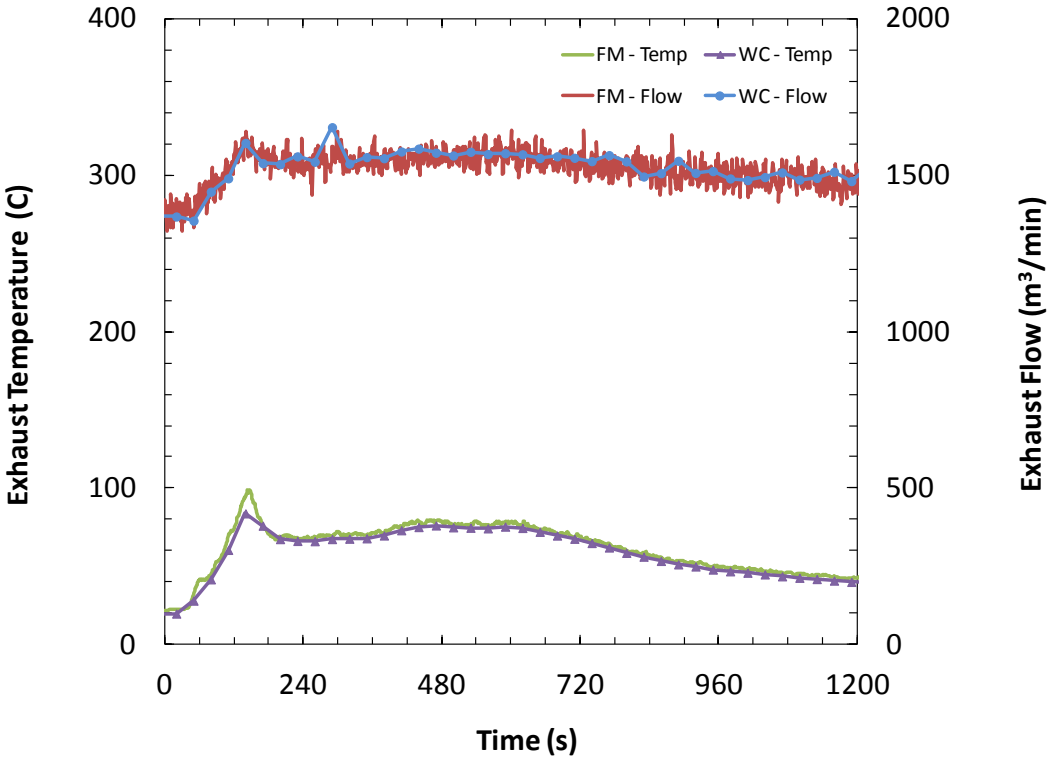

Figure 4-36: Exhaust temperature and flow for Li-ion power tool packs - Test 12

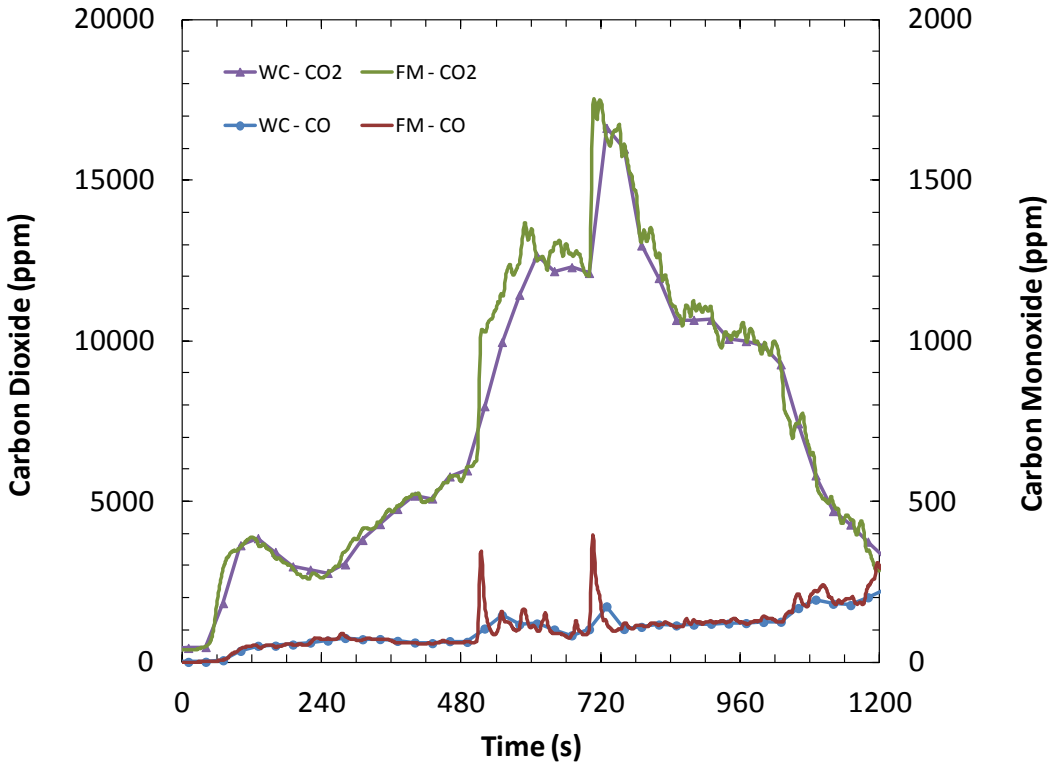

Figure 4-37: Duct concentration of CO_2 and CO for Li-ion cylindrical cells - Test 11

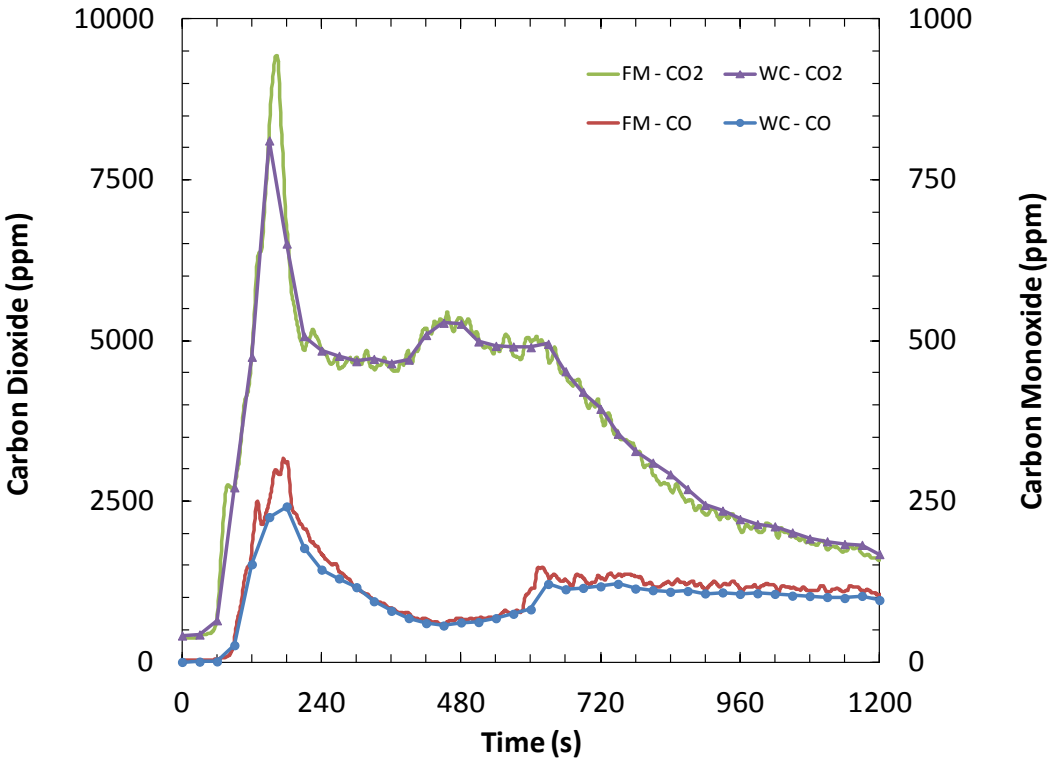

Figure 4-38: Duct concentration of CO_2 and CO for Li-ion power tool packs - Test 12

Supplemental emission testing was conducted on the exhaust gas flow by Woodard and Curran within the 5-MW exhaust duct for two of the Li-ion battery tests. The following table, labeled Table 4-10, has been extracted directly from Reference 22. In the original report the table is labeled *Table 2-1: Summary of Measured Mass Emissions* and the results are reported in pounds. Tests are referenced by date, where the test with Li-ion cylindrical cells (Test 11) was conducted on 12-Sep-12 and that with Li-ion power tool packs (Test 12) was conducted on 19-Sep-12. In addition to the mass of each species, the concentration (ppm/v) in the exhaust gas is reported for each species. Measurements were acquired in 30 s intervals and results are reported on a net basis. In total, 18 species of organic and inorganic compounds, as well as criteria pollutants, were detected during the tests. All other emission compounds not reported were below the limit of detection (Ld) for the analytical method, which ranged from 0.05 ppm to 0.5 ppm. It is important to note that in both tests minimal emissions of hydrogen fluoride gas (HF) were detected, which was a primary personnel safety concern.

For Li-ion cylindrical cells (test of 12-Sep-12), measured emissions of total hydrocarbons (THC) were 2.88 kg (6.35 lb). Of the remaining species, CO_2 and CO exhibit the highest mass emissions, distantly followed by all others at < 0.5 kg (1 lb) each for the total burn cycle. Notably, measured emission concentrations of acids (HF and HCl) were negligible. The collection period for this test extended to 46 min 30 s after ignition.

For Li-ion power tool packs (test of 19-Sep-12), overall emissions were considerably less than for the Li-ion cylindrical cells, with the exception of hydrochloric acid (HCl). Significant emissions of HCl were measured with a total mass of 1.0 kg (2.2 lbs). The measured THC emissions were 0.88 kg (1.93 lb). Of the remaining species, CO_2 and CO still exhibited the highest emission rates with total weights > 0.5 kg (1 lb). The collection period for this test extended to 59 min after ignition.

Note that an unidentifiable compound was detected at significant concentration level during the Li-ion cylindrical cell test. Subsequent qualitative analysis by FM Global has identified this compound as dimethyl carbonate ($C_2H_6O_3$). No quantitative analyses were performed. This compound has a boiling point of 90^{o}C (194^{o}F), is a non-VOC per United States Environmental Protection Agency (US EPA) and is not regulated by OSHA. Further discussion of this compound was documented in the Appendix of Reference 22.

Table 4-10: Summary of measured mass emissions for Li-ion cylindrical cell and power tool pack tests (Table 2-1 of Reference 22)

Summary of Measured Mass Emissions*
Li ion Battery Test Burns
FM Global Research Campus
12 & 19 September 2012

		Organic Compounds								
Date/Time		**Methane**	**Methanol**	**IPA**	**Acetone**	**Acrolein**	**Ethane**	**Ethylene**	**Formaldehyde**	**Acetaldehyde**
	(mw)	16	32	60.1	58.1	56	30	28	30	44
12-Sep-12 1045-1135	(ppm/v)	10.8	3.15	0.54	0.46	0.56	0.95	3.61	2.04	0.24
	(lbs**)	1.12	0.652	0.211	0.172	0.202	0.185	0.655	0.397	0.069
19-Sep-12 1325-1425	(ppm/v)	5.54	0.58	0.02	0.89	0.01	0.08	0.90	0.68	0.69
	(lbs**)	0.786	0.163	0.011	0.456	0.004	0.022	0.224	0.182	0.270

		Acids		Criteria Pollutants				Other			Exhaust	
Date/Time		**HF**	**HCL**	**NO**	**NO_2**	**CO**	**SO_2**	**CO_2**	**THC**	**N_2O**	**°F**	**SCFM**
	(mw)	20	36.5	30	46	28	64	44	(as CH_4) 16	44		
12-Sep-12 1045-1135	(ppm/v)	0.23	0.06	2.45	1.10	78.2	0.03	3,545	61.3	0.07	143	49,904
	(lbs**)	0.03	0.014	0.477	0.329	14.2	0.012	1011	6.35	0.021		
19-Sep-12 1325-1425	(ppm/v)	0.19	6.81	1.67	1.65	67.7	0.36	1,855	13.6	0.06	101	56,888
	(lbs**)	0.034	2.20	0.445	0.673	16.8	0.207	723	1.93	0.024		

* All other target constituents <Ld
** Total Mass Emissions over burn period

4.12 DISPOSAL

The disposal procedures for Li-ion batteries was developed with an outside waste management contractor. Each test was conducted within a watertight containment pan, and the use of fire suppression water was minimal. Following extinguishment, with water applied from a garden hose or fire hose, solid wastes (*e.g.,* packaging and wood pallets) were removed from the containment pan. The remaining batteries were placed in 0.21-m^3 (55-gal) non-conductive drums and covered with high-flash-point oil. The drums were filled half to three quarters of capacity

and covered with an unsecured lid. The drums were located in an outside storage array, away from combustibles, where the oil temperature was monitored until site removal by the waste management company.

Transfer of the batteries into the drums was accomplished by lab technicians wearing full firefighter turnout gear and self contained breathing apparatus (SCBA). Minimal post-test reactivity of the batteries was observed during transfer into the drums; though, slightly elevated oil temperatures and sporadic bubbles in the oil were observed for the next couple of days.

5 LARGE-SCALE FIRE TESTS

Two large-scale fire tests were conducted to evaluate the level of protection provided by a ceiling level sprinkler scheme and to validate the recommendation for Li-ion batteries in bulk storage. These tests focused on the ability of the sprinkler system to extinguish a large-scale rack-storage fire of FM Global standard CUP commodity. For protection to be considered adequate, the fire had to be nearly extinguished before the predicted time of battery involvement established for the Li-ion battery commodities in the reduced-commodity tests. In addition to the standard measurements, instrumentation was included within the test commodity and array to quantify the heating condition posed by persistent flames within the array. Acceptable performance in these tests would have greatly improved the confidence that a sprinkler system recommendation could provide effective protection for small format Li-ion batteries in bulk storage.

The test numbering sequence is continuous with the previous reduced-commodity evaluation (Tests 1 - 13); therefore the large-scale validation tests are numbered Tests 14 and 15.

5.1 LARGE BURN LABORATORY

The tests for this program were conducted under the south movable ceiling in the Large Burn Laboratory (LBL) located in the Fire Technology Laboratory at the FM Global Research Campus in West Glocester, Rhode Island, USA. Figure 5-1 is a plan view of the LBL showing the north movable ceiling, the south movable ceiling, and the 20-MW Calorimeter. The air emission control system (AECS) exhaust ducting for each movable ceiling consists of four extraction points, located at the lab ceiling, that merge into a single duct with a cross sectional area of 6.1 m^2 (66 ft^2). Gas concentration, velocity, temperature and moisture measurements are made downstream of the manifold. Beyond the measurement location, the exhaust duct connects to a wet electrostatic precipitator (WESP) prior to the gases venting to the atmosphere. The movable ceilings measure 24.4 m x 24.4 m (80 ft x 80 ft) and are adjustable for heights above the floor ranging from 3.1 m to 18.3 m (10 ft to 60 ft). All tests were conducted at an exhaust rate of 94 m^3/s (200,000 ft^3/min).

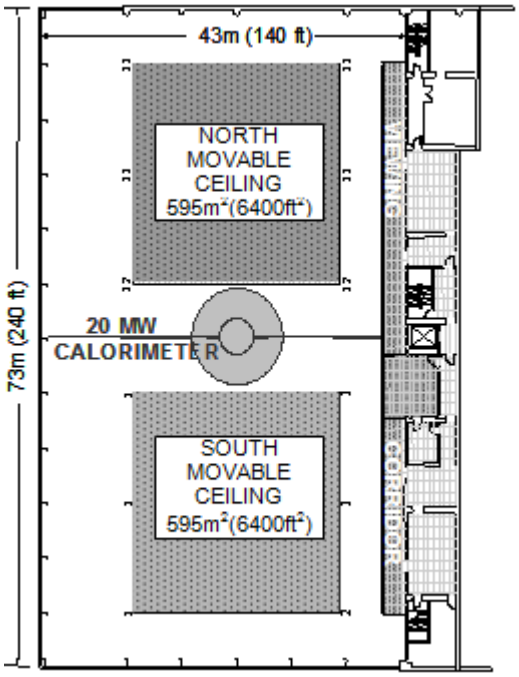

Figure 5-1: Illustration of FM Global Large Burn Laboratory test locations

5.2 TEST COMMODITY

Two rack storage fire tests were conducted using CUP commodity as described in Section 4.3.1. The pallet design for the FM Global standard CUP commodity, used in the large-scale validations tests, consisted of eight 0.53 m x 0.53 m x 0.53 m (21 in. x 21 in. x 21 in.) plastic cup filled corrugated cartons stacked 2 x 2 x 2 cartons high. Overall, the cube unit measures 1.07 m (42 in.) on the outside, and is supported on an ordinary, two-way, slatted-deck hardwood pallet, measuring 1.07 m x 1.07 m x 127 mm (42 in. x 42 in. x 5 in.). The total chemical energy for a pallet of the CUP commodity is nominally 1,430 ± 30 MJ, based on the above masses and the heat of combustion for each material.* A photo of the CUP commodity is provided in Figure 5-2.

* The heat of combustion for each material was multiplied by the mass of the material within the commodity. The referenced heat of combustion for each of the materials is included in Section 4.3.5.

Figure 5-2: Photo of cartoned unexpanded plastic (CUP) commodity

5.2.1 Selection of Test Commodity

Within the confines of the evaluation criteria detailed in Section 5.8, CUP commodity has been selected as a surrogate test material to evaluate sprinkler system performance when Li-ion batteries are not available. Section 4.9 showed that for a three-tier-high open-frame rack-storage arrangement, the carton packaging of both FM Global standard commodities (class 2 and CUP) and the Li-ion batteries used in this project exhibited similar fire development leading to operation of a quick-response sprinkler. Section 4.8 further showed that in an uncontrolled fire, CUP commodity reached a maximum HRR several minutes before significant involvement was observed for Li-ion battery products. Therefore, it is reasonable to assume that a sprinkler system found to efficiently suppress a fire involving CUP commodity will be equally able to suppress a fire of cartoned Li-ion batteries.

5.3 FUEL ARRAY

For each test, a three-pallet-load-high configuration was used, resulting in a 4.3 m (14 ft) high array, as shown in Figure 5-3. This array size is used to represent rack storage up to 4.6 m (15 ft), assuming nominally 1.5 m (5 ft) per tier. The main fuel array consisted of an open-frame, double-row steel rack erected directly on the floor. The main array dimensions measured approximately 4.9 m long x 2.3 m wide (16 ft x 7.5 ft) in a 4 x 2 pallet load arrangement. The end pallet of each row consisted of FM Global standard class 2 commodity as described in Section 4.3.1 (except for the noncombustible aluminum covering). A single-row target array

contained two pallet loads of the class 2 commodity across a 1.2 m (4 ft) aisle to the west of the main array. No target was located to the east of the main array to improve viewing angles of the ignition area, for the standard video and infrared imaging cameras. This omission had no expected impact due to the very limited tolerable fire spread precluding aisle jump. Overall the target array measured approximately 2.4 m long x 1.0 m deep (8 ft x 3.25 ft).

The ceiling was set at 9.1 m and 7.6 m (30 ft and 25 ft) above the floor for Tests 14 and 15, respectively. The rack storage arrays were oriented perpendicular to the sprinkler pipes, which run east-west across the ceiling.

Figure 5-3: Rack storage array of cartoned unexpanded plastic commodity

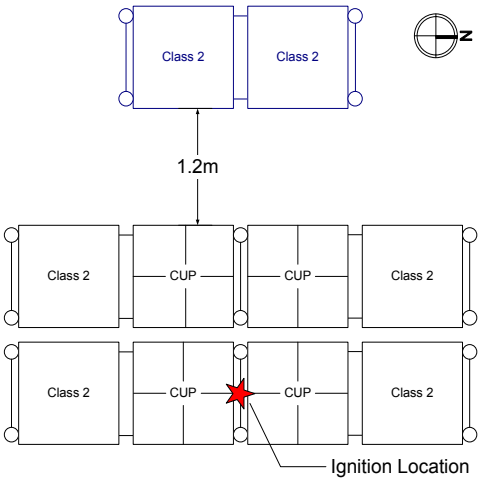

Figure 5-4: Plan view of main and target arrays

5.4 AUTOMATIC SPRINKLER PROTECTION

Sprinkler protection for the two tests was provided by different FM Approved, pendent-type, sprinklers, both with a 74°C (165°F) temperature rating and a nominal RTI of 27.6 $m^{½}s^{½}$ (50 $ft^{½}s^{½}$), Figure 5-5. The sprinklers are geometrically similar and appear identical in the figure below. Consistent with FM Global standard procedures for a large-scale fire test, each sprinkler was oriented with the sprinkler frame arms parallel to the sprinkler pipe and the sprinkler's heat-sensing link facing towards the north.

The sprinklers used in Test 14 had a K-Factor of 360 L/min/$bar^{½}$ (25.2 gpm/$psi^{½}$) and were installed with the deflectors 0.46 m (18 in.) below the ceiling. A nominal operating pressure of 172 kPa (25 psig) was chosen to provide a discharge of 477 L/min (126 gpm) per sprinkler. The sprinklers were installed on 3 m x 3 m (10 ft x 10 ft) spacing, resulting in a 51 mm/min (1.25 gpm/ft^2) water density at the floor.

The sprinklers used in Test 15 had a K-factor of 200 L/min/$bar^{½}$ (14 gpm/$psi^{½}$) and were installed with the deflectors 0.36 m (14 in.) below the ceiling. A nominal operating pressure of 517 kPa (75 psig) was chosen to provide a discharge of 454 L/min (120 gpm) per sprinkler. The sprinklers were installed on 3 m x 3 m (10 ft x 10 ft) spacing, resulting in a 49 mm/min (1.2 gpm/ft^2) water density at the floor.

Test 14
K-Factor = 360 L/min/$bar^{½}$ (25.2 gpm/$psi^{½}$)

Test 15
200 L/min/$bar^{½}$ (14 gpm/$psi^{½}$)

Figure 5-5: Selected sprinklers for Test 14 and 15

5.5 IGNITION

Ignition was achieved with two FM Global standard half igniters, which are 76 mm x 76 mm (3 in. x 3 in.) cylinders of rolled cellu-cotton. Each igniter is soaked in 118 ml (4 oz.) of gasoline and sealed in a plastic bag, Figure 5-6. The igniters were placed in an offset ignition orientation, 0.6 m (2 ft) east of center, in the center transverse flue, between the uprights, of the eastern row of the main array. The igniters were lit with a flaming propane torch at the start of each test and the fires were allowed to develop naturally.

Figure 5-6: Igniter locations within the rack, located at the rack uprights

5.6 TEST CONFIGURATION OVERVIEW

The configuration for Tests 14 and 15 is shown in Figure 5-7. In both cases, the main array was centered among four sprinklers. To fit within the extent of the ceiling, a total of 64 sprinklers were installed, although only 16 sprinklers are illustrated in Figure 5-7.

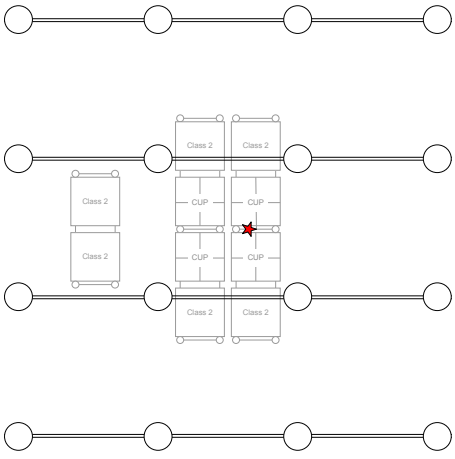

Figure 5-7: Sprinkler layout for large-scale validation tests

5.7 DOCUMENTATION AND INSTRUMENTATION

Documentation for each test included video, still photography, and audio recordings of the observations made during the test. The video documentation included two high definition digital video cameras, one standard definition video camera, and three infrared (IR) cameras for qualitative assessments of the fire. The two high definition cameras provided a view of the test from the east (main camera) and north (remote camera). The standard definition camera provided a view of the test from the east and was adjacent to the main camera. The following infrared cameras were used in this study:

- FLIR® SC655 long-wave IR (LWIR)
- FLIR® SC7600 ORION mid-wave IR (MWIR)
- THERMACAM® X90 SERIES Model PM390.

The SC655 and SC7600 cameras were adjacent to the main cameras and provided a view of the main array from the east. The X90 camera was located adjacent to the remote cameras and provided a view of the test array from the north. A detailed description of these cameras is provided in Section 4.4 and is not repeated here.

Environmental conditions, including relative humidity, dry-bulb temperature, and wet-bulb temperature of the air inside and outside of the lab, were measured just prior to each test as well as continually during each test. In addition, the following standard instrumentation was installed:

- Sprinkler protection was provided at 64 locations at the ceiling, as illustrated in Figure 5-7. Each sprinkler had its operating mechanism included in an electric circuit to determine operation times.
- Bare-bead, 0.8 mm (20-gage), chromel-alumel thermocouples, placed 165 mm (6-1/2 in.) below the ceiling at 125 locations. These thermocouples have been shown to have a response time index (RTI) of 8 ± 1 $m^{1/2}s^{1/2}$ (14.5 ± 1.8 $ft^{1/2}s^{1/2}$). See Appendix B for specific thermocouple locations.

- Bi-directional probes to measure plume velocity immediately below the ceiling. Probes were located at four orthogonal locations with radial distances from the ceiling center of 2.1 m and 4.0 m (7 ft and 13 ft) [at 0.1 m (0.4 ft) below the ceiling], and 10.4 m (34 ft) [at 0.5 m (1.5 ft) below the ceiling].
- Thermocouples imbedded in a cross-shaped steel angle, made from two 50.8 mm wide x 0.6 m long x 6.35 mm thick (2 in. x 2 ft x 0.25 in.) angle iron segments, attached to the center of the ceiling. Measurements from these thermocouples are referred to as steel temperatures.
- Flow meters and pressure controllers to monitor and control the sprinkler system.
- Gas analyzers to measure the generation of carbon dioxide (CO_2), carbon monoxide (CO), total hydrocarbons (THC), and depletion of oxygen (O_2) captured in the exhaust.

Supplementary instrumentation was added to assess the heating potential (magnitude and duration) exhibited by the burning combustibles during the fire, Figure 5-8 illustrates the instrumentation locations and Figure 5-9 illustrates the naming convention. The instrumentation consisted of:

- Sixteen stick-on thermocouples (Omega SA1XL-K-120-SRTC) adhered to the inside of the commodity on the vertical side of the carton facing the ignition flue. TCs were located at the horizontal and vertical midpoint of each carton for commodity on the south side of the ignition flue. These thermocouples are referenced by their location within the array based on tier (T1 for tier 1 or T2 for tier 2), pallet location (east or west), and carton location within a pallet (odd numbers indicate cartons adjacent to the aisle and even numbers indicate cartons adjacent the longitudinal flue). For example, T1W2 references the thermocouple located at tier 1, west pallet, adjacent to the longitudinal flue.
- Four stick-on thermocouples (Omega SA1XL-K-120-SRTC) adhered to the inside of the commodity on the horizontal top side of the carton. TCs were located at the midpoint of each carton on either side of the ignition flue. These thermocouples are referenced by their location within the array based on tier (T1 for tier 1 or T2 for tier 2), pallet location within the array (east or west), and carton relative to the central transverse flue (odd

numbers indicate cartons to the south and even numbers indicate cartons to the north). For example, T1W5 references the thermocouple located at tier 1, west pallet, south of the central transverse flue.

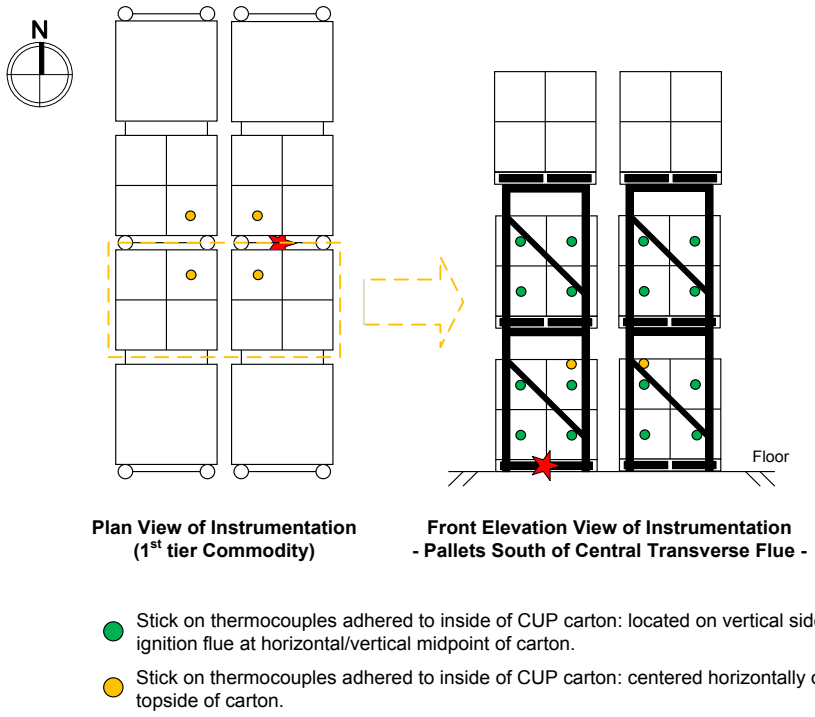

Figure 5-8: Supplementary instrumentation within main array

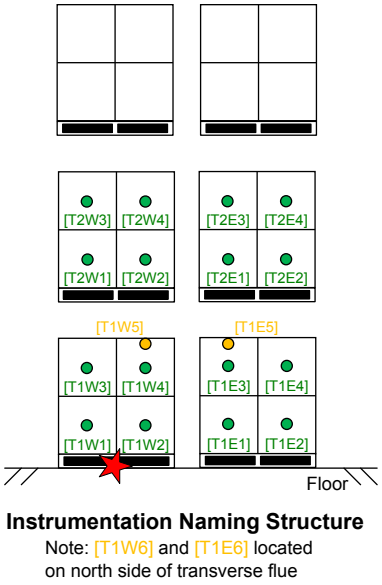

Figure 5-9: Naming convention for supplementary instrumentation

5.8 EVALUATION CRITERIA

Assessment of the system performance was based on the ability of the sprinkler system to efficiently suppress the test fire. For protection to be considered adequate, the fire must be nearly extinguished before the predicted time of battery involvement established for the Li-ion battery commodities in the reduced-commodity tests. The primary judgment criteria are the number of sprinkler operations, the extent of fire damage, heating potential for material within the commodity cartons, and the magnitude and duration of ceiling steel temperatures.

1) Sprinkler operations. Sprinkler operations should be limited to the sprinklers surrounding ignition, *i.e.*, a maximum four sprinklers for an array centered among four sprinklers.
2) Extent of fire spread. Fire damage should be largely confined to the commodity surrounding the central transverse flue (*i.e.*, ignition flue) with minimal damage across the longitudinal flue, should not propagate into the class 2 commodity capping the array, and there should be no fire spread across the aisle to the target array.
3) Heating potential. Thermocouple measurements within the test commodity, detailed in Section 5.7, should not exceed a value of 538^{o}C (1,000^{o}F) for a period of 5 min. For this assessment, TC measurements exceeding 538^{o}C (1,000^{o}F) are assumed to indicate the nearby presence of flames. This criterion is based on the reduced-commodity test results, Section 4, where involvement of cartoned Li-ion battery commodities in a three-tier-high rack storage array exposed to free-burn fire conditions occurred within 5 minutes.
4) Steel TC measurements. The maximum 1-min average allowable ceiling steel measurement is 538^{o}C (1,000^{o}F). This criterion is based on the assessment that structural steel loses 50-60 percent of its load-bearing strength upon reaching the 538^{o}C (1,000^{o}F) threshold [30,31]. The loss of strength could cause failure of the ceiling structure resulting in collapse of the roof. Additionally, the maximum instantaneous allowable ceiling steel measurement is 649^{o}C (1,200^{o}F). Values in excess of these thresholds during a test are taken as an indication of ineffective fire protection.

5.9 TEST RESULTS AND DATA ANALYSIS

This section presents the results of the two large-scale fire tests conducted to evaluate the suppression efficiency of a sprinkler system design. A summary of the test conditions and results is shown in Table 5-1. In addition, a complete analysis of each test (including time-resolved data) can be found in Appendix C.

For Test 14 a total of two sprinklers operated with the first occurring at 1 min 48 s after ignition followed by the second at 2 min 1 s. Fire spread remained within the confines of the test array; however, damage to the commodity surrounding ignition and TC measurements within the commodity both exceeded the evaluation criteria.

For Test 15 a total of four sprinklers operated between 1 min 38 s and 1 min 41 s after ignition. Fire spread was reduced compared to Test 14; however, persistent flames were observed throughout the test duration and TC measurements within the commodity exceeded the evaluation criteria.

Table 5-1: Summary of large-scale tests

Configuration and Results	**Test 14**	**Test 15**
Detailed Analysis, Appendix	Appendix C.1	Appendix C.2
Test Configuration		
Commodity	CUP, Double Row Rack	
Commodity / Ceiling Height [m (ft)]	4.6 / 9.1 (15 / 30)	4.6 / 7.6 (15 / 25)
Main Array Located Below – number of sprinklers	4	
Test Results		
Sprinklers Operations	2	4
Total Energy Released† [MJ (BTU x 10^3)]	2,000 ± 360 (1,900 ± 340)	620 ± 125 (590 ± 120)
Consumed CUP Commodity [pallet load equivalent]	1.5	0.5
Target Jump (west only) @ Time [min:s]	none	none
Maximum One-Minute Steel Temperature [^{o}C (^{o}F)] @ Time min:s]	37 (99) @ 5:09	41 (110) @ 1:48
Test Termination [min:s]	20:00	20:00

†Based on generation rates of CO and CO_2

5.9.1 Sprinkler Operation Patterns

A plan view of the sprinkler operation pattern for each test is presented in Figure 5-10.

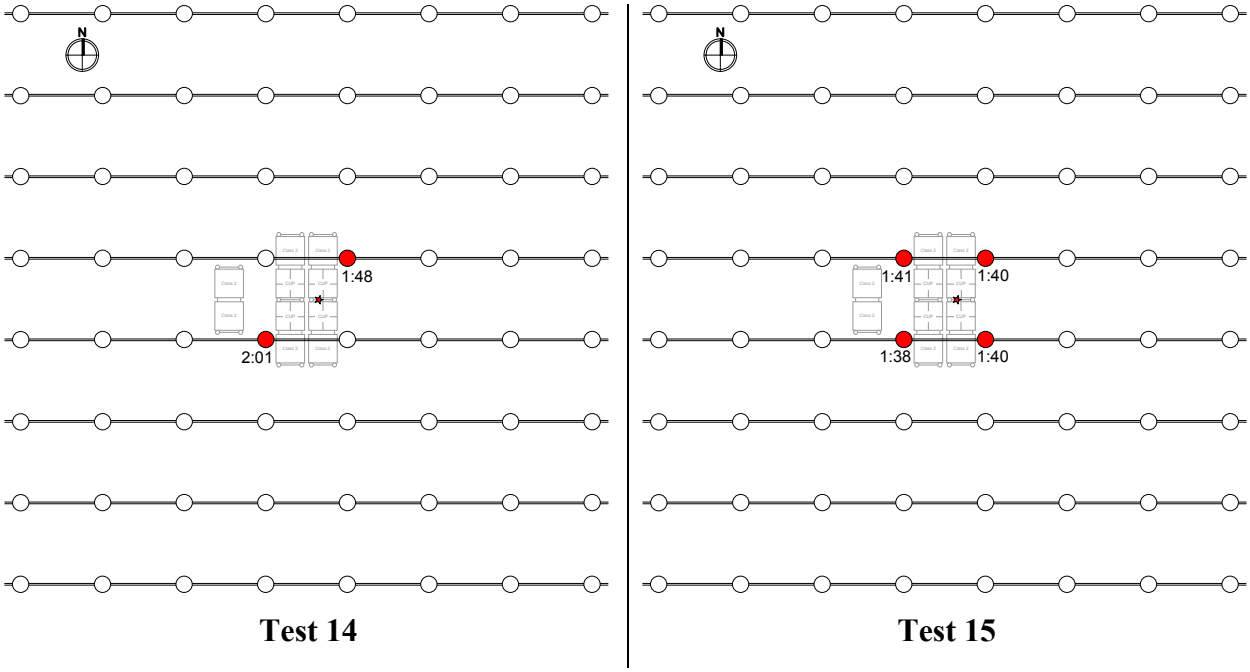

Figure 5-10: Sprinkler operation pattern for Tests 14 and 15

5.9.2 Total Energy

Figure 5-11 presents the total integrated energy produced during Tests 14 and 15. The presented data are based on the generation rates of carbon dioxide and carbon monoxide. The estimated total energy released during each test was 2,000 ± 360 MJ (1,900 ± 340 BTU x 10^3) for Test 14 and 620 ± 125 MJ (590 ± 120 BTU x 10^3) for Test 15.

Note that Figure 5-10 only shows the total energy collected during the 25-minute data collection period (20 min test plus 5 min additional data collection time). The total energy released, and reported in Table 5-1, for each test also includes an estimation of the combustion gases remaining in the laboratory space after test termination. Time-resolved HRR data for both tests are presented in Appendix C. The total energy generated was calculated by integrating the chemical HRR curve, which is possible while data are collected. After data collection is terminated, an exponential best fit curve of the decay portion of the test data is used to estimate

the tail portion of the HRR and again integrated to provide the total energy released. These two values were added to provide a value for the total energy released during the test.

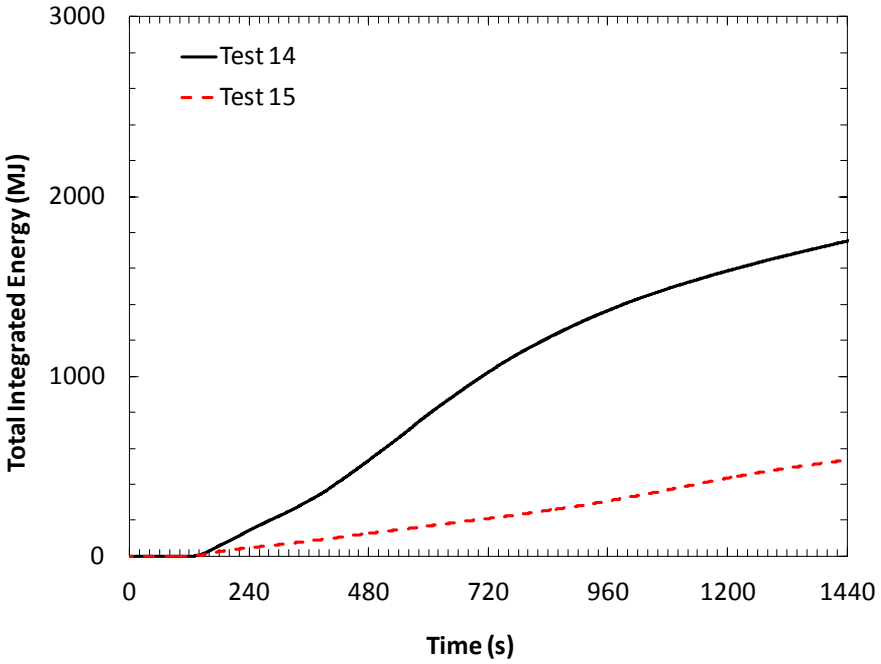

Figure 5-11: Total integrated energy for Tests 14 and 15

5.9.3 Ceiling Gas Centroid at First Sprinkler Operation

Figure 5-12 presents the ceiling TC measurement contours at first sprinkler operation and the corresponding location of the ceiling gas centroid*, for Tests 14 and 15. The position of the centroid is a measure of the axis of the fire plume above the test array. A ceiling gas centroid centered over ignition indicates that minimal ambient air current existed in the lab space during the initial fire development.

For both tests, the fire plume was nominally centered over ignition, which was located 0.6 m (2 ft) east of the ceiling center. At first sprinkler operation the centroid coordinates were 0.09 m (0.3 ft) east x 0.3 m (1 ft) south for Test 14 and 0.4 m (1.2 ft) west x 0.25 m (0.5 ft) south for Test 15. Note that the contour plot for Test 15 shows all four sprinkler operations which occurred

* Centroid refers to the geometric center of the ceiling gas layer produced by the fire, based on summation of normalized magnitude of ceiling TC measurements weighted by location.

over a 3-second timespan. The time evolution of the two coordinates of the ceiling gas centroid for each test can be found in Appendix C.

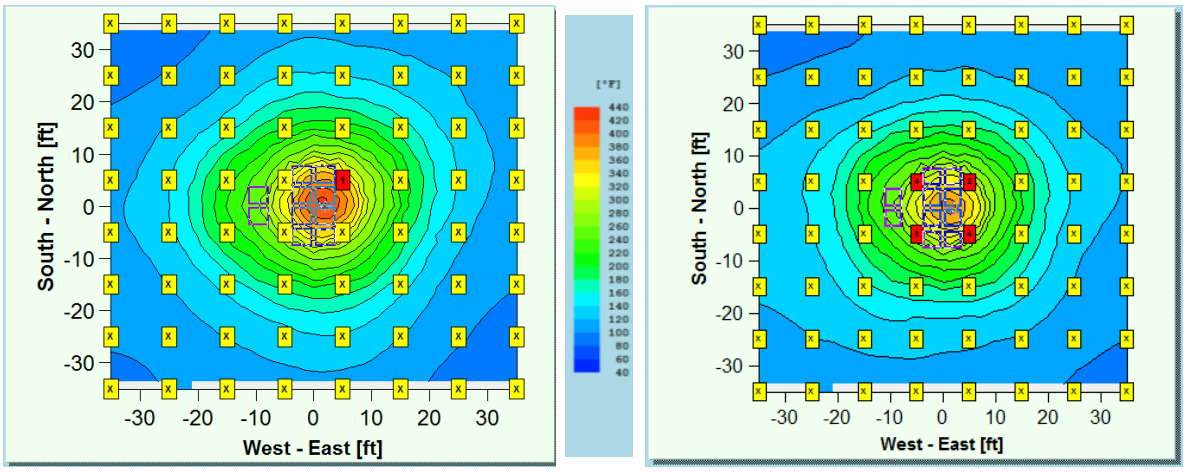

Test 14
[Centroid coordinates: 0.09 m east x 0.3 m south]

Test 15
[Centroid coordinates: 0.4 m west x 0.2 m south]

Figure 5-12: Contour plots of ceiling TC measurements at first sprinkler operation for Tests 14 and 15

5.9.4 Test Images

The fire at first sprinkler operation in Tests 14 and 15 is shown in Figure 5-13 and Figure 5-14, respectively. In each figure, the left image was recorded with a high definition video camera and the right image was recorded by the SC655 infrared camera. Though there is a slight difference in the time of first sprinkler operation, 10 s, it can be seen that the fire development leading to sprinkler operation was consistent. From the HD camera, flames spread to the front face of the array at the second and third tiers and extended ~1.5 m (5 ft) above the top of the array. Review of the infrared images shows similar results.

Figure 5-15 shows IR images 5 min after ignition for Test 14 and Test 15, which coincides with the estimated time of significant involvement of Li-ion batteries established during the reduced-commodity tests. From these images it is obvious that the sprinkler system in Test 15 was more effective at suppressing the fire; however, flames were persistent within the commodity adjacent to the central transverse flue (center of the image) for both tests. No images from the HD cameras are included here due to obscuration from smoke and sprinkler water.

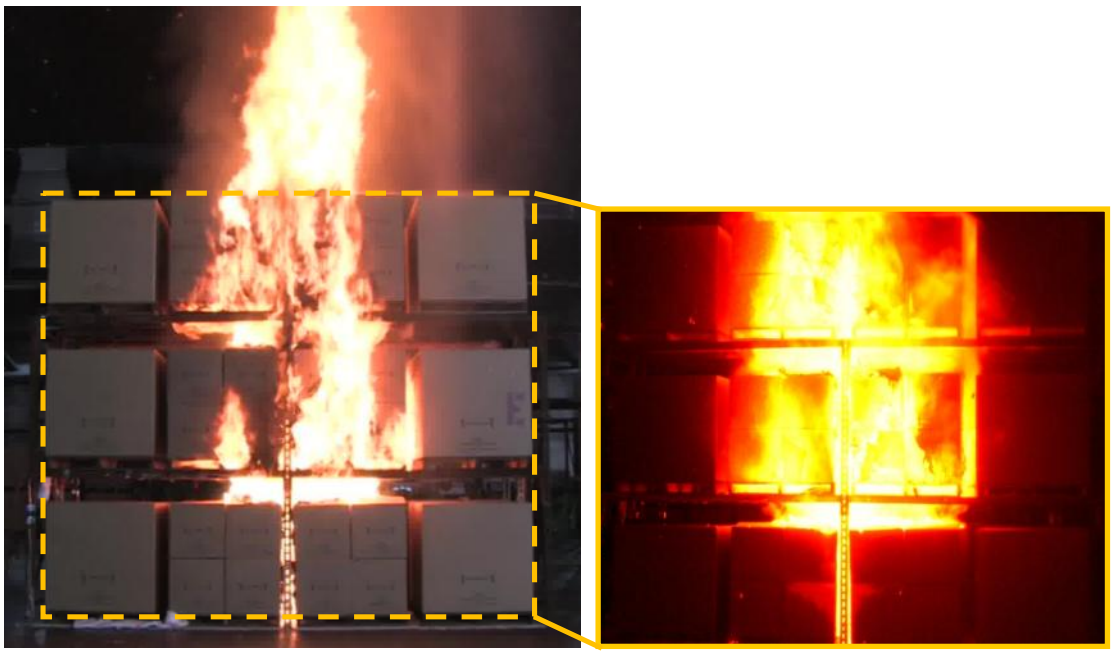

Figure 5-13: Image from HD camera (left) and IR camera (right) at first sprinkler operation [1 min 48 s] for Test 14

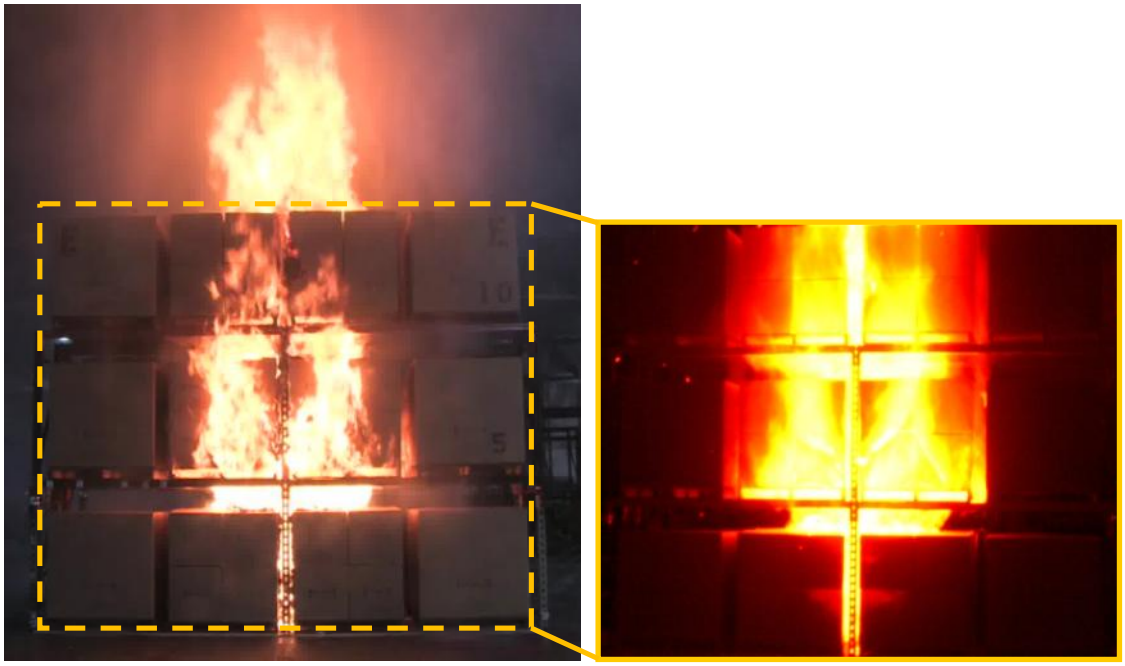

Figure 5-14: Image from HD camera (left) and IR camera (right) at first sprinkler operation [1 min 38 s] for Test 15

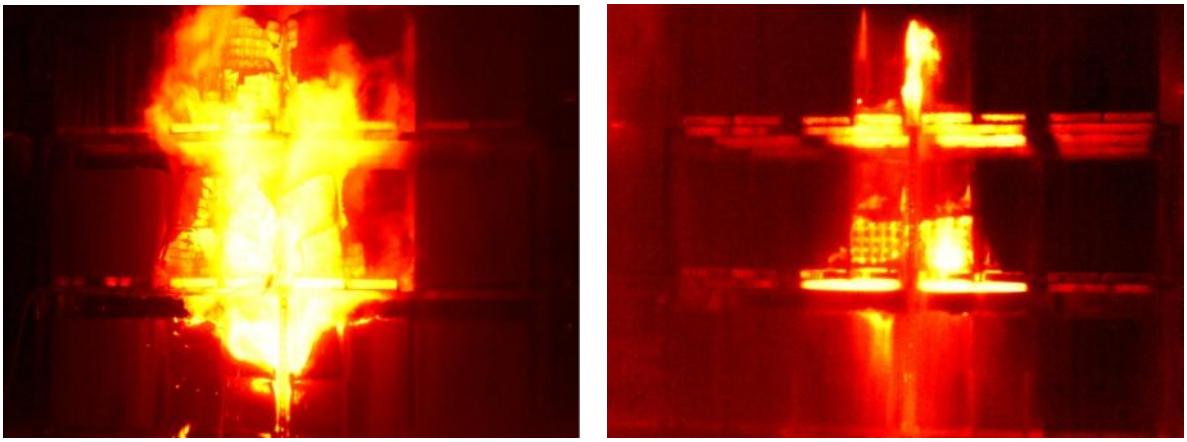

Figure 5-15: IR image of test array 5 min after ignition for Test 14 (left) and Test 15 (right)

5.9.5 Evaluation of Heating Potential

The heating potential posed by persistent flames within the array was measured by the TCs adhered to the inside of select commodity cartons surrounding ignition. TCs are referenced by their location within the array based on tier (T1 for tier 1 or T2 for tier 2), pallet location (east or west), and carton location within a pallet as illustrated in Figure 5-9.

Figure 5-16 (a) and (b) show the measurements from the TCs located within the test commodity for Test 14. The fire was initiated in the east row of the main array and the TC measurements reached > 900°C (1,650°F) starting at 1 min 30 s after ignition. These measurements are consistent with flame temperatures and indicate that the cartons were breached by the flames before the first sprinkler operation occurred at 1 min 48 s. On the west row commodity, the TC measurements were nominally 70°C (160°F) or less, which is consistent with visual observations of minimal fire damage. The exception is TCT1W3; located on the first tier adjacent to the longitudinal flue, which nominally measured 620°C (1,150°F) starting at 13 min 40 s. This measurement is consistent with the minor breach observed at the upper edge of the carton and indicates that the fire was still (slowly) propagating after the sprinklers operated.

Figure 5-17 (a) and (b) show the measurements from the TCs located within the test commodity for Test 15. The fire was initiated in the east row of the main array and the TC measurements reached > 700°C (1,290°F) starting at 1 min 5 s after ignition and reached a maximum value of

900°C (1,650°F) by 1 min 49 s. These measurements are consistent with flame temperatures and indicate that the cartons were breached by the flames before the first sprinkler operation occurred at 1 min 38 s. On the west row commodity, the TC measurements were 40°C (100°F) or less, which is consistent with visual observations of minimal fire damage.

(a)

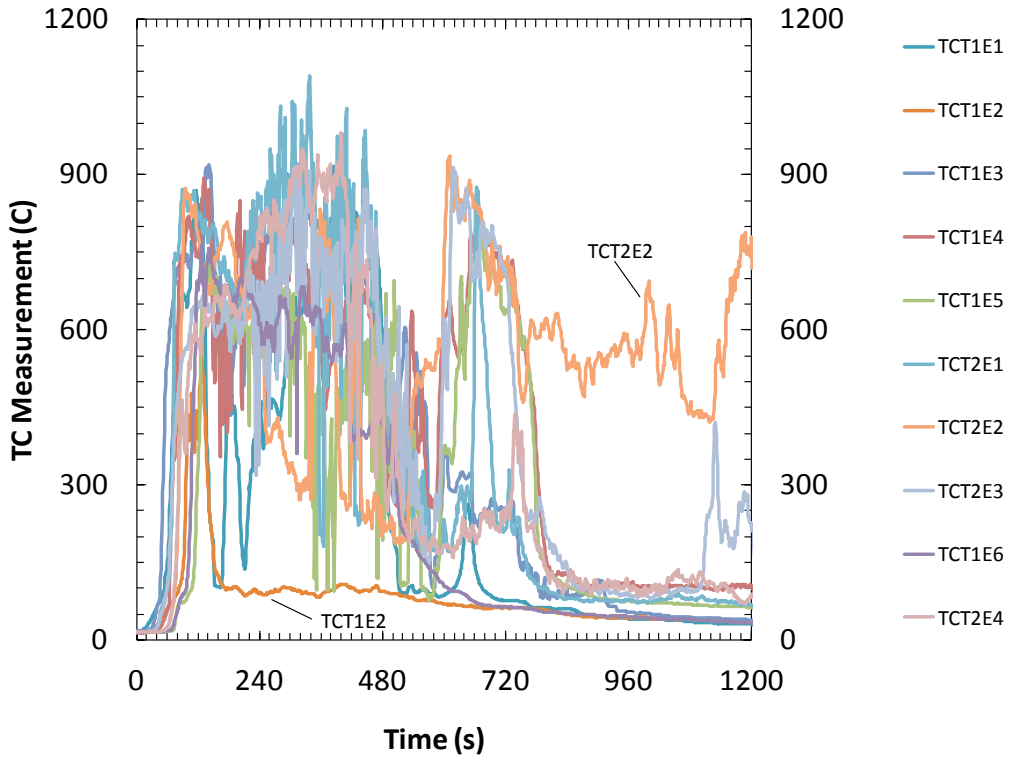

(b)

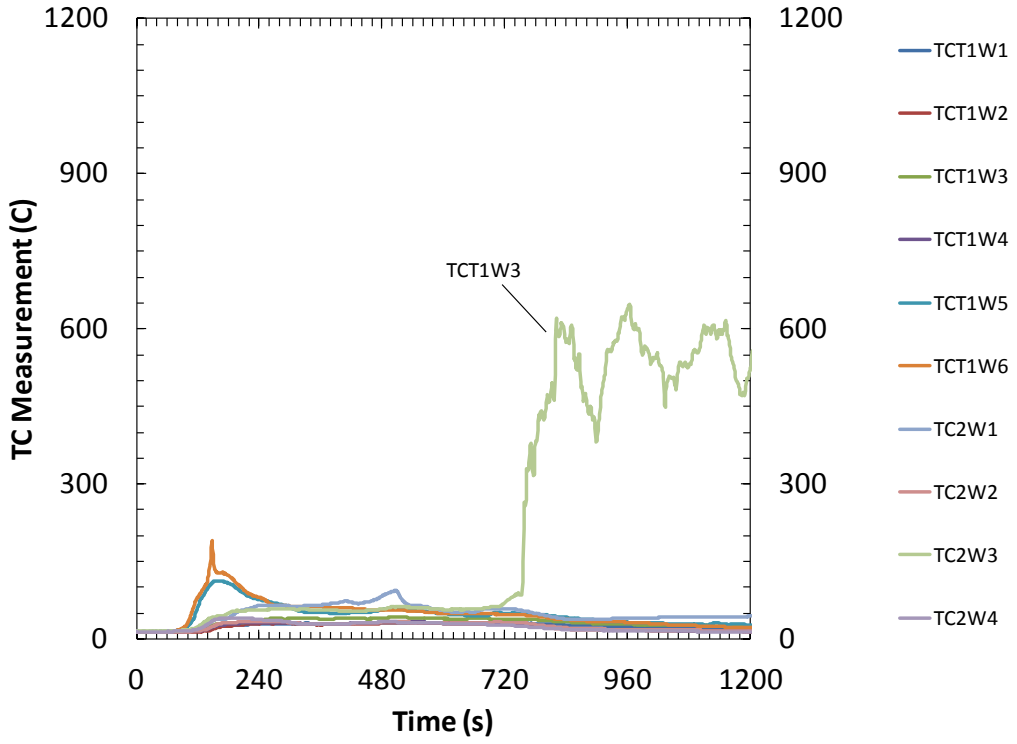

Figure 5-16: Measurements from thermocouples within commodity on east (a) and west (b) side of longitudinal flue - Test 14

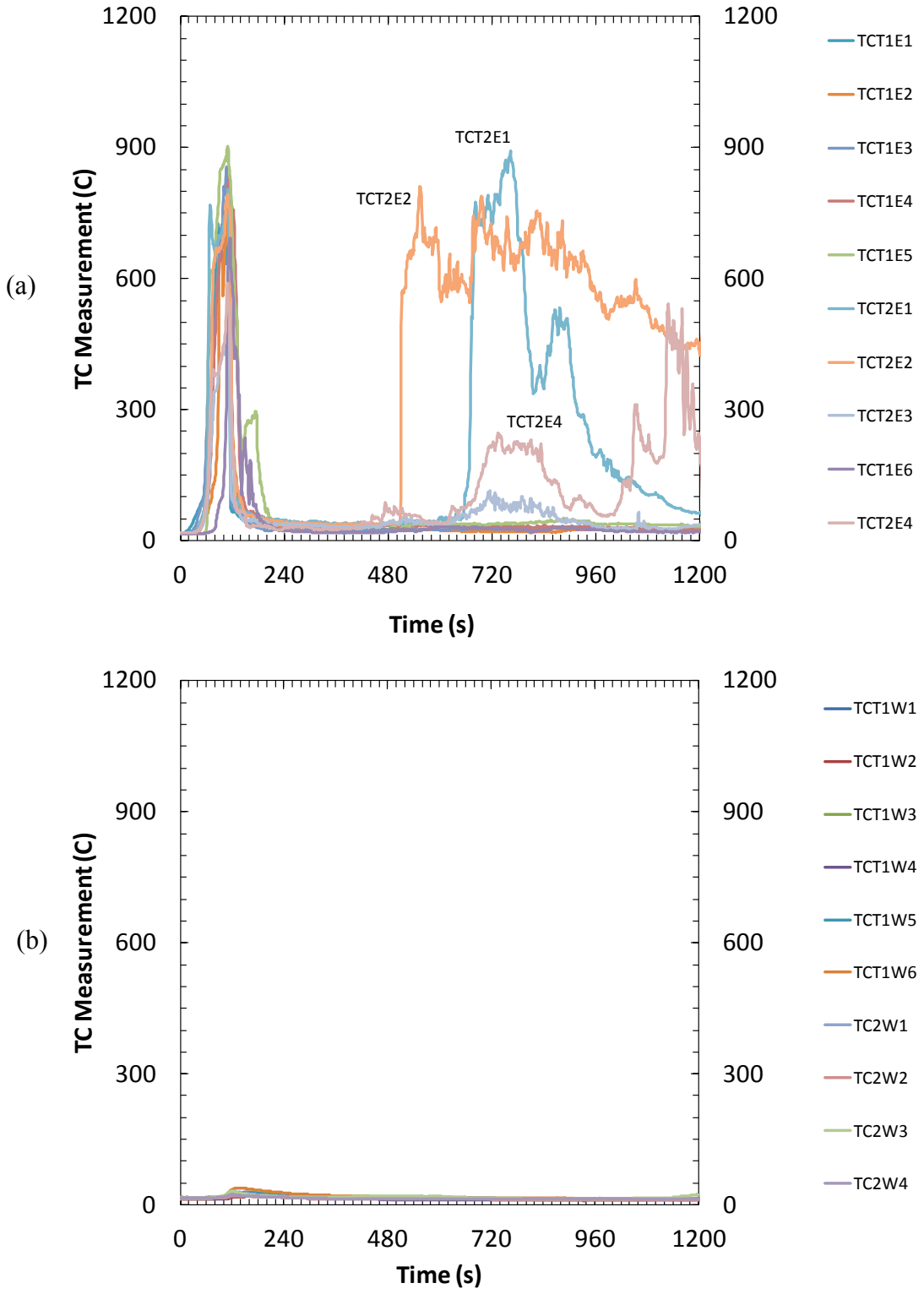

Figure 5-17: Measurements from thermocouples within commodity on east (a) and west (b) side of longitudinal flue - Test 15

6 DISCUSSION

All discussion in this report is specific to the array configurations used in the tests. The combined effects of a different array height, commodity type, ceiling height, etc., are yet to be understood and may not be inferred from these test results alone.

6.1 REPEATABILITY

Reduced-commodity testing with the two FM Global standard cartoned commodities was conducted at least three times each to assess repeatability of the initial fire growth leading to a predicted sprinkler operation. As included in Section 4.9, the characteristics of interest are the link operation times for both quick-response and standard-response sprinklers and the corresponding fire growth rate and fire size at link operation.

Table 6-1 shows the average values of fire growth parameters, such as the sprinkler activation times, etc., and one standard deviation for class 2 commodity (Tests 4 - 6, 10) and CUP commodity (Tests 7 - 9) assuming a 7.6 m (25 ft) ceiling. Excellent agreement is seen for all values with variability less than 20%. The lone exception is the fire growth rate for the CUP commodity at the operation of a standard-response sprinkler, which deviates from the average value by 30%. This measurement occurs during the transition from burning of the outer carton to the stored plastic, which was identified as a temporary plateau in the heat release curve shown in Figure 4-31. The increased deviation is a result of the minimal rate of rise in the heat release rate at the standard-response sprinkler operation time.

Table 6-2 shows the average values of fire growth parameters, such as the sprinkler activation times, etc., and one standard deviation for class 2 commodity (Tests 4 - 6, 10) and CUP commodity (Tests 7 - 9) assuming a 9.1 m (30 ft) ceiling. Values occurring after the flammability characterization period of the test, as defined in Section 4.7, are not reported. Excellent agreement is seen for all values with an uncertainty less than 20%. The lone exception is the fire growth rate for CUP commodity at the operation of a quick-response sprinkler, which deviates from the average value by 50%. Similar to the results for a 7.6 m (25 ft) ceiling, this

measurement occurs during the transition from burning of the outer carton to the contained plastic.

Table 6-1: Repeatability of flammability characteristics for Class 2 and CUP commodity assuming a 7.6 m (25 ft) ceiling

Property	Quick-response sprinkler	Standard-response sprinkler	Commodity
Link Operation Time, (s)	59 ± 6.1	77 ± 5.1	**Class 2**
Fire Growth Rate, (kW/s)	15 ± 1.8	22 ± 3.5	
Q_{be}, (kW)	209 ± 8.5	603 ± 29.0	
Link Operation Time, (s)	43 ± 2.5	70 ± 4.2	**CUP**
Fire Growth Rate, (kW/s)	16 ± 2.8	7 ± 2.2	
Q_{be}, (kW)	232 ± 4.5	431 ± 15.1	

Table 6-2: Repeatability of flammability characteristics for Class 2 and CUP commodity assuming a 9.1 m (30 ft) ceiling

Property	Quick-response sprinkler	Standard-response sprinkler	Commodity
Link Operation Time, (s)	65 ± 6.1	90 ± 4.0	**Class 2**
Fire Growth Rate, (kW/s)	24 ± 2.0	-	
Q_{be}, (kW)	367 ± 22	-	
Link Operation Time, (s)	52 ± 2.9	86 ± 3.6	**CUP**
Fire Growth Rate, (kW/s)	11 ± 5.3	-	
Q_{be}, (kW)	321 ± 47	-	

6.2 INTERNAL FAULT IGNITION SCENARIO AND PROJECTILES

The fire tests conducted for this project utilized an external fire as the ignition source. The result was rapid fire growth of the carton packaging causing heating of the stored Li-ion batteries. Another possible ignition scenario is an internal fault of a single Li-ion battery leading to preheating of many batteries before involvement of the outer cartons. Since sprinkler operation in a three-tier high rack storage arrangement typically occurs due to vertical fire growth on the carton packaging, the potential result is involvement of many Li-ion batteries before a sprinkler system operates.

A point of perspective on the impact of an internal fault leading to ignition of a Li-ion battery can be obtained with review of work conducted by the Federal Aviation Administration (FAA). A 2006 study determined that a single 18650-format cylindrical cell in thermal runaway

produces enough heat to cause other nearby cells within the shipping carton to also go into thermal runaway [32]. This result was validated in 2010 by tests involving three cartons each containing one hundred of the same cells [33]. To initiate the fire, a single cell was removed from a centrally located carton and replaced with a 100 W (340 BTU/hr) cartridge heater. The heater was selected to have a temperature profile closely matching a cell in thermal runaway. The simulated cell failure resulted in thermal-runaway of all cells in the test.

In 2012, similar cell-to-cell fire propagation was also seen for a larger test consisting of 5,000 cylindrical cells [8]. Cells were packaged in fifty 100-cell cartons and a cartridge heater was located at the bottom of the stack, Figure 6-1. Similar to the smaller tests, cell-to-cell propagation occurred slowly, gradually speeding up as the fire size increased. Significant cell rupture was observed with projectiles traveling up to 40 m (130 ft). The duration of the fire from initial smoke observation to reaction of all cells was 1 hr 5 min.

Figure 6-1: Image of 5,000 Li-ion battery test conducted by the FAA; test layout (left) and fire involving carton packaging (right) [*images taken from reference 8*]

The FAA tests raise obvious concerns for storage of large quantities of Li-ion batteries where protection options are limited, such as an aircraft cargo area. However, these concerns may be mitigated for a sprinklered warehouse scenario. Further review of the 5,000 cell test shows that the majority of cell involvement occurred after the fire spread vertically along the outer carton packaging. While a larger quantity of cells may allow for a deeper seated internal fault to occur, cell-to-cell fire propagation has been shown to occur slowly. No comments can be made relating sprinkler protection effectiveness for an external fault scenario to an internal fault scenario.

Therefore, in the absence of large-scale sprinklered test experience, the unknown impact of an internal fault must be addressed through robust sprinkler protection.

Another concern raised by the FAA testing is the potential for secondary ignition due to flaming projectiles. This concern is limited to cells with geometry advantageous for projectile, such as individual hard-cased cylindrical cells. Other cell formats are more likely to rupture in place, for instance: hard-cased prismatic cells, soft-cased polymer cells, and Li-ion battery-containing devices (power tool packs). It should be noted that the limited number of projectiles observed in the cylindrical test conducted for this project was likely due to the predominantly vertical stacking of cells not allowing a clear path for projectiles. Current solutions for commodity prone to flaming projectiles, *e.g.*, level 3 aerosols [3,34], include segregation of commodity away from other combustible materials or the use of horizontal and/or vertical barriers to contain projectiles.

6.3 CELL REIGNITION

Thermal runaway of a Li-ion cell results in ignition of the contained ignitable liquid electrolyte. Current electrolytes are composed of low-flash-point hydrocarbons and are prone to reignition. This was observed in the tests conducted for this project during water application with a hose stream during test termination. Reignition was also observed during testing by the FAA, though water was shown to effectively cool the cells and prevent further thermal runaway [33]. The largest threat of reignition occurs when fire suppression water is terminated after a fire event. Precautions should be taken to ensure that reignitions are promptly and fully extinguished.

6.4 APPLICATION OF SMALL-SCALE RESULTS

This project focused on rack storage fire testing to characterize the fire hazard of bulk stored Li-ion batteries. By focusing on the overall fire hazard and not just the contribution from Li-ion batteries, the product packaging was identified as a key factor driving protection requirements for the storage arrangement and ignition scenario used in the study. Understanding of the fire hazard can now be supplemented through bench-scale evaluations, such as the single battery tests conducted by Abraham et al. [10] or Ribière et al. [11]. However, when considering a bulk storage scenario it remains critically important to place bench-scale results into proper context with the overall packaging design. For instance, high-capacity batteries tend to be larger than

their smaller-capacity counterparts and, therefore, may actually reduce the energy density of a pallet load. In the case of power tool packs, higher capacities are often achieved by including more cells in the pack design. The result is an increase in the quantity of cell electrolyte compared to the quantity of plastic in the pack housing. Design parameters, such as chemistry, state of charge (SOC) and capacity, and case structure are known to impact cell reactivity in terms of ease and magnitude of energy release. Further bench-scale evaluation of these parameters may provide valuable insight into the ranking of the fire hazard of Li-ion cells.

7 CONCLUSIONS

Two series of rack storage fire tests were conducted to evaluate the hazard of Lithium-ion (Li-ion) batteries in bulk storage and develop protection system guidance. Both evaluations were conducted at the FM Global Research Campus in West Glocester, R.I., USA, and were identified as the reduced-commodity tests and large-scale validation tests.

This project represents a unique approach to hazard evaluation with reduced commodity that was necessary due to inordinate cost and limited availability, and personnel safety concerns. Consequently, protection recommendations for Li-ion batteries are strictly limited to the conditions included in this report. The combined effects of different storage height, ceiling height, protection system design, commodity type and composition are yet to be well understood and should not be inferred from these test results alone. Additionally, significant changes in the Li-ion cell design and chemistry may require additional research. The applicable storage conditions are:

- Rack storage heights up to 4.6 m (15 ft).
- Ceiling heights up to 9.1 m (30 ft).
- Bulk packaged small-format Li-ion batteries in corrugated board cartons (*i.e.,* 18650-format cylindrical cells), power tool packs (comprised of 18650-format cylindrical cells), and polymer cells at 50% state of charge (SOC).

The reduced-commodity test series evaluated the flammability characteristics of Li-ion batteries and FM Global standard cartoned commodities in a rack storage array. These were free-burn fire tests focused on measurement of the heat release rate of each commodity and the time of battery involvement for the Li-ion products. Subsequent predictions establish the fire hazard present in a sprinklered fire scenario and provide the basis for protection system guidance. Based on the results of the tests presented in this report the following conclusions can be made:

- The Li-ion cylindrical and polymer cells used in this project contributed to the overall fire severity of the rack storage array within 5 minutes under free-burn conditions.

- The overall agreement of the fire growth characteristics for Li-ion batteries and FM Global standard commodities supports the assumption that for three-tier-high, open-frame racks, cartoned commodities exhibit similar fire development leading to first sprinkler operation.
- Plastic content and density of packed batteries are driving factors in the commodity hazard, in particular:
    - Commodity containing significant quantities of loosely packed plastics (*i.e.,* cartoned unexpanded plastic (CUP) and power tool packs) exhibit a similar rapid increase in the released energy due to plastics involvement early in the fire development. For the Li-ion power tool packs used in this project, the plastics dominated the fire growth and there was no observable energy release contribution from the Li-ion batteries.
    - Commodity containing densely packed Li-ion batteries and minimal plastics (*i.e.,* Li-ion cylindrical and polymer cells) exhibit a delay in the battery involvement due to heating of the batteries.
- FM Global standard CUP commodity exhibits a fire hazard leading to initial sprinkler operations similar or greater than the Li-ion battery products tested in the project. This result indicates that CUP commodity is a suitable surrogate for Li-ion batteries in a bulk-packed rack-storage test scenario; provided the protection system design suppresses the fire within 5 min (*i.e.*, the time when the Li-ion batteries tested in this project contributed to the fire severity).
- In the absence of sprinklered large-scale test experience with Li-ion batteries, a protection system must preclude battery involvement by early extinguishment of the carton packaging fire.

The large-scale test series evaluated the effectiveness of a ceiling-level sprinkler system to preclude involvement of Li-ion batteries stored in corrugated board cartons. Testing was conducted with FM Global standard CUP commodity, which exhibits a fire hazard leading to initial sprinkler operation greater than or equal to the Li-ion battery products tested in the project. For protection to be considered adequate, sprinkler activation needed to occur while the fire severity was attributed to the combustion of the corrugated cartons and suppressed to the point of

near extinguishment prior to time of battery involvement established for the Li-ion battery commodities in the reduced-commodity tests.

Two tests were conducted using a three-tier-high rack-storage array that was centered among four sprinklers. This array size represents storage up to 4.6 m (15 ft) high. Protection was provided by quick-response, pendent sprinklers, having a 74°C (165°F) rated link, with either 1) a K-Factor of 360 L/min/bar$^{1/2}$ (25.2 gpm/psi$^{1/2}$) under a 9.1 m (30 ft) ceiling, or 2) a K-Factor of 200 L/min/bar$^{1/2}$ (14 gpm/psi$^{1/2}$) under a 7.6 m (25 ft) ceiling. In both tests, the CUP commodity cartons breached before the initial sprinkler operation. In accordance with the evaluation criteria established in Section 5.8, the adequacy of ceiling-level sprinkler protection could not be established due to persistent burning of the CUP commodity beyond the predicted time of battery involvement. These results indicate the effectiveness of the tested ceiling-level sprinkler protection cannot be assessed without repeating the tests using bulk-packed Li-ion batteries.

8 RECOMMENDATIONS

Protection recommendations for Li-ion batteries could not be directly and explicitly developed during this project; however, the test results do support analogous protection requirements for commodities with similar hazard characteristics. In consultation with the FM Global Engineering Standards group, which is responsible for the FM Global Property Loss Prevention Data Sheets, protection recommendations have been established based on current knowledge and may be amended if additional research specific to the hazard of Li-ion batteries is conducted.

This project concluded that bulk storage of the selected Li-ion batteries exhibit a fire hazard up to initial sprinkler operations similar to FM Global standard cartoned unexpanded plastic (CUP) commodity. For limited storage heights, this conclusion aligns with Hazard Class HC-3 of FM Global Property Loss Prevention Data Sheet 3-26, *Fire Protection Water Demand for Nonstorage Sprinklered Properties* [35], which defines protection for nonstorage facilities where the fire hazard could approach the equivalent of nominal 1.5 m (5 ft) high in-process storage of CUP commodity. Additionally, Li-ion power tool packs exhibited a fire hazard similar to CUP commodity with no observable energy release contribution from the Li-ion batteries when stored up to 4.6 m (15 ft) high). Therefore, for the storage configuration tested in this project, power tool packs can be protected as CUP commodity per FM Global Property Loss Prevention Data Sheet 8-9, *Storage of Class 1, 2, 3, 4 and Plastic Commodities* [36].

Storage beyond the above-listed conditions requires a more robust protection scheme to account for several unknowns that can negatively affect protection effectiveness, including the contribution to the fire severity from the Li-ion batteries, flaming projectiles and the ignition scenario (external fire or internal cell fault). Fire Protection Scheme A combines in-rack automatic sprinklers (IRAS) and horizontal barriers for protection of high-hazard commodities, such as rack storage of ignitable liquids or level 3 aerosols. Complete specifications and drawings can be found in Section D.2.2.1 of FM Global Property Loss Prevention Data Sheet 7-29, *Ignitable Liquid Storage in Portable Containers* [37]. Similar specifications can be found in Section E.2 of FM Global Property Loss Prevention Data Sheet 7-31 [34], *Storage of Aerosol Products*, January 2012. This system design is assumed to provide the highest level of

protection required for storage of the Li-ion batteries tested in this project and can be applied to array configurations beyond the scope of this project.

While the potential for fire spread due to flaming projectiles may exist with certain Li-ion cells, the impact of burning projectiles is expected to be minimal where commodity is segregated away from other combustibles or where Scheme A protection utilizing quick-response sprinklers is provided. The segregation distance recommendation should reflect the propensity for projectiles based on the Li-ion cell design. For instance, hard-cased cylindrical cells are more prone to be ejected far distances than soft-cased polymer cells and therefore require a greater segregation distance.

The best protection recommendations based on current knowledge, for each Li-ion battery included in this project, are summarized below:

- Li-ion cylindrical cells (*i.e.,* small-format):
    - For a single unconfined pallet load of cells stored on the floor to a maximum 1.5 m (5 ft) high, protect as an HC-3 occupancy per FM Global Property Loss Prevention Data Sheet 3-26, *Fire Protection Water Demand for Nonstorage Sprinklered Properties*, July 2011. Additionally, maintain a minimum separation of 3.0 m (10 ft) from adjacent combustibles for manufacturing occupancies; increase the separation distance to 15 m (50 ft) from areas of contiguous storage.
    - For protection of cells stored on pallets greater than one high, store pallet loads in racks and protect racks with Scheme A per Section D.2.2.1 of FM Global Property Loss Prevention Data Sheet 7-29, *Ignitable Liquid Storage in Portable Containers*, April 2012.
- Li-ion polymer cells (*i.e.,* small-format):
    - For a single unconfined pallet load of cells stored on the floor to a maximum of 1.5 m (5 ft) high, protect as an HC-3 occupancy per FM Global Property Loss Prevention Data Sheet 3-26, *Fire Protection Water Demand for Nonstorage Sprinklered Properties*, July 2011. Additionally, maintain a minimum of 3.0 m (10 ft) separation between adjacent combustibles.

- For protection of cells stored on pallets greater than one high, store pallet loads in racks and protect racks with Scheme A per Section D.2.2.1 of FM Global Loss Prevention Data Sheet 7-29, *Ignitable Liquid Storage in Portable Containers*, April 2012.

- Li-ion power tool packs (*i.e.,* small-format cylindrical cells)
  - For cells stored on pallets up to three high (*i.e.*, 4.6 m (15 ft)) under a ceiling up to 9.1 m (30 ft) high, store pallet loads in racks and protect as FM Global standard cartoned unexpanded plastic (CUP) commodity per FM Global Property Loss Prevention Data Sheet 8-9, *Storage of Class 1, 2, 3, 4 and Plastic Commodities*, FM Global, July 2011.
  - For protection of cells stored on pallets greater than three high (*i.e.*, 4.6 m (15 ft)), store pallet loads in racks and protect racks with Scheme A per Section D.2.2.1 of FM Global Property Loss Prevention Data Sheet 7-29, *Ignitable Liquid Storage in Portable Containers*, April 2012.
  - For protection of cells stored beneath a ceiling greater than 9.1 m (30 ft), regardless of storage height, store pallet loads in racks and protect racks with Scheme A per Section D.2.2.1 of FM Global Property Loss Prevention Data Sheet 7-29, *Ignitable Liquid Storage in Portable Containers*, April 2012.

9 REFERENCES

[1] D. Lisbona and T. Snee, "A Review of Hazards Associated with Primary Lithium and Lithium-ion Batteries," Process Safety and Environmental Protection, Volume 89, Issue 6, pp. 434-442, November 2011.

[2] C. Arbizanni, G. Gabrielli, and M. Mastragostino, "Thermal Stability and Flammability of Electrolytes for Lithium-ion Batteries," Journal of Power Sources, Volume 196, Issue 10, pp. 4801–4805, May 2011.

[3] National Fire Protection Association Standard 13 (NFPA 13), "Standard for the Installation of Sprinkler Systems," 2010.

[4] C. Mikolajczak, M. Kahn, K. White, and R. Long, "Lithium-Ion Batteries Hazard and Use Assessment," Report prepared for the Fire Protection Research Foundation, June 2011. http://www.nfpa.org/assets/files/pdf/research/rflithiumionbatterieshazard.pdf, accessed on January 28, 2103.

[5] M. Buser, "Lithium Batteries: Hazards and Loss Prevention," S+S Report International, pp. 10-17, February 2011.

[6] R.T. Long, M. Kahn, and C. Mikolajczak, "Lithium-Ion Battery Hazards," Fire Protection Engineering, pp. 20-36, 4th Quarter, 2012.

[7] S.M. Summer, "Flammability Assessment of Lithium-Ion and Lithium-Ion Polymer Battery Cells Designed for Aircraft Power Usage," DOT/FAA/AR-09/55, Springfield, VA, U.S. Department of Transportation Federal Aviation Administration, 2010.

[8] H. Webster, "Preliminary Full-Scale Fire Tests with Bulk Shipments of Lithium Batteries," 2012 FAA Fire Safety Highlights, U.S. Department of Transportation Federal Aviation Administration, 2012.

[9] E.P. Roth, C. Crafts, D.H. Doughty, and J. McBreen, "Advanced Technology Development Program for Lithium-Ion Batteries: Thermal Abuse Performance of 18650 Li-Ion Cells," SANDIA REPORT SAND2004-0584, Unlimited Release, March 2004.

[10] D.P. Abraham, E.P. Roth, R. Kostecki, K. McCarthy, and D.H. Doughty, "Diagnostic Examination of Thermally Abused High-Power Lithium-ion Cells," Journal of Power Sources, Volume 161, pp. 648–657, 2006.

[11] P. Ribière, S. Grugeon, M. Morcrette, S. Boyanov, S. Laruelle, and G. Marlair, "Investigation on the Fire-Induced Hazards of Li-ion Battery Cells by Fire Calorimetry," Energy and Environmental Science, Volume 5, pp. 5271-5280, 2012. DOI: 10.1039/c1ee02218k

[12] Y. Xin and F. Tamanini, "Assessment of Commodity Classification for Sprinkler Protection Using Representative Fuels," Journal of Fire Safety Science, Volume 9, pp. 527-538, 2008. DOI:10.3801/IAFSS.FSS.9-527

[13] Y. Xin, "Storage Height Effects on Fire Growth Rates of Cartoned Commodities," for presentation at the Seventh International Seminar on Fire and Explosion Hazards, Providence RI USA, May 5-10, 2013.

[14] G. Marlair and A. Tewarson, "Effects of the Generic Nature of Polymers on Their Fire Behavior," Proceedings of the 7th International Symposium on Fire Safety Science, Worcester (USA), pp. 629-642, 2002. DOI:10.3801/IAFSS.FSS.7-629

[15] H. Biteau, "Thermal and Chemical Behaviour of an Energetic Material and a Heat Release Rate Issue," PhD thesis, University of Edinburgh, 2010.

[16] H. Biteau, T. Steinhaus, C. Schemel, A. Simeoni, G. Marlair, N. Bal, and J.L. Torero, "Calculation Methods for the Heat Release Rate of Materials of Unknown Composition," Fire Safety Science, Volume 9, pp. 1165-1176, 2009. doi:10.3801/IAFSS.FSS.9-1165

[17] S.J. Harris, A. Timmons, W.J. Pitz, "A Combustion Chemistry Analysis of Carbonate Solvents in Li-Ion Batteries," Journal of Power Sources, Volume 193, pp. 855-858, 2009.

[18] A. Tewarson, "Generation of Heat and Chemical Compounds," SFPE Handbook of Fire Protection Engineering, 4th Edition, P. DiNenno (Ed.), Section 3, Chapter 4, pp. 3-109 to 3-194, 2008.

[19] ASTM E 2058-09, "Standard Test Methods for Measurement of Synthetic Polymer Material Flammability Using a Fire Propagation Apparatus (FPA)," American Society for Testing Materials, Philadelphia, PA. DOI: 10.1520/E2058-09

[20] A. Tewarson, "Flammability Parameters of Materials: Ignition, Combustion, and Fire Propagation," Journal of Fire Science, Volume 10, pp. 188–241, 1994.

[21] International Standards Organization (ISO/IEC) 17025:2005, General Requirements for the Competence of Testing and Calibration Laboratories, International Standards Organization, Geneva, Switzerland, 2005.

[22] "Li Ion Battery Test Burn," Woodard and Curran Technical Report prepared for FM Global, 225590.00, January 2013.

[23] H.C. Kung, H.Z. You and R.D. Spaulding, "Ceiling Flows of Growing Rack Storage Fires," Twenty-first Symposium (International) on Combustion, The Combustion Institute, pp. 121-128, 1986.

[24] G. Heskestad, "Investigation of a New Sprinkler Sensitivity Approval Test: The Plunge Test," FMRC Technical Report, Serial No. 22485, RC 76-T-50, 1976.

[25] G. Heskestad and H.F. Smith, "Plunge Test for Determination of Sprinkler Sensitivity," FMRC Technical Report, J.I. 3A1E2.RR, December, 1980.

[26] H.Z. You and H.C. Kung, "Strong buoyant plumes of growing rack storage fires", Twentieth Symposium (International) on Combustion, The Combustion Institute, pp. 1547-1554, 1984.

[27] G. Heskestad, "Pressure Profiles Generated by Fire Plumes Impacting on Horizontal Ceilings," FMRC Technical Report, 0F0E1.RU, August, 1980.

[28] J. de Vries and B. Ditch, "Multi-Spectral Infrared Analysis of Lithium-Ion Battery Bulk-Storage Fire Tests," for presentation at the Seventh International Seminar on Fire and Explosion Hazards, Providence RI, USA May 5-10, 2013.

[29] D. Abraham, "Diagnostic Examination of Thermally Abused High-Power Lithium-Ion Cells," Journal of Power Sources, Volume 161, pp. 648-657, 2006.

[30] J. Milke, "Analytical Methods for Determining Fire Resistance of Steel Members," SFPE Handbook of Fire Protection Engineering, 3rd Edition, Section 4, Chapter 9, pp. 4-212 to 4-238, 2002.

[31] *Specifications for the Design, Fabrication, and Erection of Structural Steel for Building,* American Institute of Steel Construction, New York, 1978.

[32] H. Webster, "Flammability Assessment of Bulk-Packed, Rechargeable Lithium-Ion Cells in Transport Category Aircraft," U.S. Department of Transportation Federal Aviation Administration, DOT/FAA/AR-06/38, September 2006.

[33] H. Webster, "Fire Protection for the Shipment of Lithium Batteries in Aircraft Cargo Compartments," U.S. Department of Transportation Federal Aviation Administration, DOT/FAA/AR-10/31, November 2010.

[34] "Storage of Aerosol Products," FM Global Property Loss Prevention Data Sheet 7-31, FM Global, January 2012.

[35] "Fire Protection Water Demand for Nonstorage Sprinklered Properties," FM Global Loss Prevention Data Sheet 3-26, July 2011.

[36] "Storage of Class 1, 2, 3, 4 and Plastic Commodities," FM Global Loss Prevention Data Sheet 8-9, July 2011.

[37] "Ignitable Liquid Storage in Portable Containers," FM Global Loss Prevention Data Sheet 7-29, April 2012.

A APPENDIX A – REDUCED-COMMODITY TEST DATA AND RESULTS

Tests 1 - 3 were conducted with FM Global standard commodities as a preliminary evaluation of the instrumentation setup for the reduced-commodity test methodology. Limited data were acquired and the results are not included in this report.

A.1 CLASS 2 COMMODITY

Tests 4 - 6 and 10 were conducted using FM Global standard class 2 commodity as described in Section 4.3.1. Due to the strong agreement between the tests, Section 6.1, only Test 10 is described in full detail and comparable graphs are provided for Tests 4 - 6.

The fourth test was conducted on August 21, 2012, at 11:15 am under the 5-MW fire products collector (FPC) located in the Calorimetry Laboratory. Environmental conditions inside the lab were as follows: dry-bulb temperature, 25^{o}C (77^{o}F) and relative humidity, 42%.

The fifth test was conducted on August 22, 2012, at 1:30 pm under the 5-MW FPC located in the Calorimetry Laboratory. Environmental conditions inside the lab were as follows: dry-bulb temperature, 25^{o}C (77^{o}F) and relative humidity, 43%.

The sixth test was conducted on August 23, 2012, at 1:30 pm under the 5-MW FPC located in the Calorimetry Laboratory. Environmental conditions inside the lab were as follows: dry-bulb temperature, 26^{o}C (79^{o}F) and relative humidity, 48%.

The tenth test was conducted on August 30, 2012, at 2:00 pm under the 5-MW FPC located in the Calorimetry Laboratory. Environmental conditions inside the lab were as follows: dry-bulb temperature, 25^{o}C (77^{o}F) and relative humidity, 34%.

For all tests, the fuel array consisted of an open-frame, single-row rack in a reduced-commodity pallet design as described in Section 4.2 The array dimensions measured approximately 2.4 m long x 1 m wide (8 ft x 3.25 ft) in a 2 pallet load long x 1 pallet load wide arrangement. A three-pallet-load-high configuration was used, representing storage up to 4.6 m (15 ft) high. Ignition

was achieved with a 0.4 m (16 in.) diameter propane ring burner centered in the transverse flue 0.15 m (6 in.) below the second-tier test commodity. Propane was supplied at a rate of 30 L/min (1.06 ft^3/min) for the entire test, resulting in a nominal 45 kW continuous heat release rate.

Visual observations were made looking at the north face of the test array, which consisted of the reduced-commodity portion of the pallet load design, shown in Figure 4-1 of Section 4.2 in the main text. Figure A-1 through Figure A-4 show a photographic time evolution of the fire in 30 s increments for Tests 4 through 6 and 10, respectively. The propane burner was lit and the test time started at 0 min. For Test 10, during initial growth the fire spread upward in the central flue with flames extending above the top of the array 50 s after ignition. At 1 min 10 s, flames reached the north face of the array on the third tier and began to spread laterally. By 1 min 40 s the entire north face of the commodity was involved in the fire and flames extended three-quarters across the underside of the wood pallets on the third tier. By 5 min the majority of the commodity on both tiers was involved in the fire. The test was terminated by a water hose stream at 6 min 8 s. A similar fire development was seen for Tests 4 through 6 and is not reiterated here.

Time-resolved heat release rate data based on convective flow measurements for Tests 4 through 6 and 10 are shown in Figure A-5. Comparable heat release rate data based on oxygen consumption and carbon monoxide/dioxide care shown in Figure A-6 and Figure A-7, respectively. In each figure, the test time has been slightly offset to align the initial fire growth periods. Additionally, the notable increase in the heat release rate starting at 200 s for Test 6 occurred as the aluminum foil covering part of the carton fell away, allowing unwanted fire propagation along the previously unexposed combustible material. Due to an instrumentation failure, no heat release based on carbon monoxide/dioxide generation was reported for Tests 4 through 6 in Figure A-7.

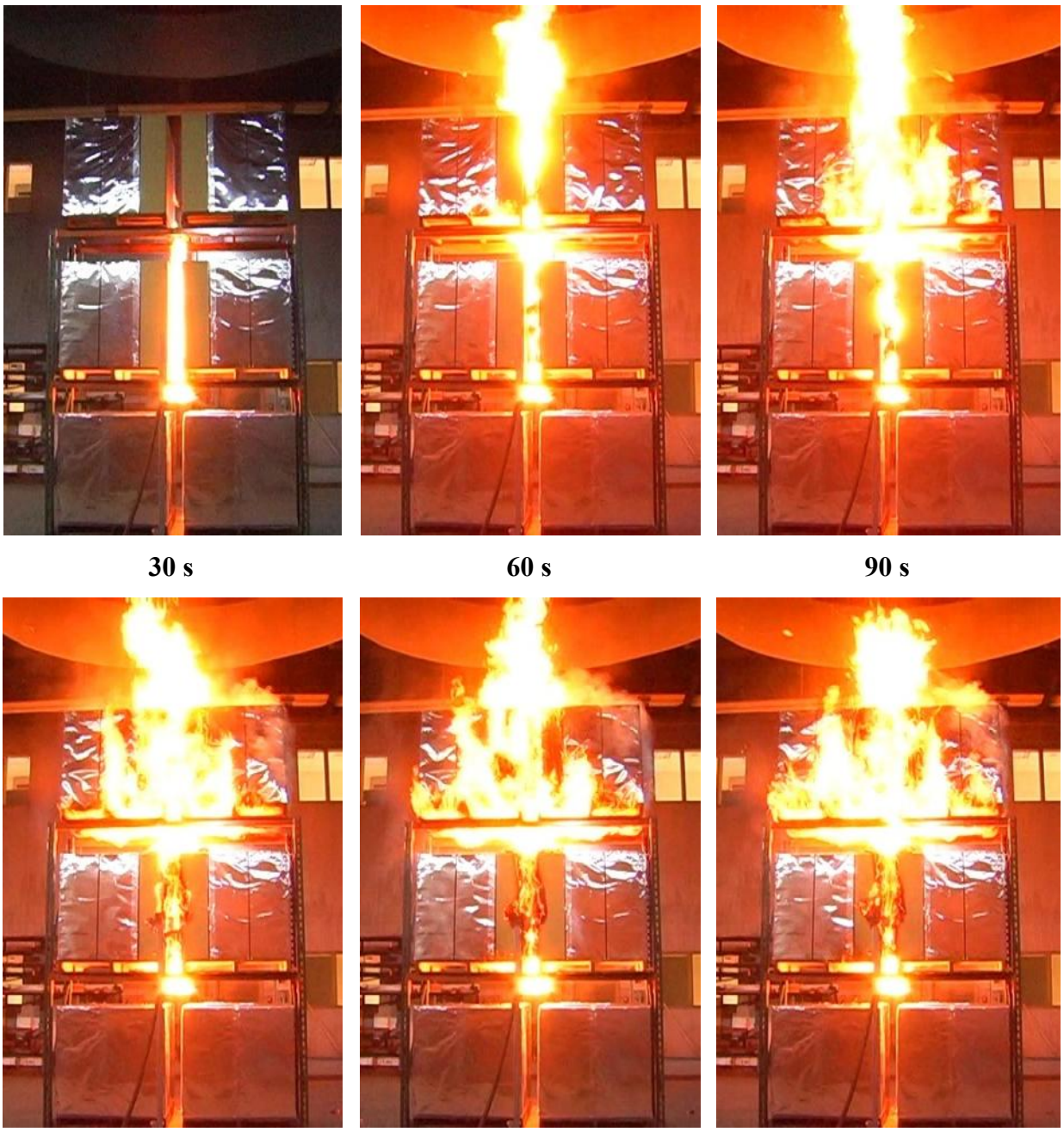

30 s **60 s** **90 s**

120 s **150 s** **180 s**

Figure A-1: Photographic time evolution of fire - Test 4

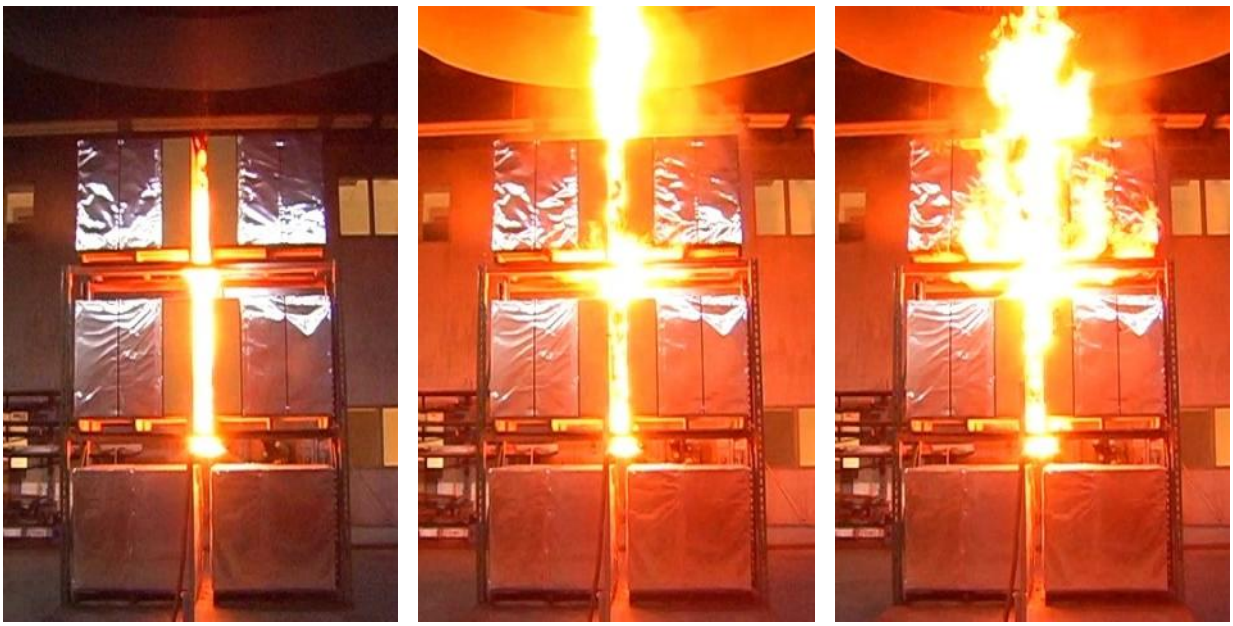

30 s **60 s** **90 s**

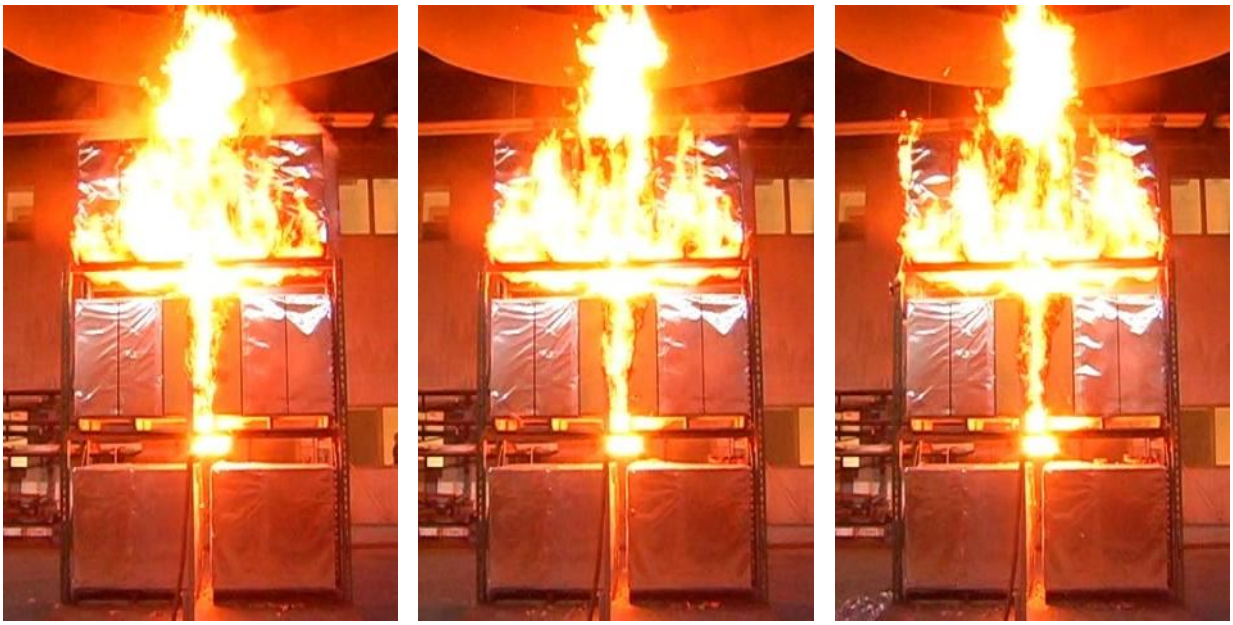

120 s **150 s** **180 s**

Figure A-2: Photographic time evolution of fire - Test 5

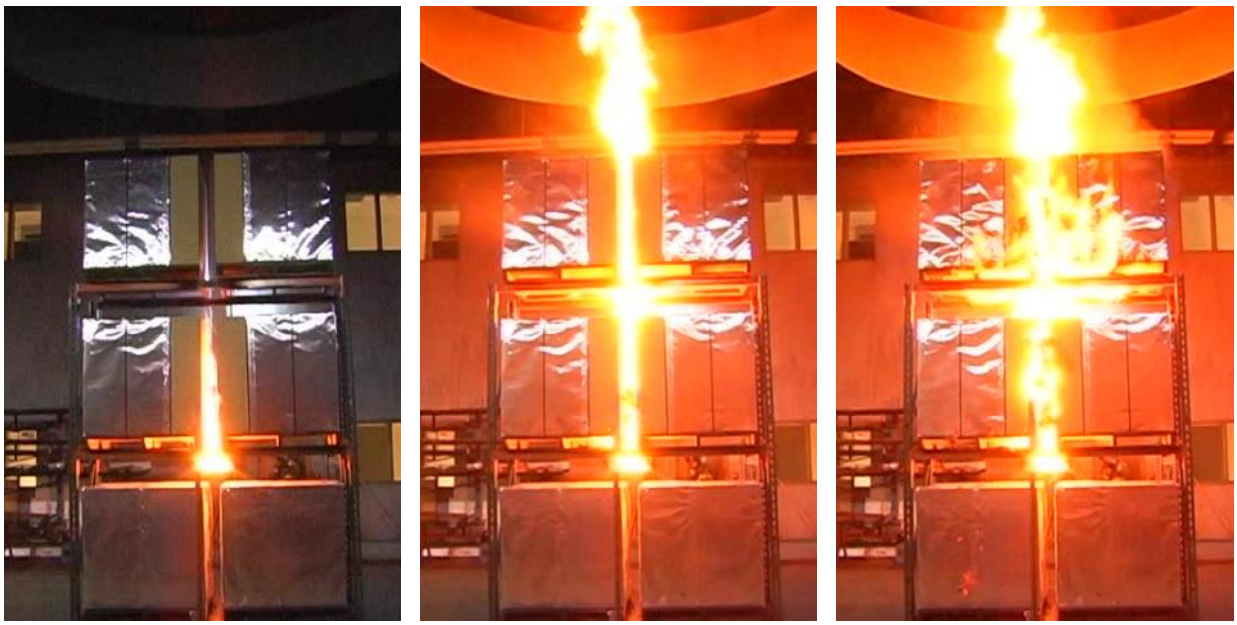

30 s **60 s** **90 s**

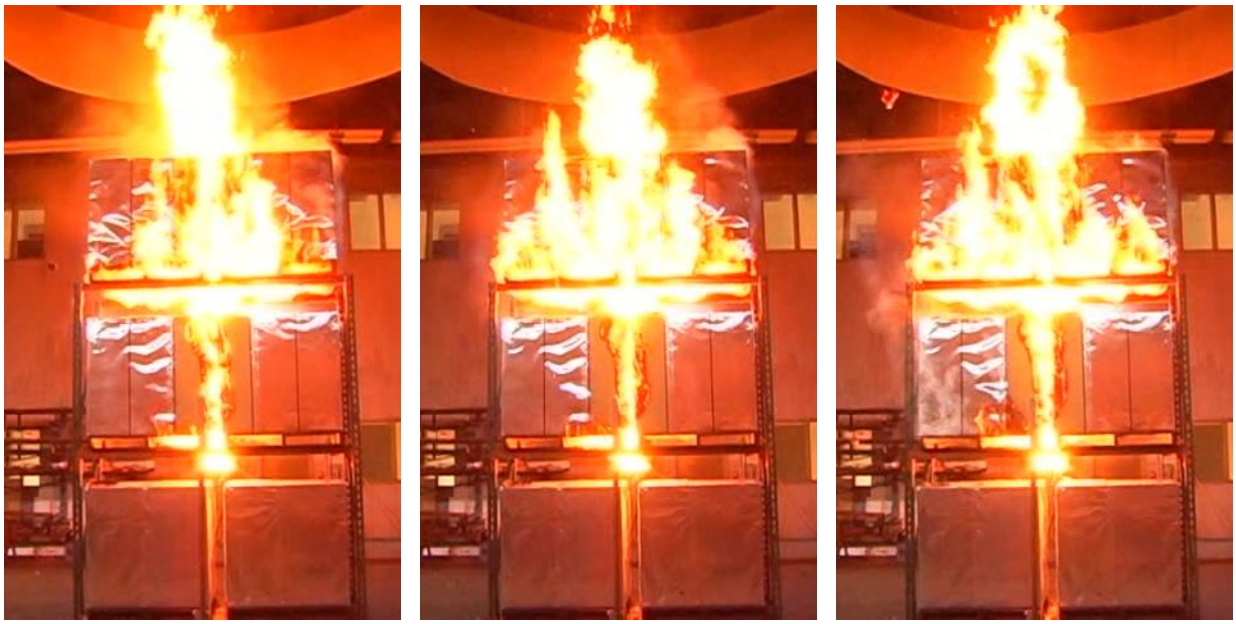

120 s **150 s** **180 s**

Figure A-3: Photographic time evolution of fire - Test 6

30 s **60 s** **90 s**

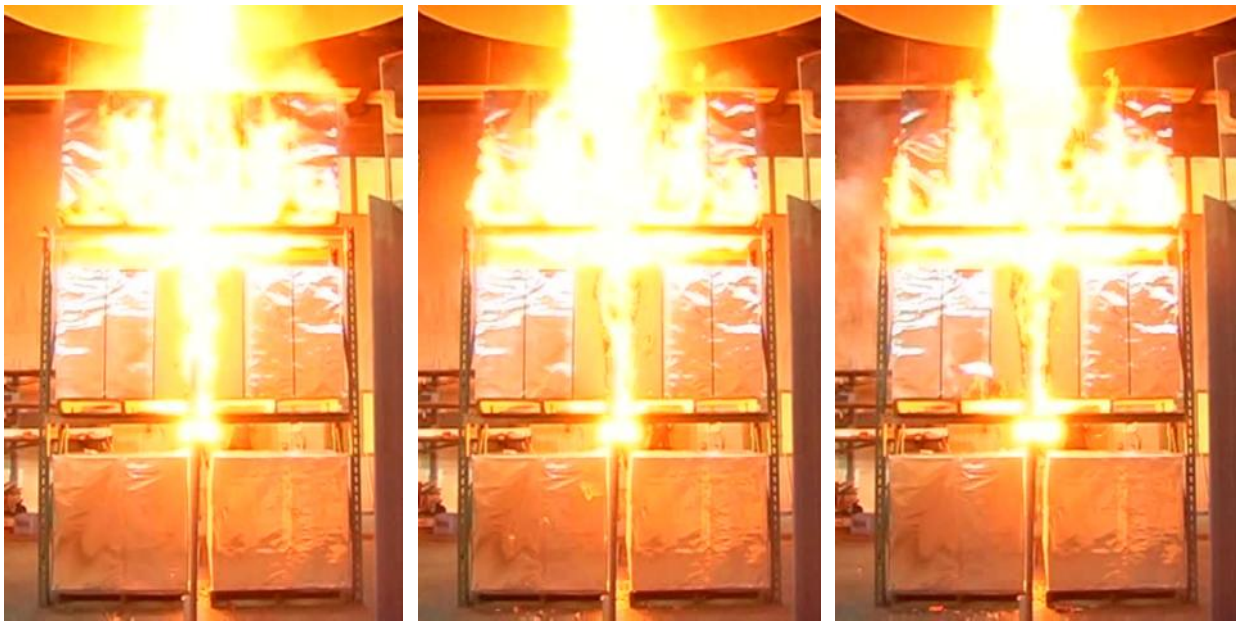

120 s **150 s** **180 s**

Figure A-4: Photographic time evolution of fire - Test 10

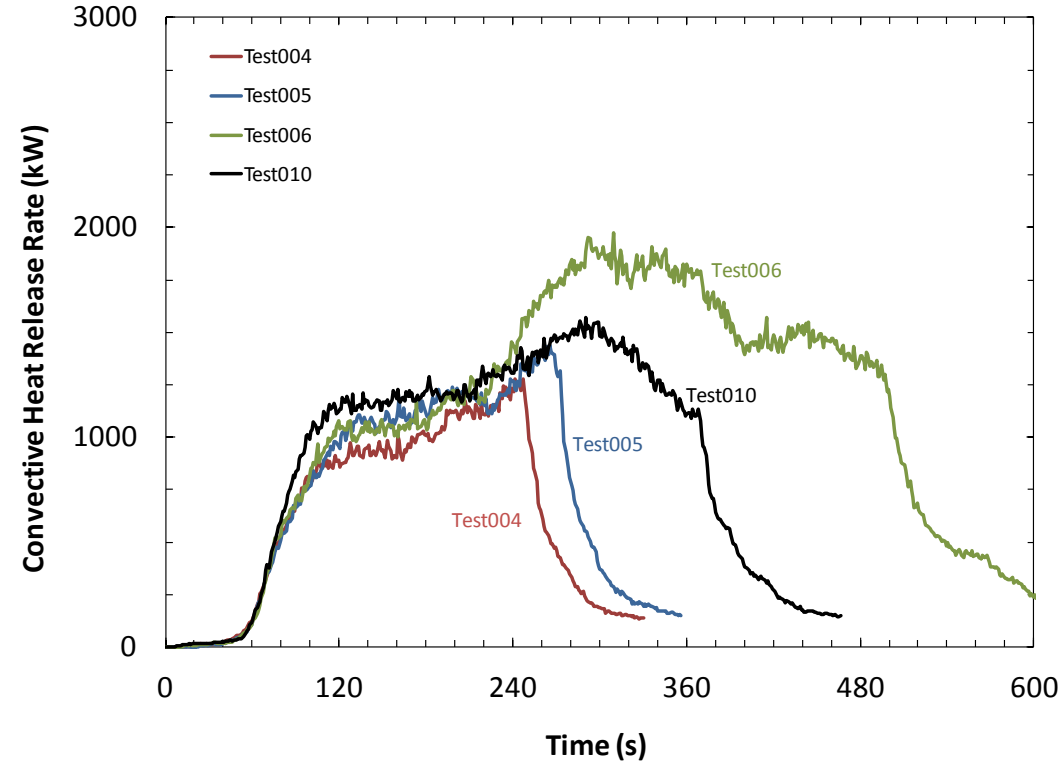

Figure A-5: Convective heat release rates for Tests 4 - 6, 10

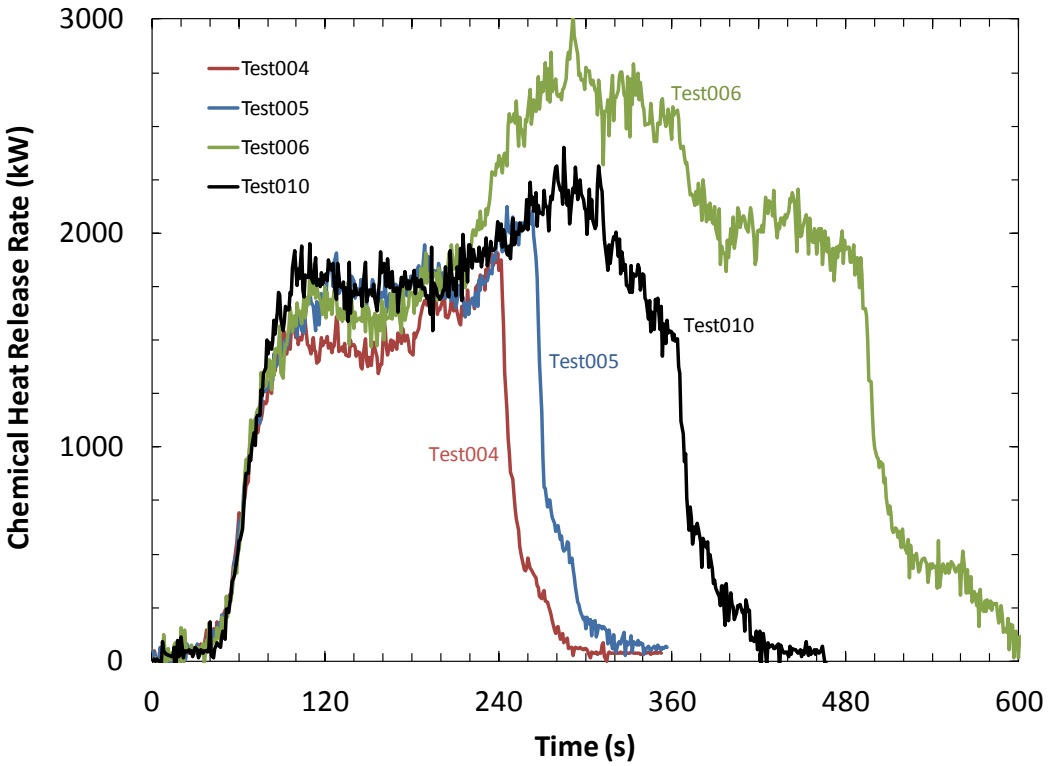

Figure A-6: Chemical heat release rates based on oxygen consumption (HRRO2) for Tests 4 - 6, 10

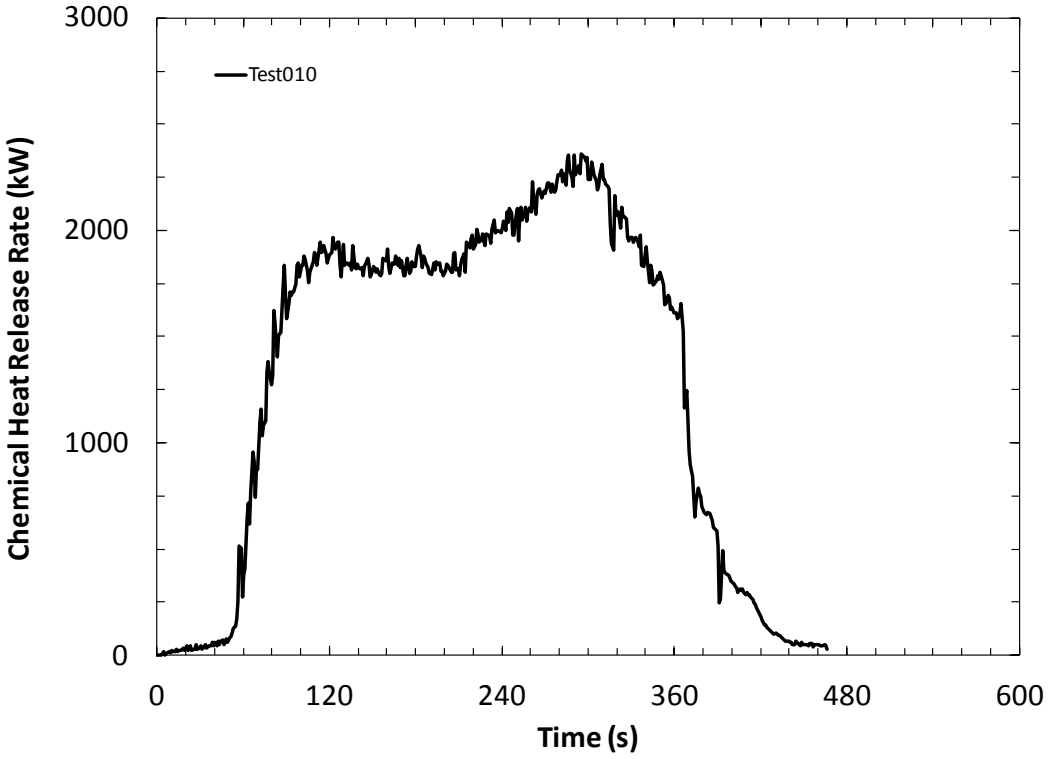

Figure A-7: Chemical heat release rates based on carbon monoxide/dioxide generation (HRRCOCO2) for Tests 4 - 6, 10

A.2 CUP COMMODITY

Tests 7 through 9 were conducted using FM Global standard cartoned unexpanded plastic (CUP) commodity as described in Section 4.3.1. Due to the strong agreement between the tests, discussed in Section 6.1, only Test 7 is described in full detail and comparable graphs are provided for Tests 8 and 9.

The seventh test was conducted on August 24, 2012, at 2:15 pm under the 5-MW fire products collector (FPC) located in the Calorimetry Laboratory. Environmental conditions inside the lab were as follows: dry-bulb temperature, 26^{o}C (79^{o}F) and relative humidity, 49%.

The eighth test was conducted on August 27, 2012, at 1:15 pm under the 5-MW FPC located in the Calorimetry Laboratory. Environmental conditions inside the lab were as follows: dry-bulb temperature, 26^{o}C (78^{o}F) and relative humidity, 59%.

The ninth test was conducted on August 28, 2012, at 1:45 pm under the 5-MW FPC located in the Calorimetry Laboratory. Environmental conditions inside the lab were as follows: dry-bulb temperature, 26°C (79°F) and relative humidity, 62%.

For each test, the fuel array consisted of an open-frame, single-row rack in a reduced-commodity pallet design as described in Section 4.2. The array dimensions measured approximately 2.4 m long x 1 m wide (8 ft x 3.25 ft) in a two-pallet-load-long x one-pallet-load-wide arrangement. A three-pallet-load-high configuration was used, representing storage up to 4.6 m (15 ft) high. Ignition was achieved with a 0.4 m (16 in.) diameter propane ring burner centered in the transverse flue 0.15 m (6 in.) below the second-tier test commodity. Propane was supplied at a rate of 30 L/min (1.06 ft^3/min) for the entire test, resulting in a nominal 45 kW continuous heat release rate.

Visual observations were made looking at the north face of the test array, which consisted of the reduced-commodity portion of the pallet load design, shown in Figure 4-1 of Section 4.2. Figure A-8 through Figure A-10 show a photographic time evolution of the fire in 30 s increments for Tests 7 through 9, respectively. The propane burner was lit and the test time started at 0 min. For Test 7, during initial growth the fire spread rapidly upward in the central flue with flames extending above the top of the array 30 s after ignition. At 50 s, flames reached the north face of the array on the third tier and began to spread laterally. By 1 min 25 s the entire north face of the commodity was involved in the fire and flames extended three-quarters across the underside of the wood pallets on the third tier. A small quantity of plastic was dripping from the commodity and pooling at the base of the array. By 2 min 15 s the majority of the commodity on both tiers was involved in the fire. The test was terminated by a water hose stream at 4 min 8 s. A similar fire development was seen for Tests 8 and 9 and is not reiterated here.

Time-resolved heat release rate data based on convective flow measurements for Tests 7 through 9 are shown in Figure A-11. Comparable heat release rate data based on oxygen consumption and carbon monoxide/dioxide are shown in Figure A-12 and Figure A-13, respectively. In all cases the data show good repeatability for the duration of the test.

It should be noted that, for this composite commodity comprised of corrugated board cartons and unexpanded plastic cups, the HRR-COCO2 calculation has up to 10% greater uncertainty than HRR-O2. This is due to the net heats of complete combustion per unit of species measured, which are similar for oxygen consumption but vary by ~10% for carbon monoxide/dioxide generation[a]. This is evident in Figure A-13 as an under-prediction of the HRR-COCO2 after the initial fire growth phase (~100 s) when the plastic cups become involved in the fire.

[a] A. Tewarson, "Generation of Heat and Chemical Compounds," SFPE Handbook of Fire Protection Engineering, 3rd Edition, Section 3, Chapter 4, pp. 3-82 to 3-161, March 2002.

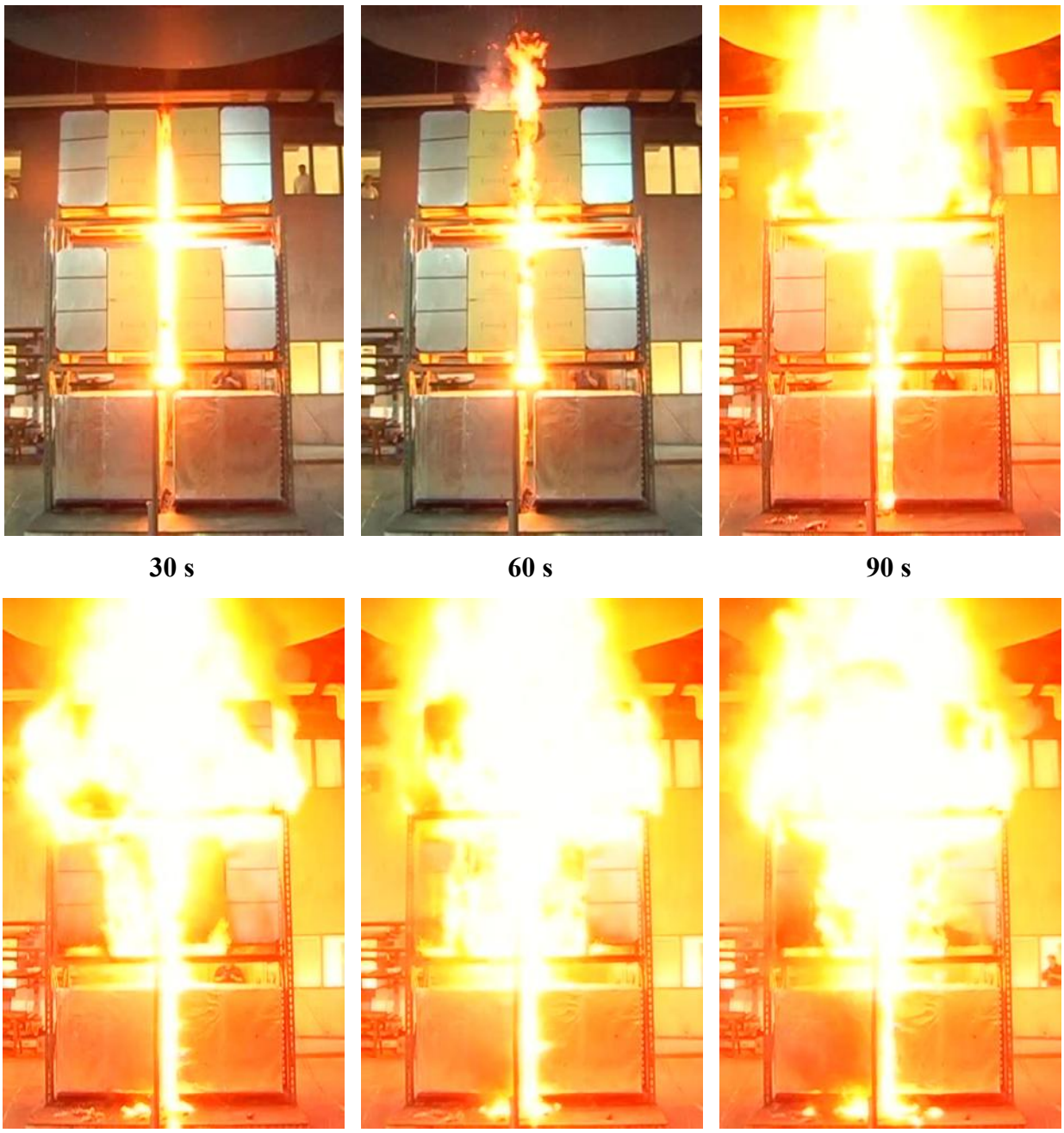

Figure A-8: Photographic time evolution of fire - Test 7

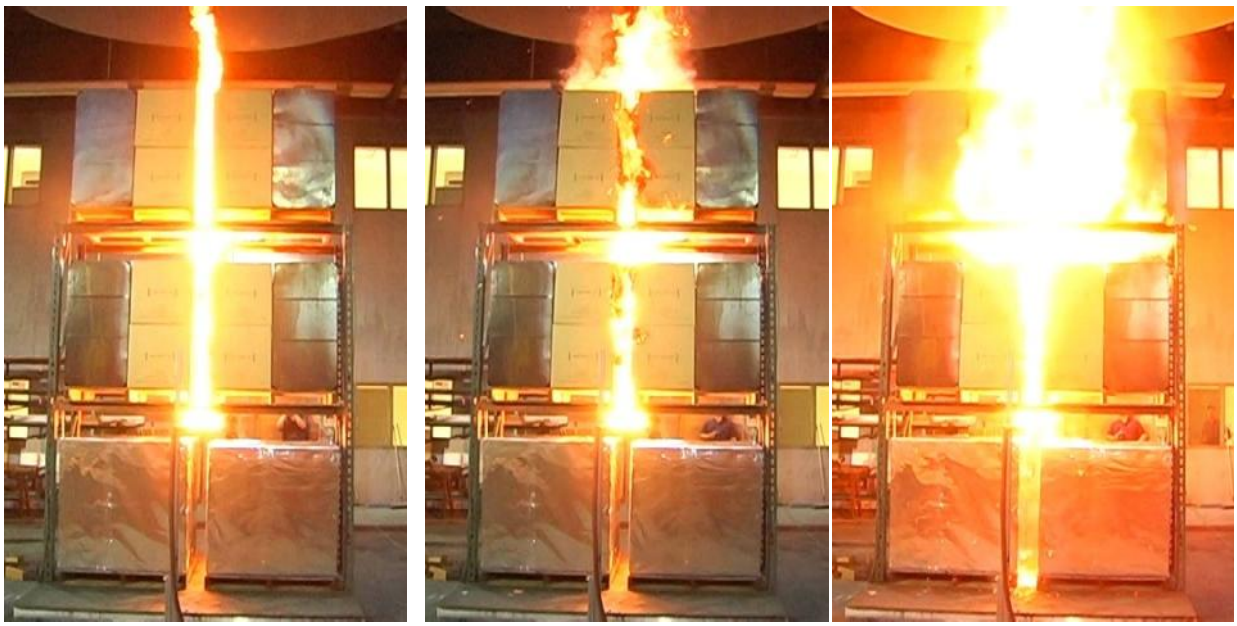

30 s **60 s** **90 s**

120 s **150 s** **180 s**

Figure A-9: Photographic time evolution of fire - Test 8

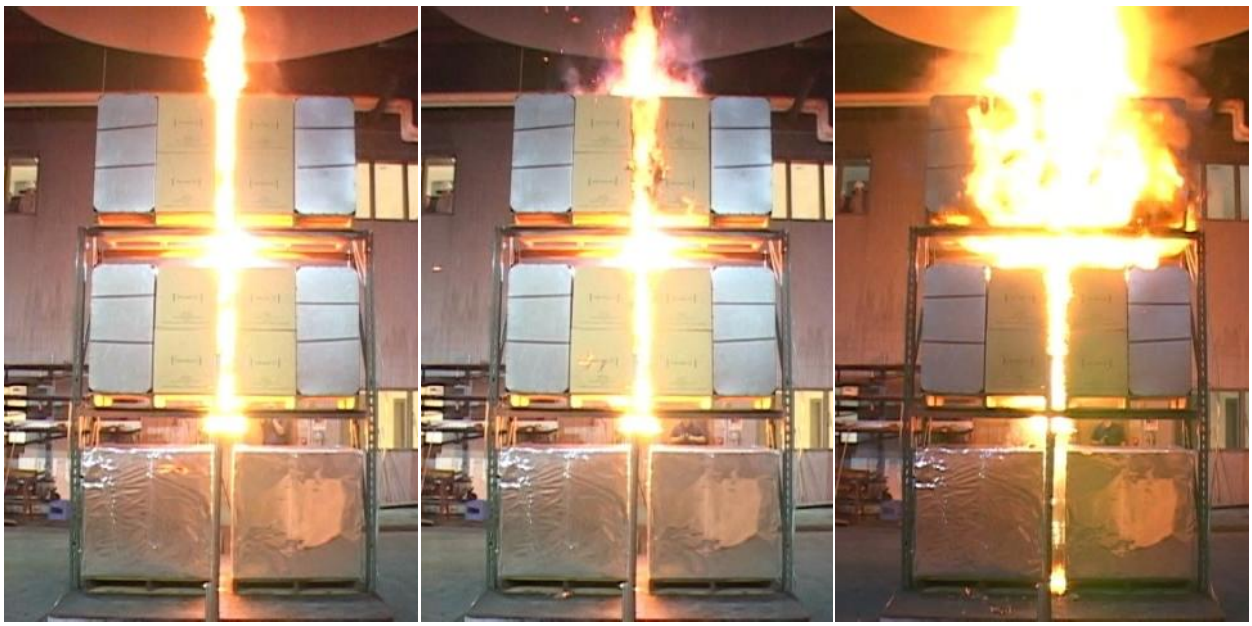

30 s **60 s** **90 s**

120 s **150 s** **180 s**

Figure A-10: Photographic time evolution of fire - Test 9

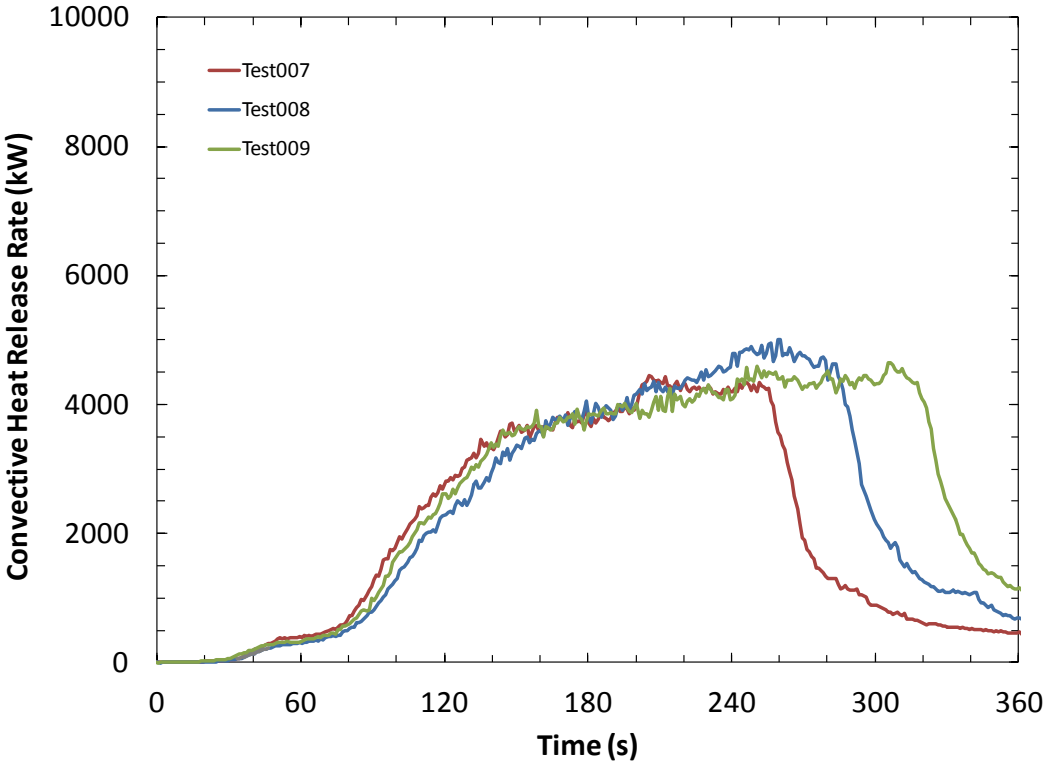

Figure A-11: Convective heat release rates for Tests 7 - 9

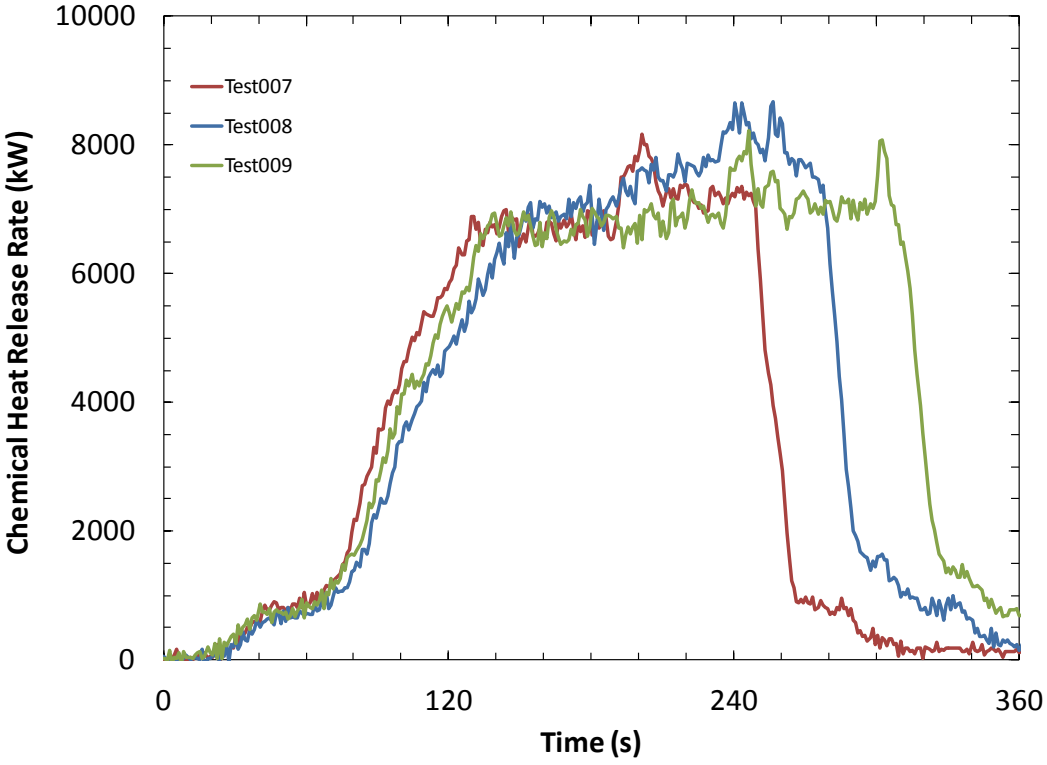

Figure A-12: Chemical heat release rates based on oxygen consumption (HRRO2) for Tests 7 - 9

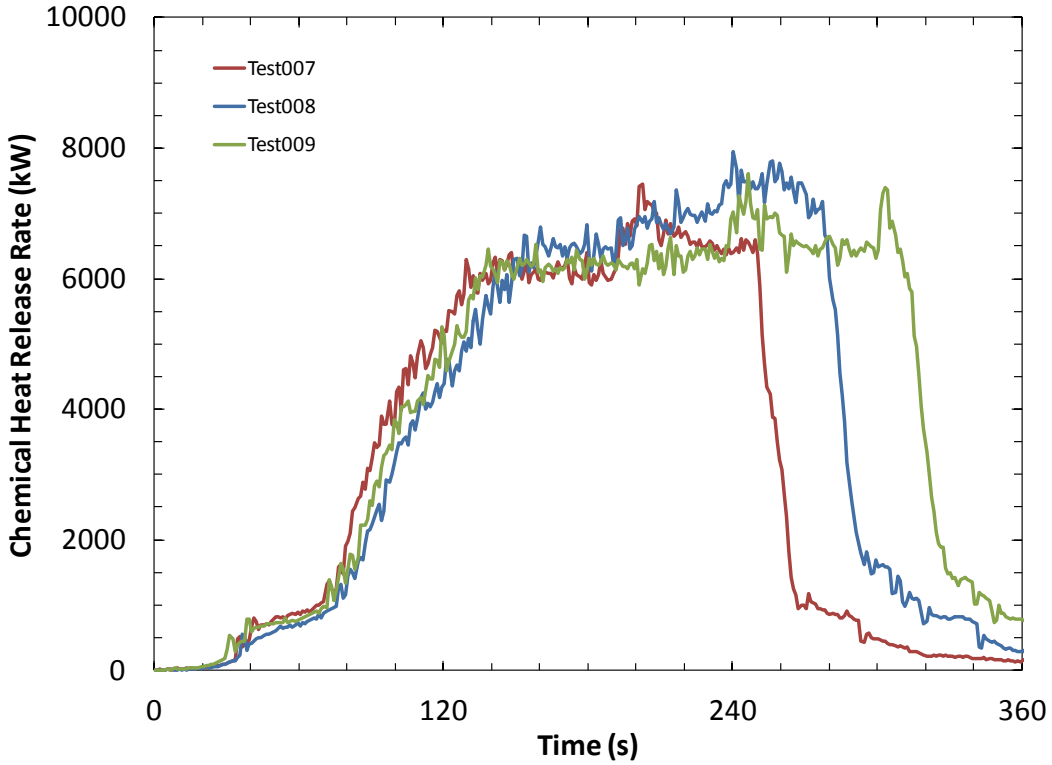

Figure A-13: Chemical heat release rates based on carbon monoxide/dioxide generation (HRRCOCO2) for Tests 7 - 9

Figure A-14 shows the measurements from the TCs located at the interface between the test commodity and the metal liner as detailed in Section 4.4 for Test 7. TCs were mechanically fastened to the metal liner along the horizontal centerline of each commodity at elevations of 0.36 m (14 in.) and 0.72 m (28 in.) above the wood pallet. These TCs are referenced by their location with the array based on tier (T2 for tier 2 or T3 for tier 3), pallet location within the array (east or west) and elevation (low = 0.36 m above pallet or high = 0.72 m above pallet). The convective heat release rate is included for reference to the time evolvement of the fire. The threshold temperature of 180°C (356°F) was added based on the oxidation temperature of electrolyte that results in a high-rate runaway reaction (peak rates > 100°C/min). For this test, the threshold temperature was first exceeded by the TC located on tier 3, east commodity, high elevation (T3EH) at 145 s after ignition. Note that the sudden reduction in measured temperature occurring after 240 s reflects the application of suppression water to terminate the test. Similar results are shown in Figure A-15 (T3EH exceeded threshold temperature at 171 s) and Figure A-16 (T3WH exceeded threshold temperature at 158 s) for Tests 8 and 9, respectively.

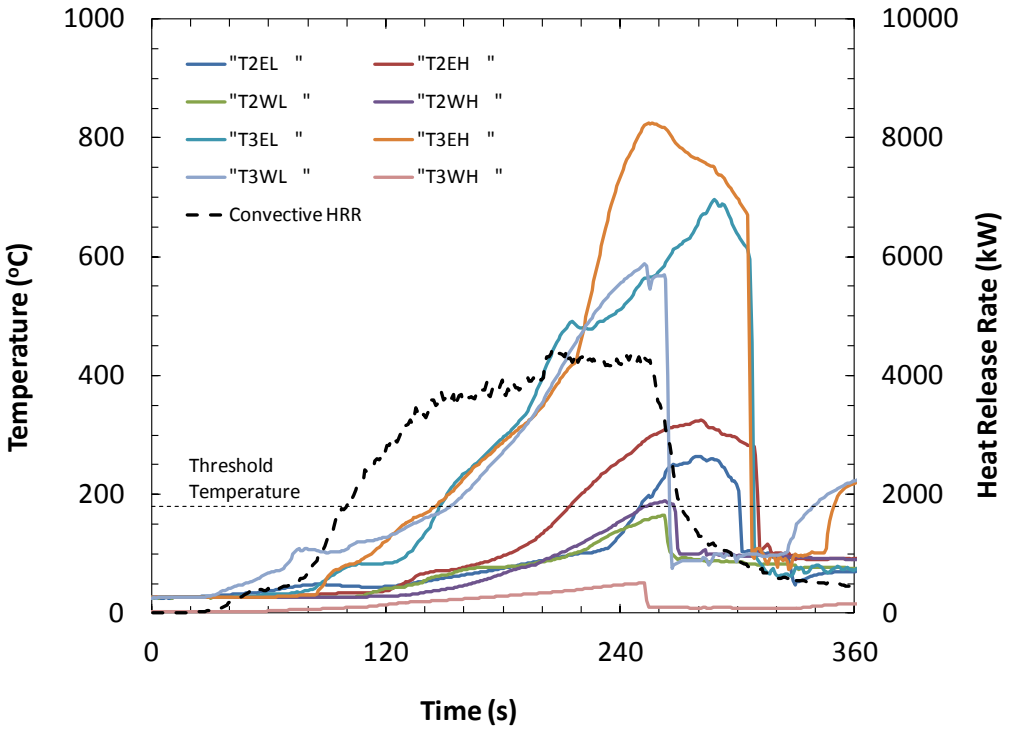

Figure A-14: Liner thermocouples - Test 7

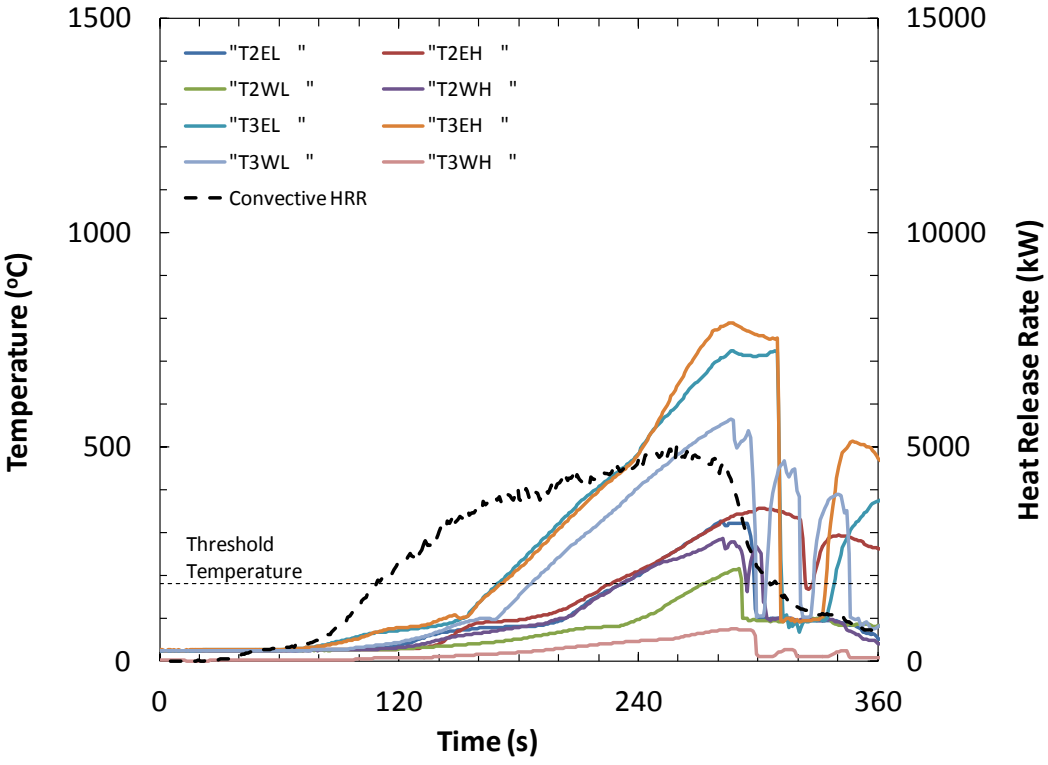

Figure A-15: Liner thermocouples - Test 8

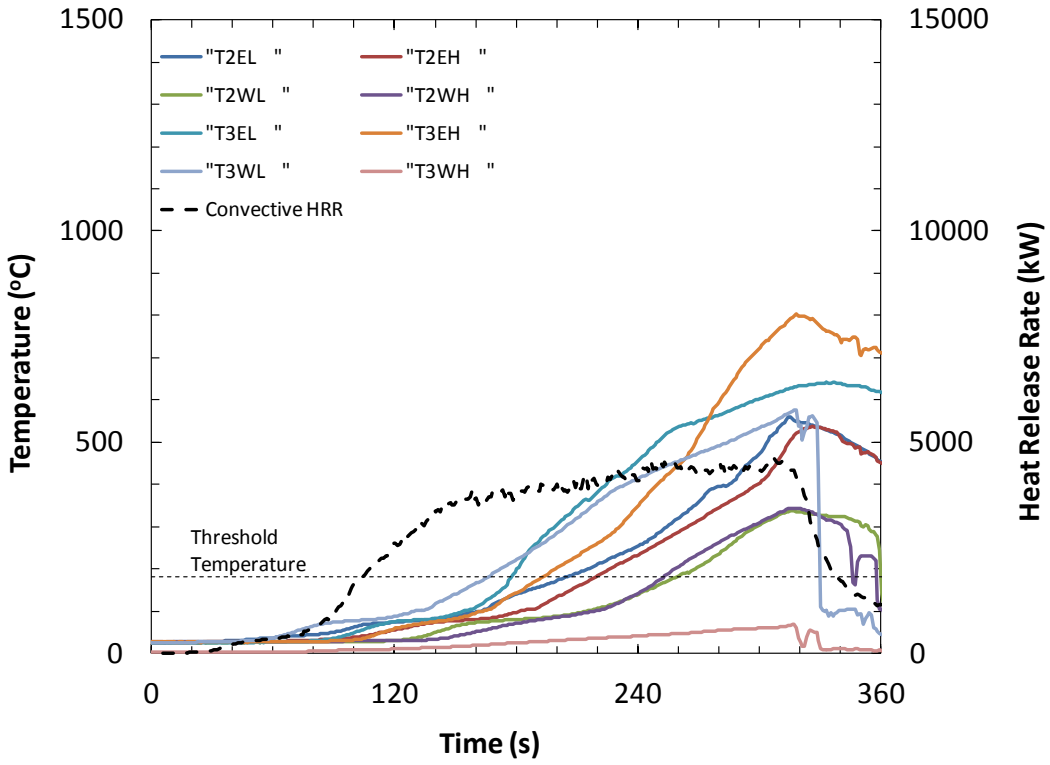

Figure A-16: Liner thermocouples - Test 9

A.3 LI-ION BATTERY COMMODITES

Tests 11 through 13 were conducted with Li-ion battery products as described in Section 4.3.2 through Section 4.3.4. The fuel array consisted of an open-frame, single-row rack in a reduced-commodity pallet design as described in Sections 4.3.2 - 4.3.4. The array dimensions measured approximately 2.4 m long x 1 m wide (8 ft x 3.25 ft) in a two-pallet-load-long x one-pallet-load-wide arrangement. A three–pallet-load-high configuration was used, representing storage heights up to 4.6 m (15 ft). Ignition was achieved with a 0.4 m (16 in.) diameter propane ring burner centered in the transverse flue 0.15 m (6 in.) below the second-tier test commodity. Propane was supplied at a rate of 30 L/min (1.06 ft^3/min) for the entire test, resulting in a nominal 45 kW continuous heat release rate.

A.3.1 Cylindrical Cells

The eleventh test was conducted on September 12, 2012, at 10:45 am under the 5-MW FPC located in the Calorimetry Laboratory. Environmental conditions inside the lab were as follows: dry-bulb temperature, 23°C (74°F) and relative humidity, 45%. The test commodity was cartoned bulk-packed 18650-format Li-ion cylindrical cells as described in Section 4.3.2.

Visual observations were made looking at the north face of the test array, which consisted of the reduced-commodity portion of the pallet load design, shown in Figure 4-1 of Section 4.2 in the main text. Figure A-17 and Figure A-18 show a photographic time evolution of the fire. The propane burner was lit and the test time started at time 0. The initial fire growth spread rapidly upward in the central flue with flames extending above the top of the array 41 s after ignition. At 1 min 0 s, flames began to spread laterally on the third-tier north face. Sporadic collapse of power tools began at 1 min 4 s with an estimated 19 packs (of the 200 in the test array) falling over a 30 s period. By 1 min 25 s the entire north face of the commodity was involved in the fire and flames extended halfway across the underside of the wood pallets on the third tier. Additional collapse of the power tool packs occurred at 1 min 45 s. The majority of the cartons and contained power tool packs was involved in the fire by 2 min 30 s and blue flames were visible on both tiers. Intermittent suppression water was applied to the collapsed commodity burning away from the test array from approximately 46 min to 48 min. The test was terminated by a water hose stream at 48 min. No reignition of suppressed batteries occurred during the extinguishment process.

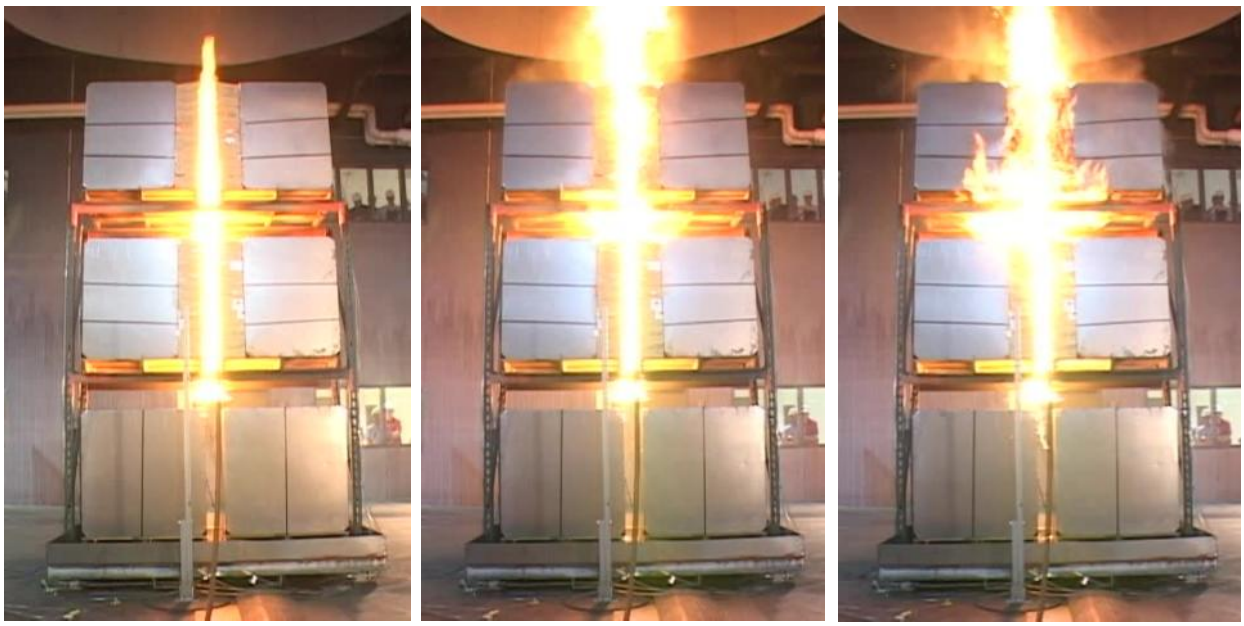

30 s **60 s** **90 s**

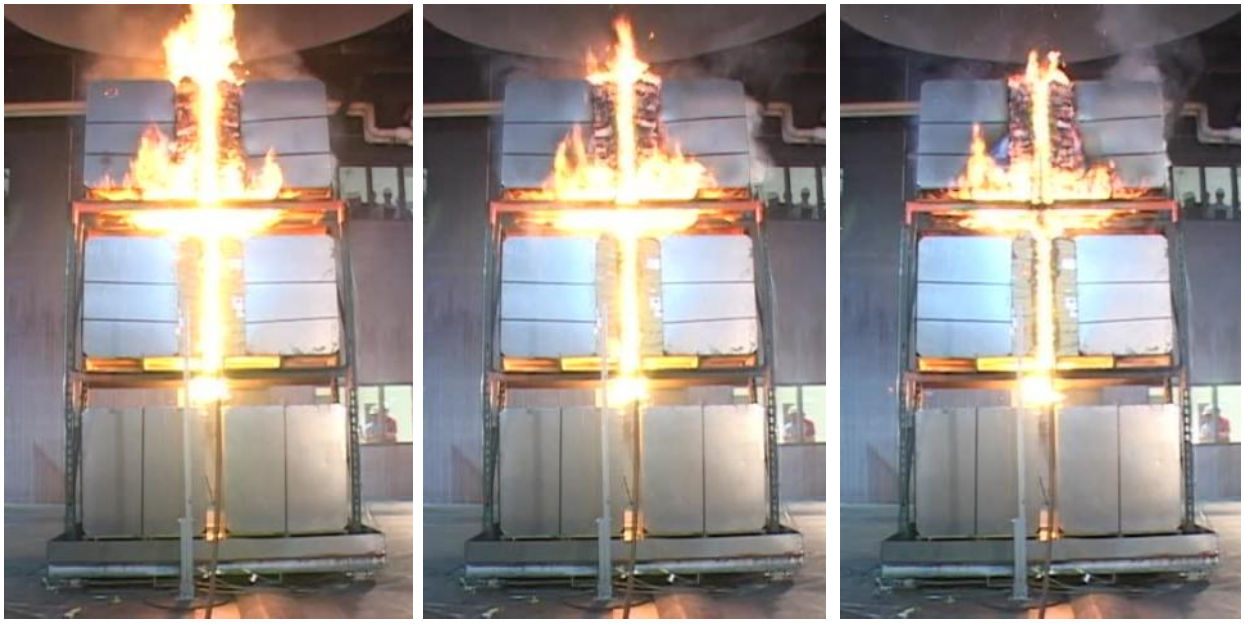

120 s **150 s** **180 s**

Figure A-17: Photographic time evolution of fire - Test 11

240 s **360 s** **480 s**

600 s **720 s** **840 s**

Figure A-18: Photographic time evolution of fire - Test 11 (continued)

Figure A-19 presents the convective heat release rate measurements based on the gas flow within the exhaust duct. Based on these measurements, an estimated 2,400 ± 250 MJ (230 ± 240 BTUx10^3) of convective energy was released during data collection (1,420 s total). Generation rates of carbon dioxide and carbon monoxide (HRR-$COCO_2$), and oxygen depletion (HRR-O_2) were also acquired. However, due to measurement uncertainties related to the battery electrolyte discussed in Section 2.2, chemical heat release rates are not calculated for testing with Li-ion batteries.

Figure A-20 shows the measurements from the TCs located at the interface between the test commodity and the metal liner as detailed in Section 4.4. TCs were mechanically fastened to the metal liner along the horizontal centerline of each commodity at elevations of 0.36 m (14 in.) and 0.72 m (28 in.) above the wood pallet. These TCs are referenced by their location with the array based on tier (T2 for tier 2 or T3 for tier 3), pallet location within the array (east or west) and elevation (low = 0.36 m above pallet or high = 0.72 m above pallet). The convective heat release rate is included for reference to the time evolvement of the fire. The threshold temperature of 180^{o}C (356^{o}F) was added based on the oxidation temperature of electrolyte that results in a high-rate runaway reaction (peak rates > 100^{o}C/min). For this test, the threshold temperature was first exceeded by the TC located on tier 3, east commodity, high elevation (T3EH) at 309 s after ignition. Note that several of the data series are truncated (T3EH, T3WL, T2WL) due to damage to the TCs, which occurred after the temperature threshold was substantially exceeded.

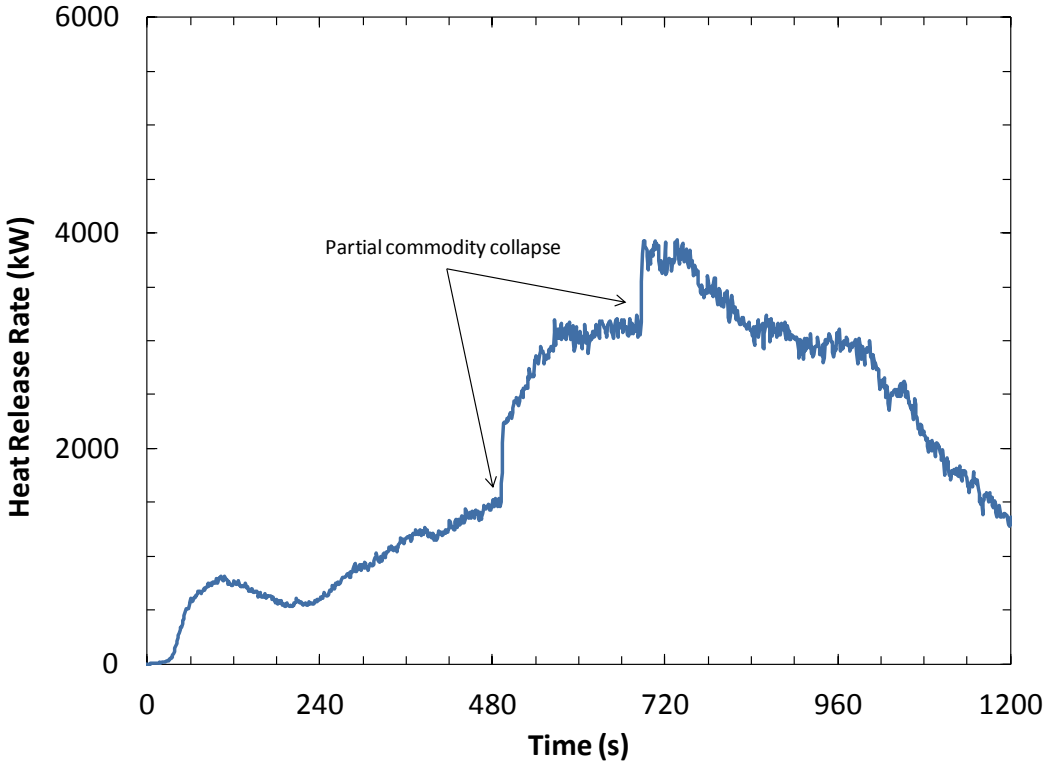

Figure A-19: Convective heat release rate - Test 11
(Chemical HRRs not included for Li-ion battery tests)

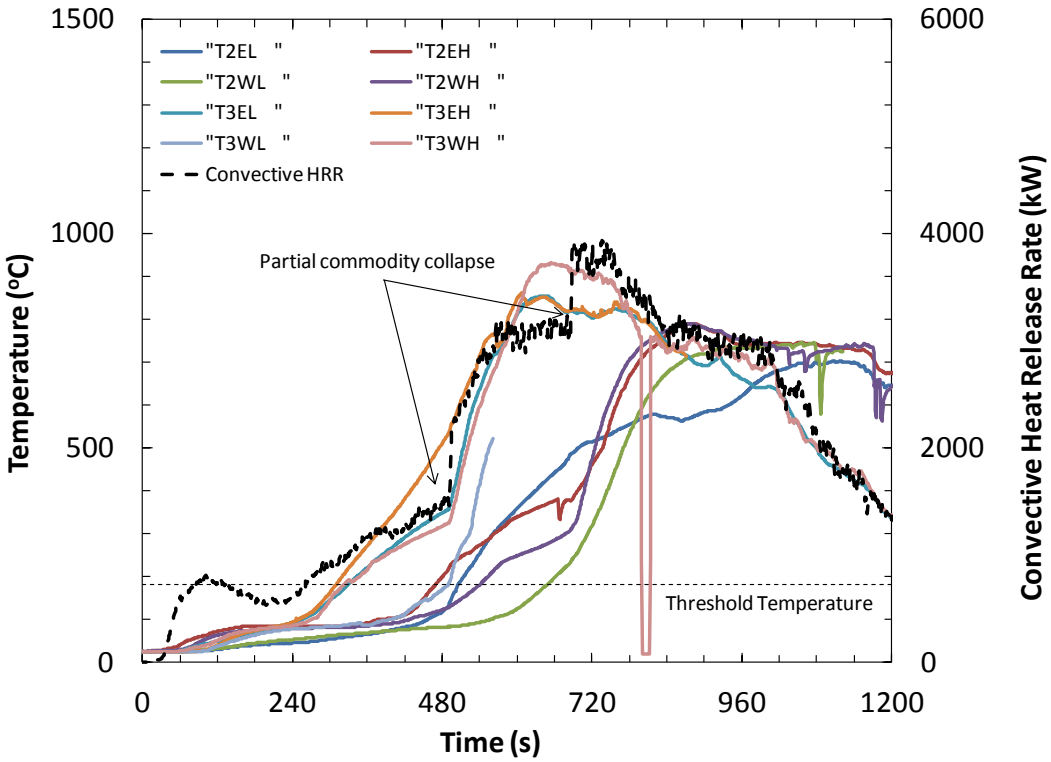

Figure A-20: Liner thermocouples - Test 11

A.3.2 Power Tool Packs

The twelfth test was conducted on September 19, 2012, at 1:15 pm under the 5-MW FPC located in the Calorimetry Laboratory. Environmental conditions inside the lab were as follows: dry-bulb temperature, 24^{o}C (75^{o}F) and relative humidity, 33%. The test commodity was cartoned bulk-packed 18 V Li-ion power tool packs cells as described in Section 4.3.3.

Visual observations were made looking at the north face of the test array, which consisted of the reduced-commodity portion of the pallet load design, shown in Figure 4-1 of Section 4.2 in the main text. Figure A-21 and Figure A-22 show a photographic time evolution of the fire. The propane burner was lit and the test time started at time 0. During initial growth the fire spread rapidly upward in the central flue with flames extending above the top of the array 28 s after ignition. At 50 s, flames began to spread laterally on the third-tier north face of commodity with full involvement occurring by 1 min 20 s. Occasional popping sounds could be heard indicating rupture of Li-ion batteries. Minor commodity collapse on the third tier occurred at 4 min 8 and small jet fires were visible exiting ruptured cells. A major collapse of the third tier commodity occurred at 8 min 17 s followed by a second tier collapse at 11 min 40 s. Intermittent suppression water was applied to the collapsed commodity burning away from the test array from approximately 17 min to 42 min. The test was terminated by a water hose stream at 42 min. Minor reignition of suppressed batteries occurred sporadically during the extinguishment process. No projectiles from ruptured cells were observed throughout the test.

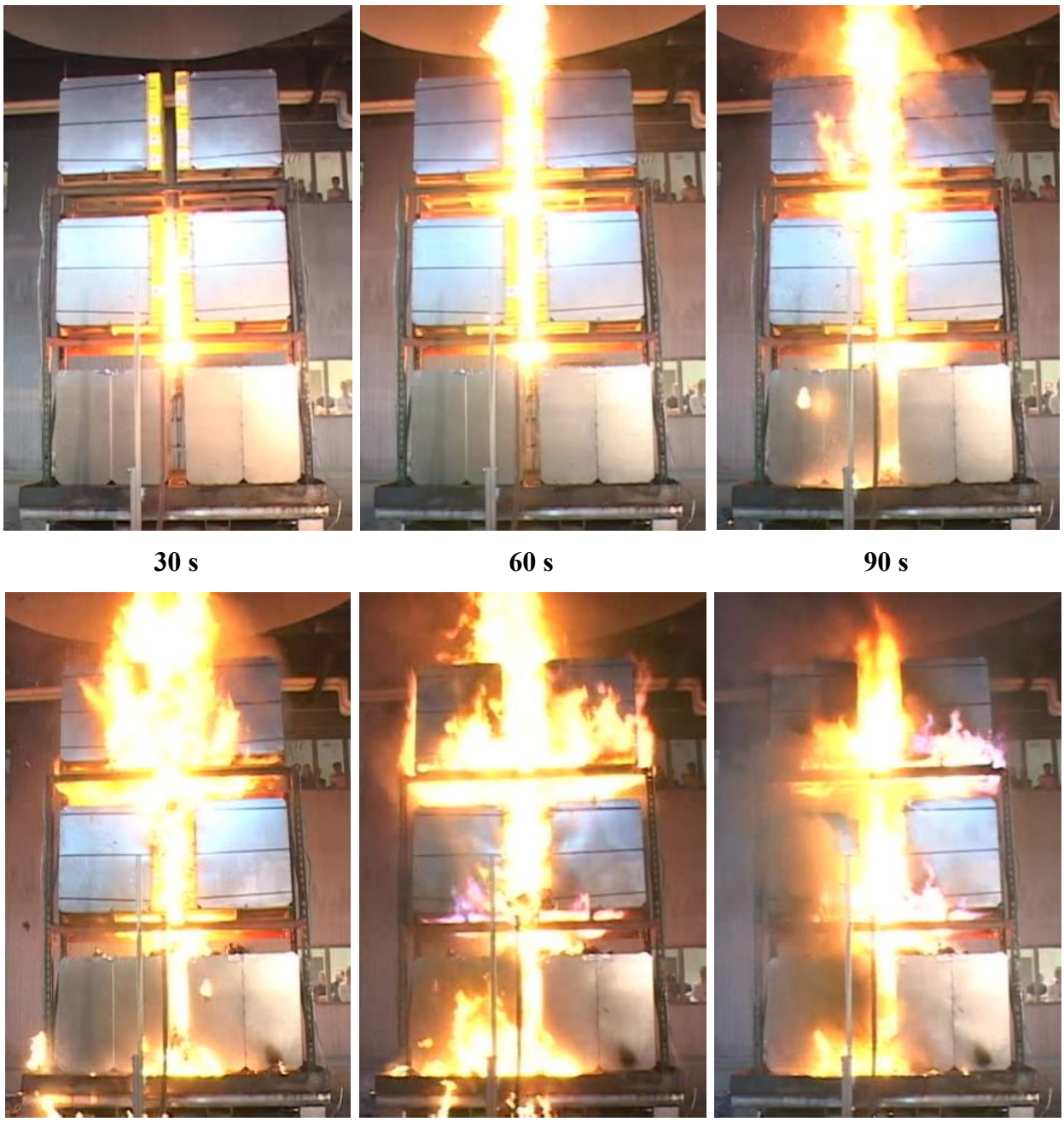

30 s **60 s** **90 s**

120 s **150 s** **180 s**

Figure A-21: Photographic time evolution of fire - Test 12

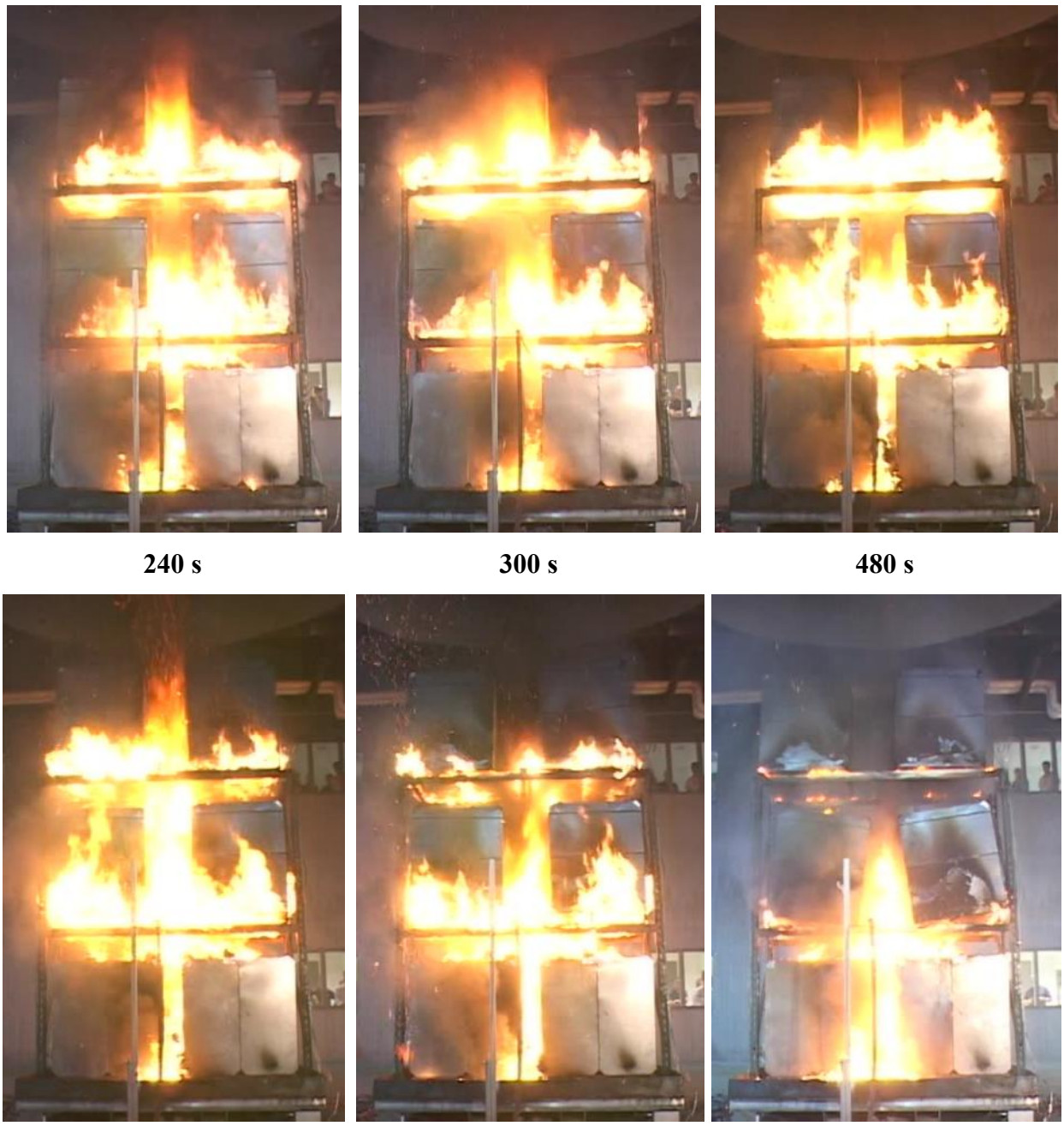

240 s **300 s** **480 s**

600 s **720 s** **1200 s**

Figure A-22: Photographic time evolution of fire - Test 12 (continued)

Figure A-23 presents the convective heat release rate measurements based on the gas flow within the exhaust duct. Based on these measurements, an estimated 1,440 ± 150 MJ (1,300 ± 140 BTUx10^3) of convective energy was released during data collection (2,440 s total). Generation rates of carbon dioxide and carbon monoxide (HRR-$COCO_2$), and oxygen depletion (HRR-O_2) were also acquired. However, due to measurement uncertainties related to the battery electrolyte discussed in Section 2.2, chemical heat release rates are not calculated for testing with Li-ion batteries.

Figure A-24 shows the measurements from the TCs located at the interface between the test commodity and the metal liner as detailed in Section 4.4. Thermocouples were mechanically fastened to the metal liner along the horizontal centerline of each commodity at elevations of 0.36 m (14 in.) and 0.72 m (28 in.) above the wood pallet. These thermocouples are referenced by their location with the array based on tier (T2 for tier 2 or T3 for tier 3), pallet location within the array (east or west) and elevation (low = 0.36 m above pallet or high = 0.72 m above pallet). The convective heat release rate is included for reference to the time evolvement of the fire. The threshold temperature of 180^{o}C (356^{o}F) was added based on the oxidation temperature of electrolyte that results in a high-rate runaway reaction (peak rates > 100^{o}C/min). For this test, the relatively low content density of the power tool packs resulted in rapid flame penetration through the commodity. The threshold temperature was first exceeded by the thermocouple located on the second tier, east commodity, high elevation (T2EH) at 122 s after ignition.

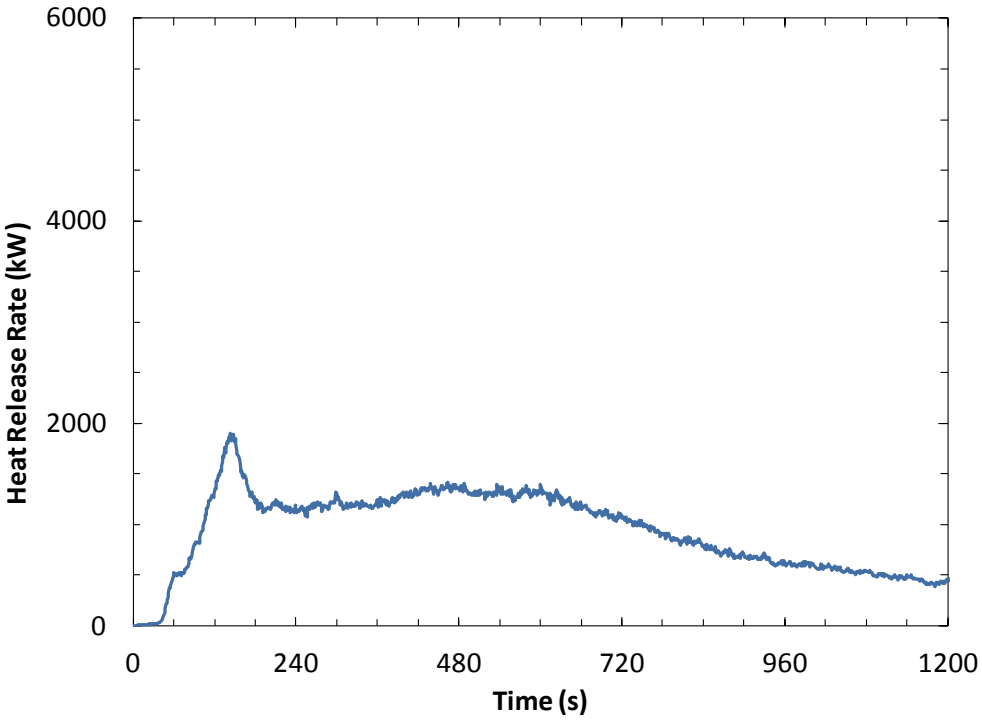

Figure A-23: Convective heat release rate - Test 12
(Chemical HRRs not included for Li-ion battery tests)

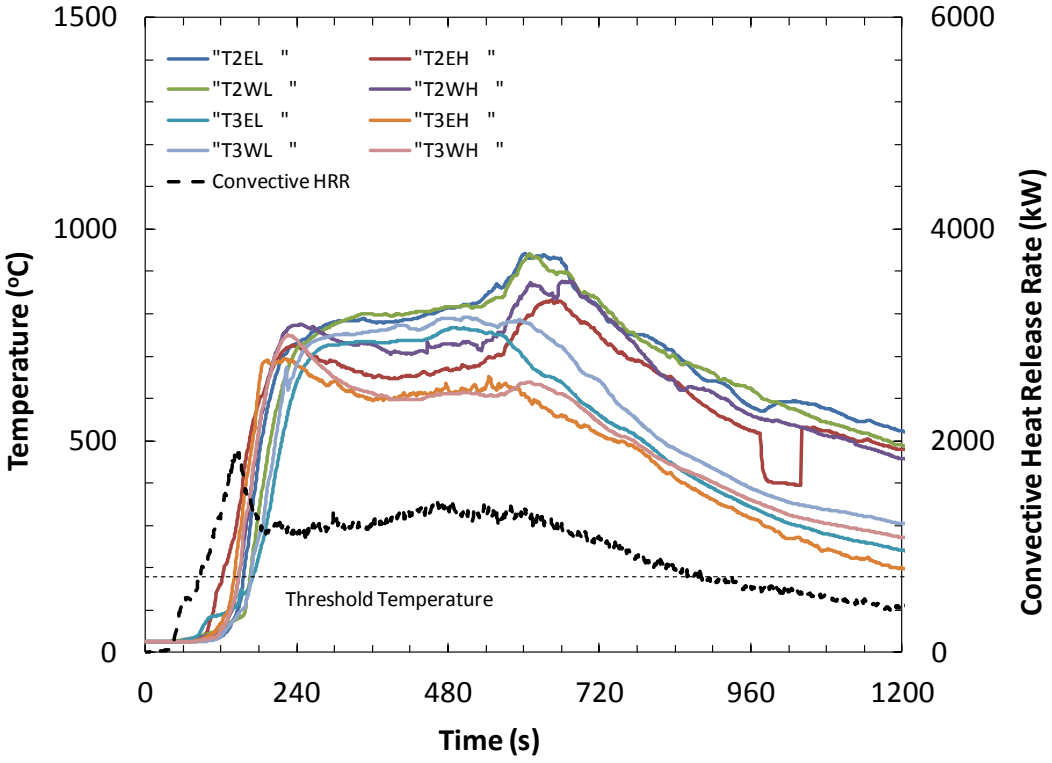

Figure A-24: Liner thermocouples - Test 12

A.3.3 Polymer Cells

The thirteenth test was conducted on October 3, 2012, at 12:15 pm under the 5-MW FPC located in the Calorimetry Laboratory. Environmental conditions inside the lab were as follows: dry-bulb temperature, 23°C (74°F) and relative humidity, 60%. The test commodity was cartoned bulk-packed Li-ion polymer cells as described in Section 4.3.4.

Visual observations were made looking at the north face of the test array, which consisted of the reduced-commodity portion of the pallet load design, shown in Figure 4-1 of Section 4.2 in the main text. Figure A-25 and Figure A-26 show a photographic time evolution of the fire. The propane burner was lit and the test time started at time 0. During initial growth the fire spread rapidly upward in the central flue with flames extending above the top of the array 23 s after ignition. At 1 min 5 s, flames began to spread laterally on the third-tier north face of commodity with full involvement occurring by 1 min 20 s. Occasional popping sounds could be heard indicating rupture of Li-ion batteries. At 5 min 50 s, a similar lateral flame spread began on the second tier and the wood pallets on the third tier were fully involved in the fire. The fire size continued to grow and blue flames were observed at several locations throughout the array. Minor commodity collapse on the third tier occurred at 8 min 35 s, followed by a major collapse at 9 min 0 s. Intermittent suppression water was applied to the collapsed commodity burning away from the test array from approximately 14 min to 15 min. The test was terminated by a water hose stream at 16 min. Minor reignition of suppressed batteries occurred sporadically during the extinguishment process.

30 s

60 s

90 s

120 s

150 s

180 s

Figure A-25: Photographic time evolution of fire - Test 13

240 s **360 s** **480 s**

600 s **720 s** **960 s**

Figure A-26: Photographic time evolution of fire - Test 13 (continued)

Figure A-27 presents the convective heat release rate measurements based on the gas flow within the exhaust duct. Based on these measurements, an estimated 2,660 ± 300 MJ (2,500 ± 280 BTUx10^3) of convective energy was released during data collection (2,380 s total). Generation rates of carbon dioxide and carbon monoxide (HRR-$COCO_2$), and oxygen depletion (HRR-O_2) were also acquired. However, due to measurement uncertainties related to the battery electrolyte discussed in Section 2.2, chemical heat release rates are not calculated for testing with Li-ion batteries.

Figure A-28 shows the measurements from the TCs located at the interface between the test commodity and the metal liner as detailed in Section 4.4. Thermocouples were mechanically fastened to the metal liner along the horizontal centerline of the each commodity at elevations of 0.36 mm (14 in.) and 0.72 mm (28 in.) above the wood pallet. These thermocouples are referenced by their location with the array based on tier (T2 for tier 2 or T3 for tier 3), pallet location within the array (east or west) and elevation (low = 0.36 m above pallet or high = 0.72 m above pallet). The convective heat release rate is included for reference to the time evolvement of the fire. The threshold temperature of 180°C (356°F) was added based on the oxidation temperature of electrolyte that results in a high-rate runaway reaction (peak rates > 100°C/min). For this test, the threshold temperature was first exceeded by the thermocouple located on tier 3, east commodity, high elevation (T3EH) at 315 s after ignition.

Figure A-29 shows the measurements from the TCs located within the test commodity. A single TC was located 0.18 m (7 in.) in from the face of each commodity at the horizontal and vertical midpoint of the commodity. These thermocouples were placed between commodity cartons and are referenced based on tier (T2 for tier 2 or T3 for tier 3) and pallet location within the array (east or west). For example, T3EC references the thermocouple located at tier 3, east pallet, at the center height of the commodity. The convective heat release rate is again included for reference to the time evolvement of the fire. The 180°C (356°F) temperature threshold was first exceeded by the thermocouple located on the east commodity on the third tier at approximately 508 s followed closely by the west commodity at 537 s; these times coincide with collapse of the third-tier commodity. The approximate 200 s delay in the heating of these thermocouples compared to the liner TCs (Figure A-28) is an unexpected result assuming heating of the TCs

was solely related to conduction through the commodity. It should be noted that the backside of the liner TCs, *i.e.*, side facing the inside of the metal liner, was not insulated. This result therefore indicates that the liner TCs probably experience additional heating from the air inside the metal liners.

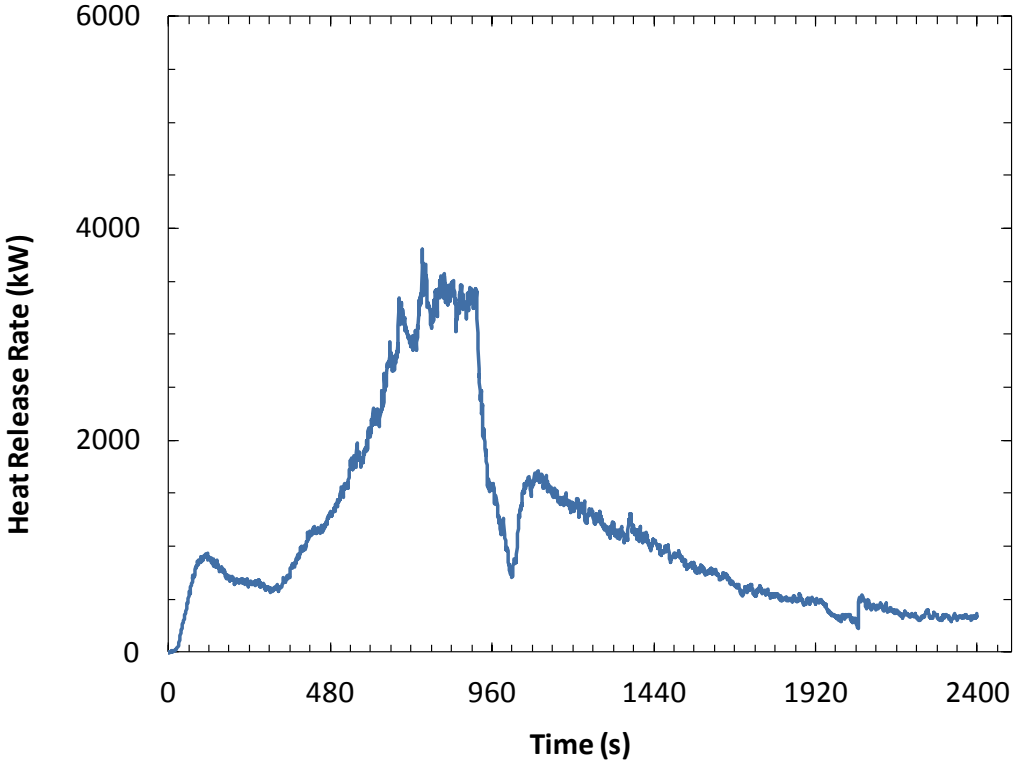

Figure A-27: Convective heat release rate - Test 13
(Chemical HRRs not included for Li-ion battery tests)

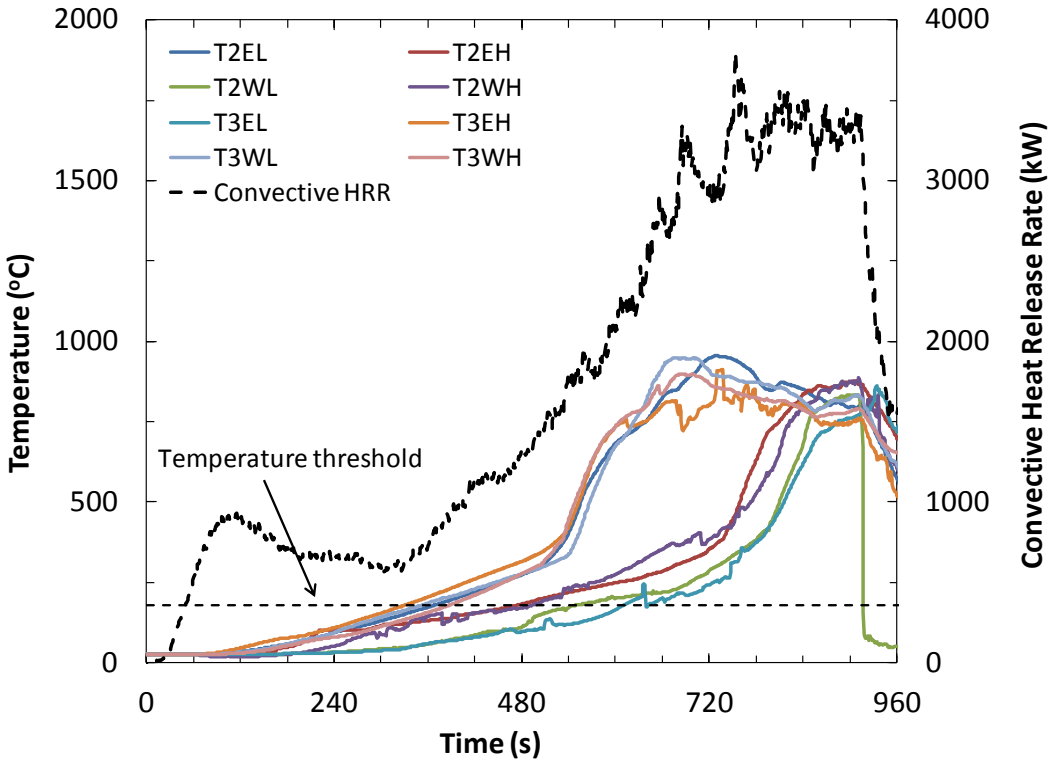

Figure A-28: Liner thermocouples - Test 13

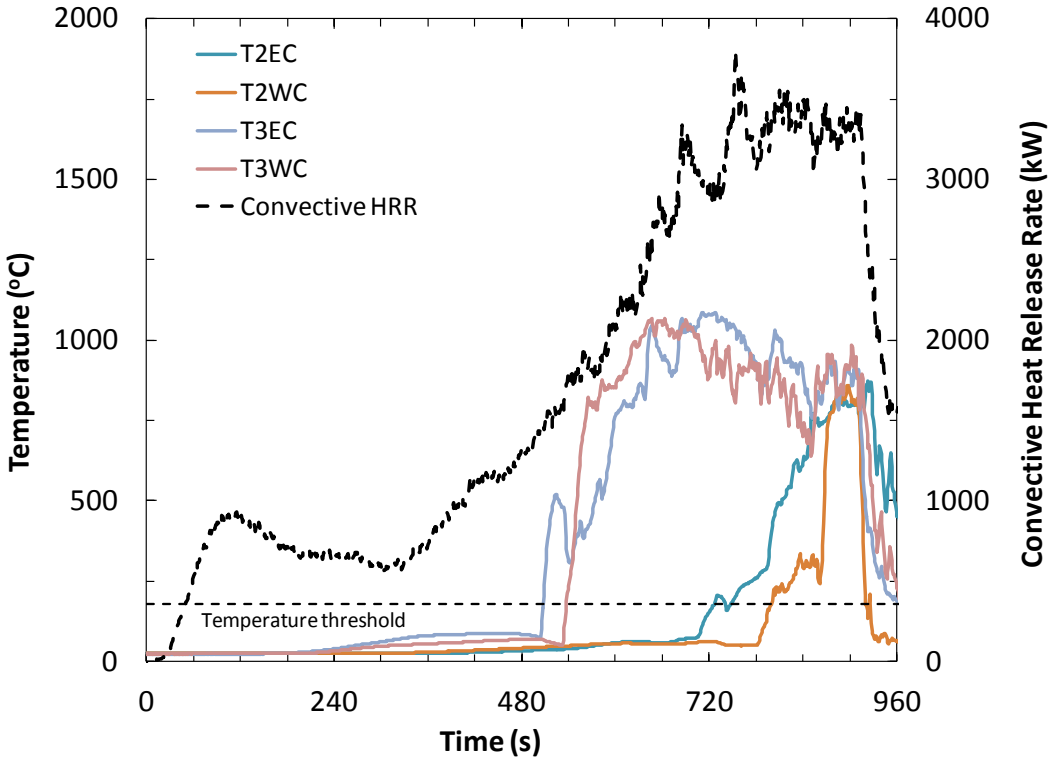

Figure A-29: Commodity thermocouples - Test 13

A.4 TEST CHRONOLOGIES

Visual observations were made looking at the north face of the test array, which consisted of the reduced-commodity portion of the pallet load design, shown in Figure 4-1 of Section 4.2.

A.4.1 Class 2 Commodity

Test: #4
Date: August 21, 2010
Test Commodity: FM Global standard class 2 commodity
Observer: Benjamin Ditch

Time (mm:ss)	Observation
0:00	Ignition; propane burner at 30 L/min
0:30	Flames at bottom of third tier
0:45	Flames extend 3-5 ft above array
1:05	Flames spread to north face of array at third tier at ignition flue
1:15	Flame attachment extends horizontally across cartoned commodity to edge of metal liner on third tier above wood pallet; flames still contained to ignition flue on second tier
1:25	North face of commodity carton on third tier fully involved in fire, flame attachment halfway across underside of wood pallets on third tier.
1:30	North face of commodity carton on second tier becomes involved in fire, flame attachment three-quarters across underside of wood pallets on third tier.
4:00	Test termination by water hose stream; minimal horizontal flame spread on the north face of second tier commodity
5:44	Data collection ended

Test: #5
Date: August 22, 2010
Test Commodity: FM Global standard class 2 commodity
Observer: Benjamin Ditch

Time (mm:ss)	Observation
0:00	Ignition; propane burner at 30 L/min
0:25	Flames at bottom of third tier
0:40	Flames extend 3-5 ft above array
1:00	Flames spread to north face of array at third tier at ignition flue
1:25	Flame attachment extends horizontally across cartoned commodity to edge of metal liner on third tier above wood pallet; flames still contained to ignition flue on second tier
1:30	North face of commodity carton on third tier fully involved in fire, flame attachment three-quarters across underside of wood pallets on third tier.
1:45	North face of commodity carton on second tier becomes involved in fire; third tier wood pallet fully involved in fire
4:15	Test termination by water hose stream; minimal horizontal flame spread on the north face of second tier commodity
5:40	Data collection ended

Test: #6
Date: August 23, 2010
Test Commodity: FM Global standard class 2 commodity
Observer: Benjamin Ditch

Time (mm:ss)	Observation
0:00	Ignition; propane burner at 30 L/min
0:30	Flames at bottom of third tier
0:50	Flames extend 3-5 ft above array
1:05	Flames spread to north face of array at third tier at ignition flue
1:25	Flame attachment extends horizontally across cartoned commodity to edge of metal liner on third tier above wood pallet; flames spread to north face of array at second tier at ignition flue
1:40	North face of commodity carton on third tier fully involved in fire, flame attachment halfway across underside of wood pallets on third tier
2:40	Flame attachment begins to spread horizontally across the north face of cartoned commodity on second tier; foil encasing third tier commodity breached exposing some commodity not intended for this test
8:35	Test termination by water hose stream; minimal horizontal flame spread on the north face of second tier commodity
10:09	Data collection ended

Test: #10
Date: August 30, 2010
Test Commodity: FM Global standard class 2 commodity
Observer: Benjamin Ditch

Time (mm:ss)	Observation
0:00	Ignition; propane burner at 30 L/min
0:45	Flames at bottom of third tier
0:50	Flames extend 3-5 ft above array
1:10	Flames spread to north face of array at third tier at ignition flue
1:25	Flame attachment extends horizontally across cartoned commodity to edge of metal liner on third tier above wood pallet; flames still contained to ignition flue on second tier
1:40	North face of commodity carton on third tier fully involved in fire, flame attachment three-quarters across underside of wood pallets on third tier.
1:50	North face of commodity carton on second tier becomes involved in fire; third tier wood pallet fully involved in fire
5:00	Majority of combustible material on both tiers involved in fire
6:08	Test termination by water hose stream
6:45	Data collection ended

A.4.2 CUP Commodity

Test: #7
Date: August 24, 2010
Test Commodity: FM Global standard CUP commodity
Observer: Benjamin Ditch

Time (mm:ss)	Observation
0:00	Ignition; propane burner at 30 L/min
0:22	Flames at bottom of third tier
0:33	Flames extend 3-5 ft above array
0:50	Flames spread to north face of array at third tier at ignition flue
1:15	Flame attachment extends horizontally across cartoned commodity to edge of metal liner on third tier above wood pallet; flames still contained to ignition flue on second tier
1:25	North face of commodity carton fully involved in fire, flame attachment three-quarters across underside of wood pallets on third tier.
1:32	Flames extend to aisle face of array at second tier
2:15	Majority of the commodity on both tiers involved in the fire
4:08	Test termination by water hose stream
9:09	Data collection ended

Test: #8
Date: August 27, 2010
Test Commodity: FM Global standard CUP commodity
Observer: Benjamin Ditch

Time (mm:ss)	Observation
0:00	Ignition; propane burner at 30 L/min
0:21	Flames at bottom of third tier
0:32	Flames extend 3-5 ft above array
0:50	Flames spread to north face of array at third tier at ignition flue
1:15	Flame attachment extends horizontally across cartoned commodity to edge of metal liner on third tier above wood pallet (biased towards west), flames extend to the north face of second tier at ignition flue; plastic dripping and pooling at base of ignition flue
1:30	North face of commodity carton fully involved in fire, flame attachment three-quarters across underside of wood pallets on third tier.
4:10	Majority of the commodity on both tiers involved in the fire
4:32	Test termination by water hose stream
6:11	Data collection ended

Test: #9
Date: August 28, 2010
Test Commodity: FM Global standard CUP commodity
Observer: Benjamin Ditch

Time (mm:ss)	Observation
0:00	Ignition; propane burner at 30 L/min
0:17	Flames at bottom of third tier
0:26	Flames extend 3-5 ft above array
0:40	Flames spread to north face of array at third tier at ignition flue
1:11	Flame attachment extends horizontally across cartoned commodity to edge of metal liner on third tier above wood pallet (biased towards west), flames extend to the north face of second tier at ignition flue; plastic dripping and pooling at base of ignition flue
1:30	North face of commodity carton full involved in fire, flame attachment across entire underside of wood pallets on third tier.
3:10	Majority of the commodity on both tiers involved in the fire
6:20	Test termination by water hose stream
7:08	Data collection ended

A.4.3 Li-ion Battery Commodities

Test: #11
Date: September 12, 2012
Test Commodity: Li-ion 18650-format cylindrical cells
Observer: Benjamin Ditch

Time (mm:ss)	Observation
0:00	Ignition; propane burner at 30 L/min
0:22	Flames at bottom of third tier
0:28	Flame tips extend above top of array
0:33	Flames extend 3-5 ft above array
0:50	Flames spread to north face of array at third tier at ignition flue
1:20	Flame attachment extends horizontally across cartoned commodity to edge of metal liner on third tier above wood pallet; flames still contained to ignition flue on second tier
1:30	North face of commodity carton fully involved in fire, flame attachment half-way across underside of wood pallets on third tier
3:30	Flame spread across entire underside of wood pallets on third tier; flames still contained to ignition flue on second tier
4:08	Very minor collapse of third tier commodity on west side of array; flames spread to north face of array at second tier at ignition flue
5:00	Fire appears to be growing on third tier
6:20	Significant fire growth on third tier; flame attachment extends horizontally across cartoned commodity to edge of metal liner on second tier
8:17	Significant collapse of commodity primarily from third tier; followed by sporadic collapse at both tiers; Collapsed cells burning at bottom of array
9:40	Additional cell collapse from third tier, majority of second tier commodity still in place
11:40	Significant collapse of second tier commodity
16:59 - 20:47, 25:05 - 27:10, 27:25 - 29:26, 30:06 - 30:16, 35:44 - 37:58, 38:13 - 38:18, 38:27 - 38:38, 39:02 - 39:13, 39:54 - 40:26, 40:36 - 41:03, 41:12 - 41:19, 41:42 - 41:46, 42:04 - 42:19	Intermittent water application (fire hose) to suppress commodity burning outside of collection pan surrounding test array; Test termination by water hose stream
40:40	Data collection ended (occurred during water application)

Test: #12
Date: September 19, 2012
Test Commodity: Li-ion power tool packs
Observer: Benjamin Ditch

Time (mm:ss)	Observation
0:00	Ignition; propane burner at 30 L/min
0:34	Flames at bottom of third tier
0:41	Flame tips extend above top of array
0:45	Flames extend 3-5 ft above array
1:00	Flames spread to north face of array at third tier at ignition flue
1:04	Sporadic collapse of few power packs (based on audio and video 19 packs collapsed over 30 s period, ending at 1:04)
1:10	Flame attachment begins to spread laterally across commodity carton on north face of array at third tier
1:25	North face of commodity cartons fully involved in fire at third tier, flame attachment half-way across underside of wood pallets on third tier
1:40	Flames spread to north face of array at second tier in ignition flue
1:45	Additional collapse of power packs
2:00	North face of commodity cartons fully involved in fire at second and third tier, flame attachment across entire underside of wood pallets on third tier
2:30	Majority of cartons and wood pallets surfaces on both tiers involved in fire; bluish flames visible around wood pallets at second and third tier
45:52 - 46:35	Intermittent water application (fire hose) to suppress small quantity of commodity burning outside of collection pan surrounding test array; Test termination by water hose stream
39:40	Data collection ended (occurred during water application)

Test: #13
Date: October 3, 2012
Test Commodity: Li-ion polymer cells
Observer: Benjamin Ditch

Time (mm:ss)	Observation
0:00	Ignition; propane burner at 30 L/min
0:16	Flames at bottom of third tier
0:23	Flame tips extend above top of array
0:30	Flames extend 3-5 ft above array
0:45	Flames spread to north face of array at third tier in ignition flue
0:55	Flames tips extend horizontally to edge of metal liner on third tier above wood pallet
1:05	Flame attachment begins to spread laterally across commodity carton on north face of array at third tier
1:20	North face of commodity carton fully involved in fire, flame attachment half-way across underside of wood pallets on third tier
3:00	Flame spread across entire underside of wood pallets on third tier; flames still contained to ignition flue on second tier
4:00	Third tier commodity sagging towards ignition flue
5:50	Flame spread along north face of commodity on second tier; wood pallets on third tier fully involved in fire
7:00	Second tier commodity sagging towards ignition flue
8:35	Minor collapse of batteries (only a few batteries); Significant fire growth on third tier
9:00	Major collapse of commodity from third tier
11:25 - 12:00	Intermittent water application (fire hose) to suppress commodity burning outside of collection pan surrounding test array; bluish flames visible from burning of Li-ion cells
14:00 - 14:15, 14:30 - 14:40, 15:07 - 15:12	Intermittent water application (fire hose) to suppress commodity burning outside of collection pan surrounding test array
16:00	Test termination by water hose stream
20:00	Data collection ended

B APPENDIX B – SOUTH CEILING THERMOCOUPLE LAYOUT

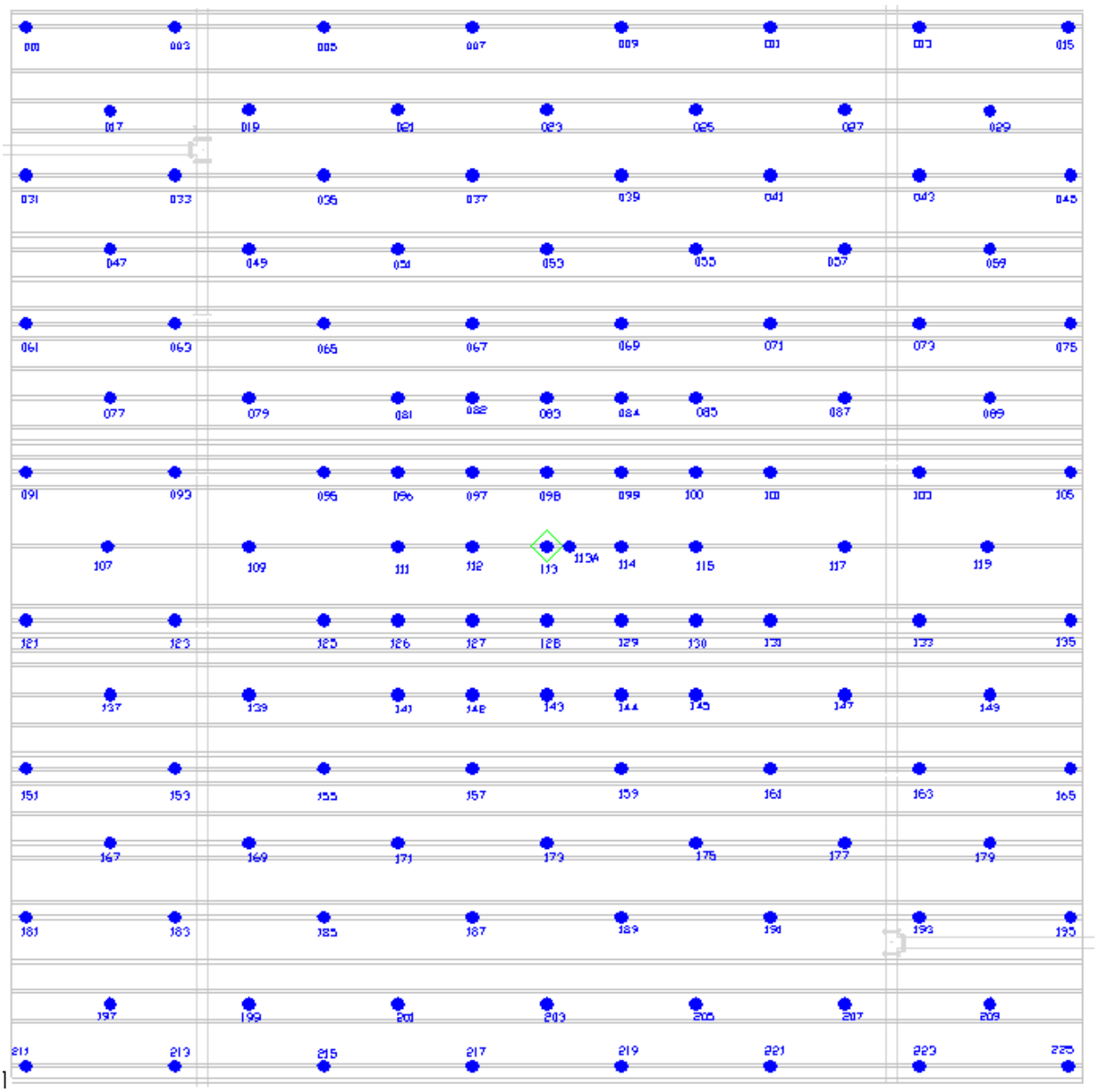

C APPENDIX C – LARGE-SCALE VALIDATION TEST DATA AND RESULTS

C.1 TEST 14

The fourteenth test was conducted on January 7, 2013, at 2:00 pm under the south movable ceiling portion of the Large Burn Lab. Environmental conditions inside the lab were as follows: dry-bulb temperature, 13°C (55°F) and relative humidity, 29%. Weather conditions outside the lab were as follows: dry-bulb temperature, 4°C (40°F) and relative humidity, 40%.

The main fuel array consisted of an open-frame, double-row rack of cartoned unexpanded plastic (CUP) commodity as described in Section 5.2. The array dimensions measured approximately 4.9 m long x 2.3 m wide (16 ft x 7.5 ft) in a 4 x 2 pallet load arrangement. The end pallet of each row consisted of FM Global standard class 2 commodity as described in Section 4.3.1 (except for the noncombustible aluminum covering). A single-row target array contained two pallet loads of the class 2 commodity across a 1.2 m (4 ft) aisle to the west of the main array[a]. Overall the target array measured approximately 2.4 m long x 1.0 m deep (8 ft x 3.25 ft). For each array, a three-pallet-load-high configuration was used, representing storage heights up to 4.6 m (15 ft) high. The ceiling was set at a height of 9.1 m (30 ft) above the floor. The rack storage arrays were oriented perpendicular to the sprinkler pipes, which run east-west across the ceiling.

The main array was centered among four sprinklers. Ignition was accomplished with two FM Global standard half igniters, offset 0.6 m (2 ft) east in the central transverse flue, located at the rack uprights.

The sprinkler system was comprised of quick-response pendent sprinklers with a K-Factor of 360 L/min/bar$^{1/2}$ (25.2 gal/min/psi$^{1/2}$) and a 74°C (165°F) rated link installed with the thermal element 0.46 m (18 in.) below the ceiling. A nominal operating pressure of 172 kPa (25 psig) was chosen to provide a discharge of 477 L/min (126 gpm) per sprinkler. The sprinklers were installed on 3 m x 3 m (10 ft x 10 ft) spacing, resulting in a 51 mm/min (1.25 gpm/ft^2) water density at the floor.

[a] No target was located to the east of the main array to improve viewing angles of the ignition area.

Visual observations were made looking at the east aisle face of the main test array, as shown in Figure 5-4 of Section 5.3. The igniters were lit and the test time started at time 0. The initial fire growth spread rapidly upward in the central transverse flue and extended 1 m to 1.5 m (3 ft to 5 ft) over the top of the array at approximately 1 min 5 s after ignition. By 1 min 33 s, the fire had spread across the underside of the pallets adjacent to ignition and to the east (front) face of the array at the second and third tiers. The first sprinkler, northeast of ignition, operated at 1 min 48 s, followed by the second (and final) operation, southwest of ignition, at 2 min 1 s. The fire intensity was reduced; however, persistent burning occurred on all three tiers until test termination by water hose streams at 20 min. A total of two sprinklers operated and the fire was mostly contained to the commodity on either side of the central transverse flue (ignition flue), with minimal damage to the commodity across the longitudinal flue.

Figure C-1 shows images of Test 14 at initial sprinkler operation and during test termination. No additional images are shown before test termination due to obscuration of the test array from smoke and sprinkler water.

[1 min 48 s] **[> 20 min]**

Figure C-1: Images of Test 14 at initial sprinkler operation (left) and test termination (right)

Figure C-2 shows images from the FLIR® SC655 long-wave IR (LWIR) infrared camera at initial sprinkler operation and 5 min after ignition. These images indicate that the sprinkler system was not effective at suppressing the fire and deep-seated burning continued within the commodity surrounding ignition on the upper two tiers. The image at 5 min was selected to coincide with the predicted time of battery involvement from the reduced-commodity tests conducted with Li-ion batteries.

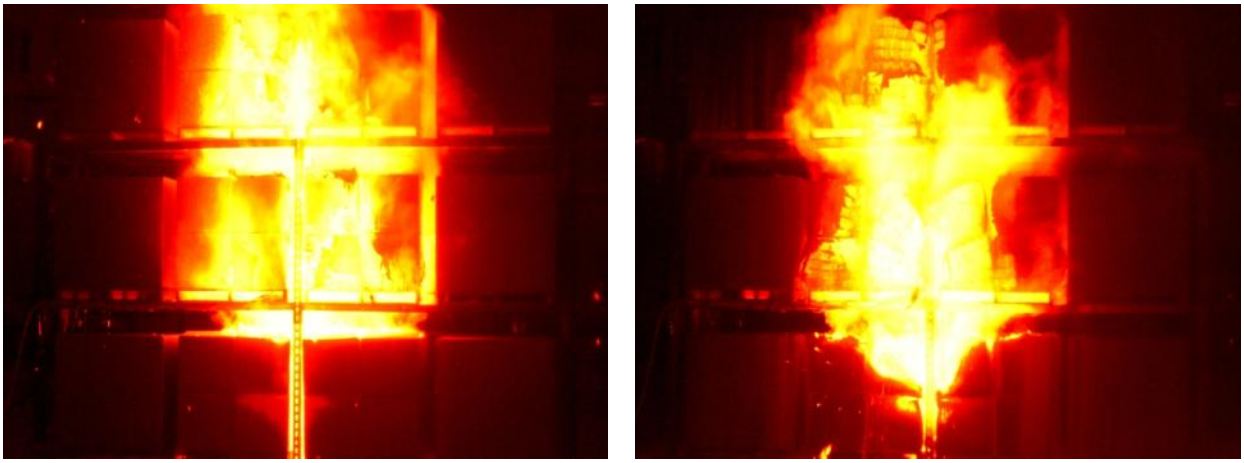

[1 min 48 s] **[5 min]**

Figure C-2: IR images of Test 14 at initial sprinkler operation (left) and 5 min after ignition (right)

A schematic overview of the sprinkler operation sequence and operation times can be found in Figure C-3. As indicated, the first sprinkler, northeast of the main array center, operated at 1 min 48 s. The second (and final) sprinkler, southwest of the main array center, operated at 2 min 1 s.

The overall extent of fire damage for Test 14 is represented by the shaded areas in Figure C-4 for the main array. As shown, damage represents visual observation of burning on the outside faces of the commodity. Damage was primarily contained to the commodity on either side of the central transverse flue, surrounding the ignition location. Limited damage across the longitudinal flue also occurred on the second and third tiers. The fire spread remained within the confines of the main array and there was no damage to the target array.

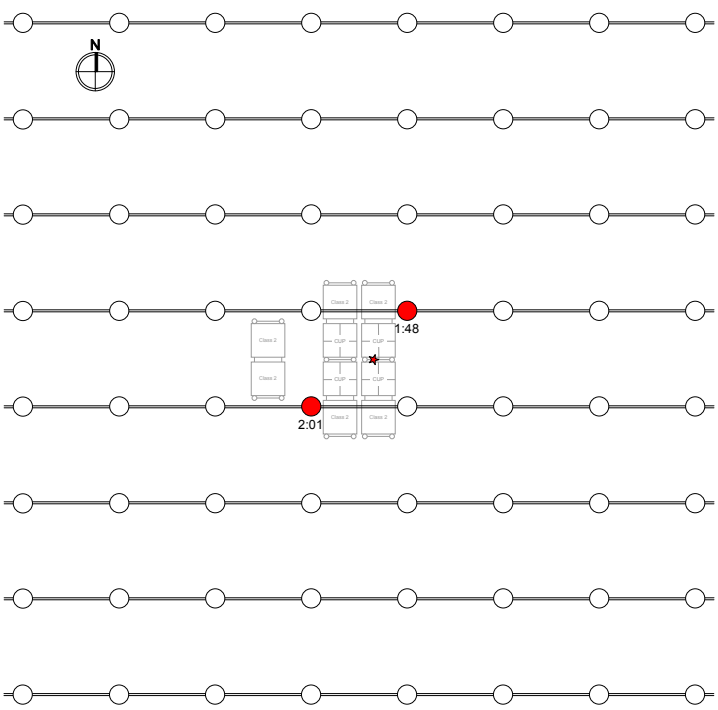

Figure C-3: Plan view of sprinkler operation pattern - Test 14

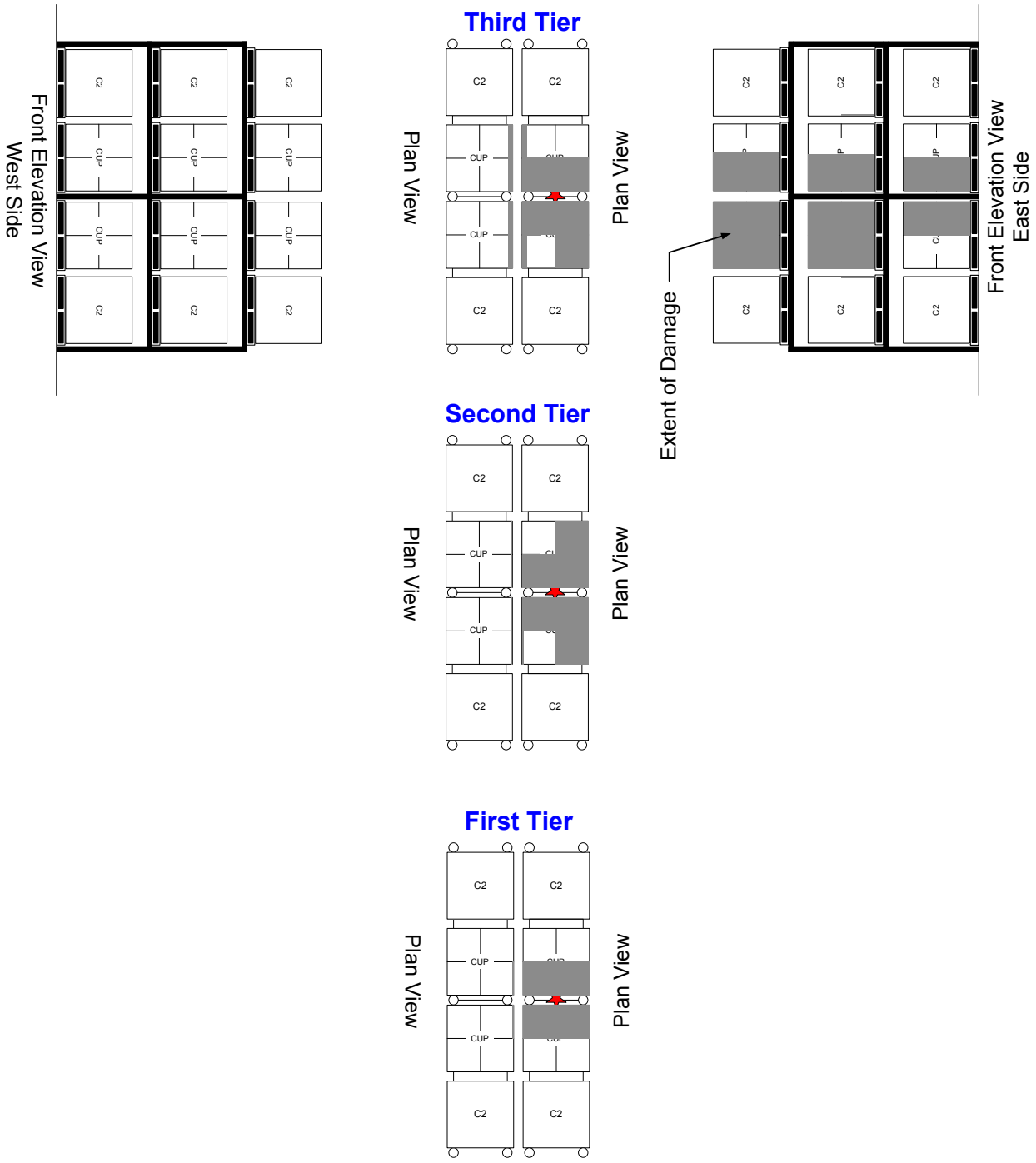

Figure C-4: Extent of damage - Test 14

Figure C-5 (a) through (f) shows various near-ceiling measurements for Test 14. The branch-line water discharge pressure, as shown in Figure C-5 (a), closely matched the target value of 172 kPa (25 psig). To minimize the expected pressure drop due to sprinkler operation, the initial pressure was set higher than the target value. Figure C-5 (b) – (d) show the near-ceiling TC measurements and steel TC measurements centered over the main array, and the ceiling TCs at a radial distance of 1.5 m (5 ft) and 3.0 m (10 ft) from center. The TC centered over the main array recorded a peak measurement of 341^{o}C (645^{o}F) coinciding with first sprinkler operation at 1 min 48 s. The peak steel TC measurement of approximately 37^{o}C (99^{o}F) was recorded at 5 min 9 s. Steel temperatures shown in the graph represent the average of all nine thermocouples located out to 0.3 m (12 in.) in all four directions from the center of the ceiling. The thermocouples located radially 1.5 m (5 ft) and 3.0 m (10 ft) recorded peak TC measurements of 249^{o}C (480^{o}F) and 148^{o}C (298^{o}F) both north of the ceiling center, respectively, at first sprinkler operation. Figure C-5 (e) and (f) show the near-ceiling gas velocities at 2.1 m (7 ft) and 4.0 m (13 ft), with recorded peak velocities of 6.9 m/s and 5.2 m/s, both to the east of the ceiling center, respectively, at first sprinkler operation.

Figure C-6 (a) and (b) show the measurements from the TCs located within the test commodity, as detailed in Section 5.7. The TCs were adhered to the inside of the commodity cartons, facing the ignition flue. The fire was initiated in east row of the main array and the TC measurements reached > 900^{o}C (1,650^{o}F) starting at 1 min 30 s after ignition. These measurements are consistent with flame temperatures and indicate that the cartons were breached by the flames before the first sprinkler operation occurred at 1 min 48 s. On the west row commodity, the TC measurements were nominally 70^{o}C (158^{o}F) or less, which is consistent with visual observations of minimal fire damage. The exception is TCT1W3; located on the first tier adjacent to the longitudinal flue, which nominally measured 620^{o}C (1,150^{o}F) starting at 13 min 40 s. This measurement is consistent with the minor breach observed at the upper edge of the carton and indicates that the fire was still (slowly) propagating after the sprinklers operated.

Figure C-7 presents the time evolution of the two coordinates of the ceiling gas layer centroid. At first sprinkler operation, 1 min 48 s, the coordinates were 0.09 m (0.3 ft) to the east and 0.3 m (1 ft) to the north. For convenience, Figure C-8 presents the corresponding ceiling TC

measurement contours, which illustrate the extent of the fire plume at first sprinkler operation. Ceiling gas centroid and contour plots are calculated using the 125 TCs located 152 mm (6 in.) below the ceiling. The zero coordinate values at the beginning and end of the test are due to a preset condition of the calculation where a zero value is reported when minimal temperature variations are measured across the entire ceiling.

Figure C-9 presents the chemical heat release rate, based on the generation rates of carbon dioxide and carbon monoxide (HRR-COCO2) and oxygen depletion (HRR-O2), during Test 14. Note that the heat release rate measurements do not account for lag and smear of the data, which can be significant, due to complex mixing of the gases above the movable ceiling or transport time through the collection ducts. Therefore, time-resolved heat release rates (HRR) cannot be determined directly from the calorimetry data. However, the total energy generated can be calculated by integrating the chemical HRR curve, calculated from mass flow rate and gas analysis data for CO and CO_2. Integration under the data curve is possible up to test termination. After the test is terminated, an exponential best-fit curve of the decay portion of the test data is used to estimate the tail portion of the HRR and integrated to estimate energy released during that period. These two values were added to provide a value for the total energy released during the test. For error analysis, it was assumed that the total energy up to test termination has ± 10% error and the post-test curve fit data have 50% error. Based on the HRR-COCO2 measurements, an estimated 2,000 ± 360 MJ (1,900 ± 340 BTU x 10^3) of total energy was measured during the test. Dividing by the energy content of a pallet load of CUP commodity discussed in Section 5.2, an equivalent of 1.5 pallet loads of CUP was consumed during this test. A similar value was calculated based on the HRR-O2 measurements.

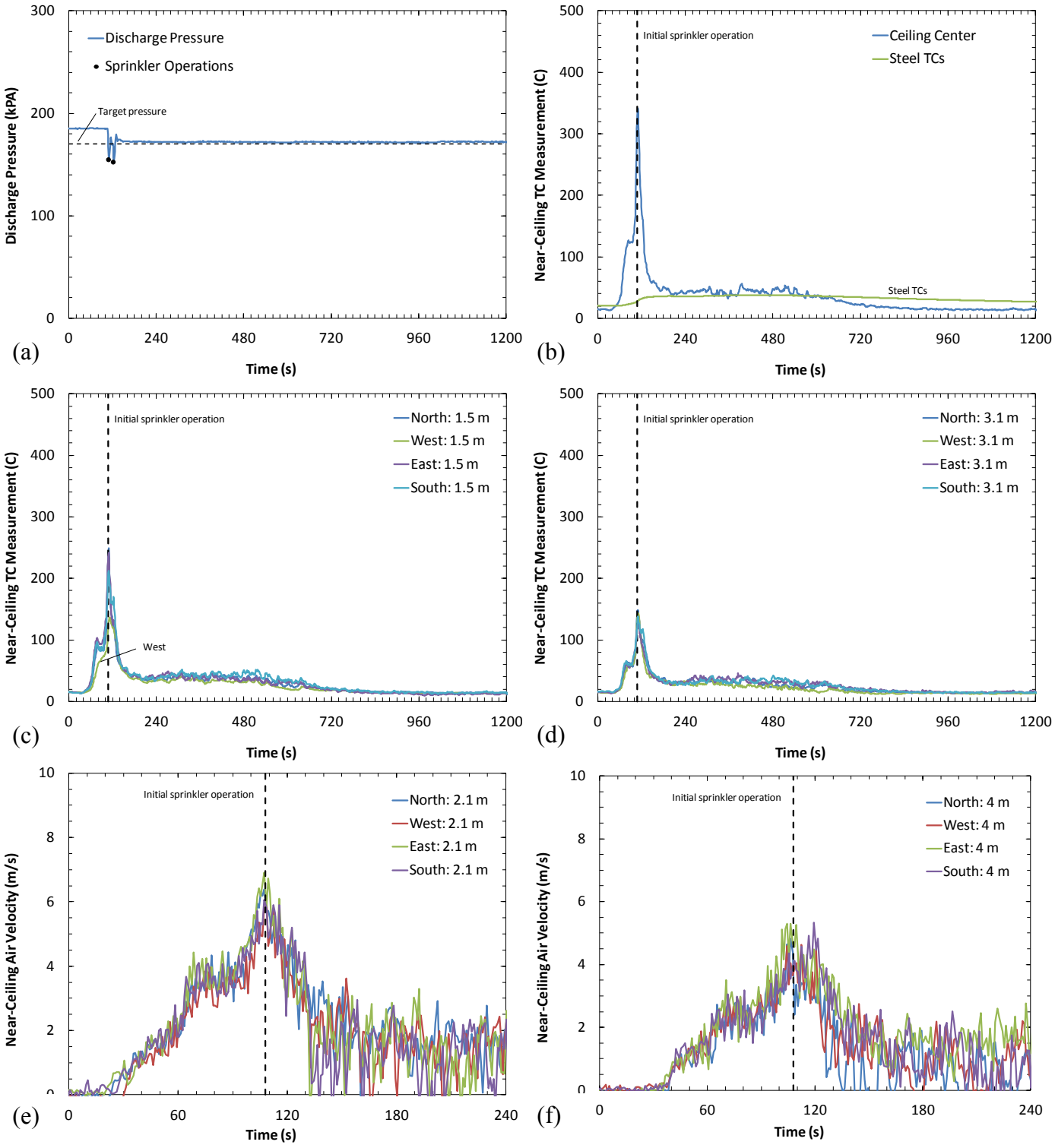

Figure C-5: Various near-ceiling measurements - Test 14

(a)

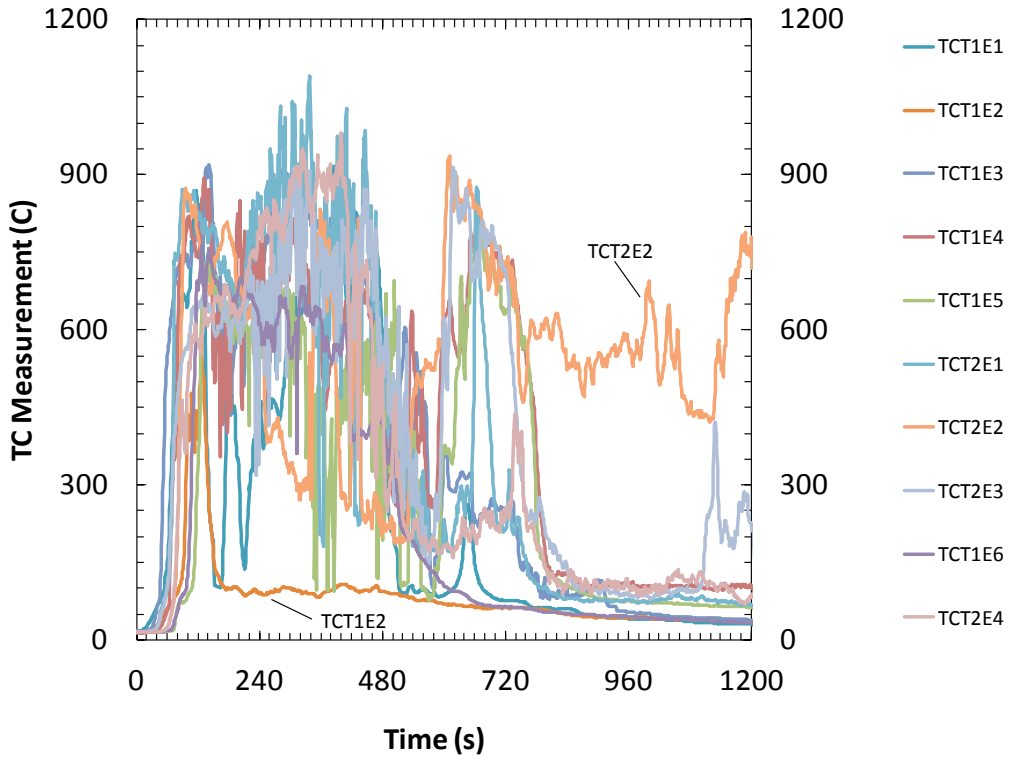

(b)

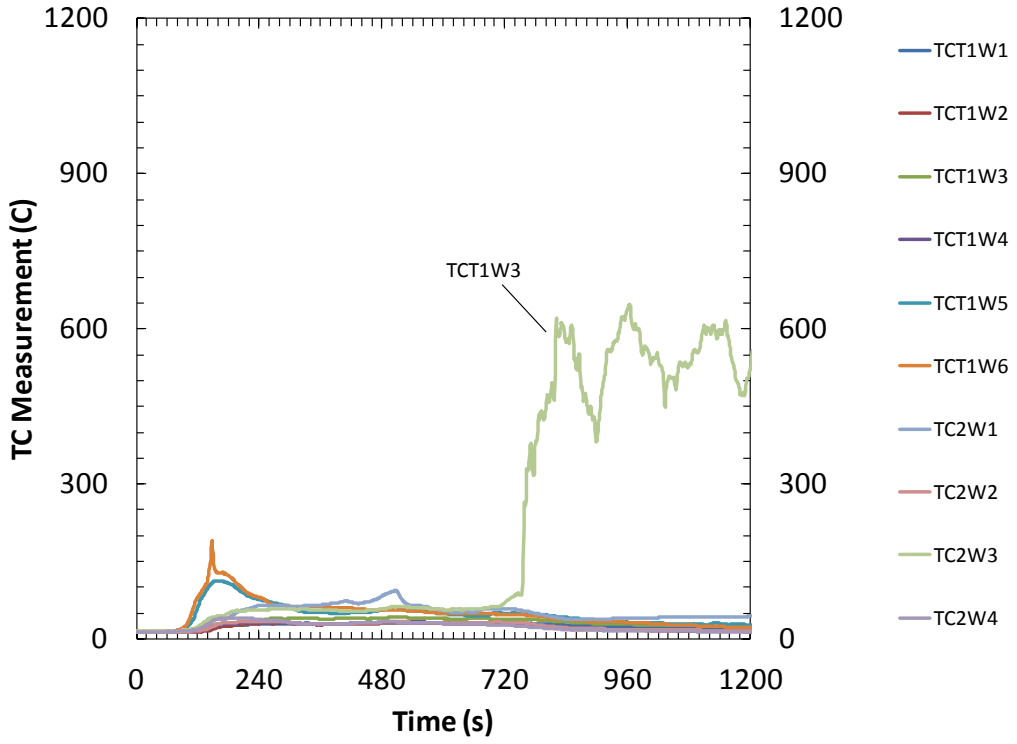

Figure C-6: Measurements from thermocouples within the commodity on the east (a) and west (b) side of the longitudinal flue - Test 14

(a)

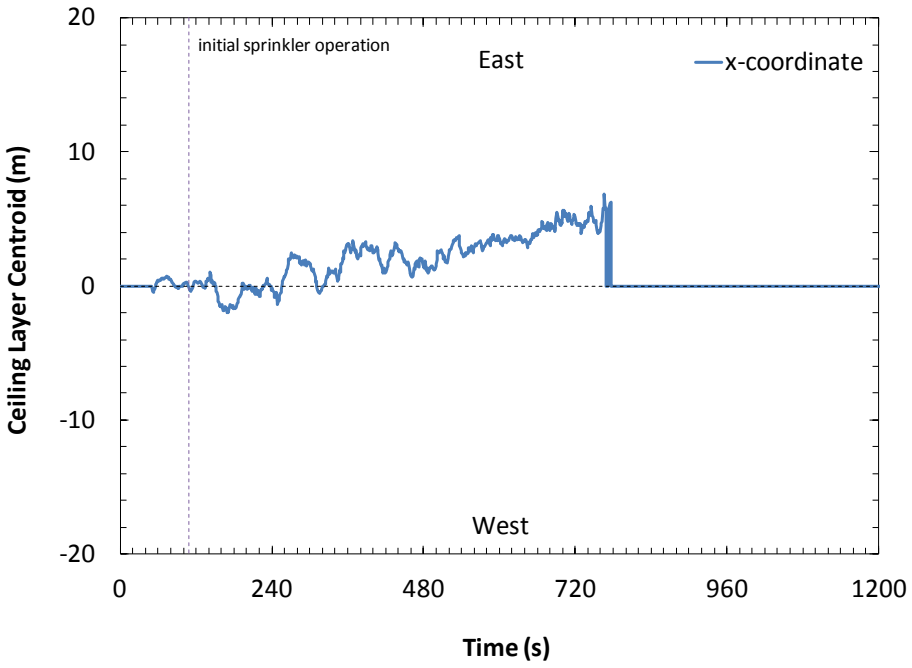

(b)

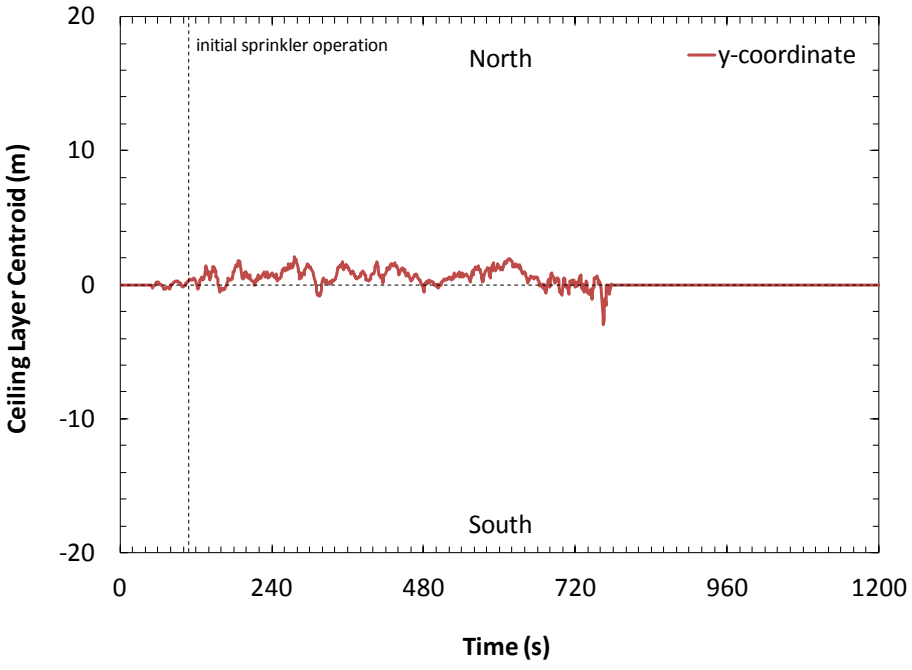

Figure C-7: Time evolution of x- (a) and y-coordinate (b) of ceiling layer centroid - Test 14

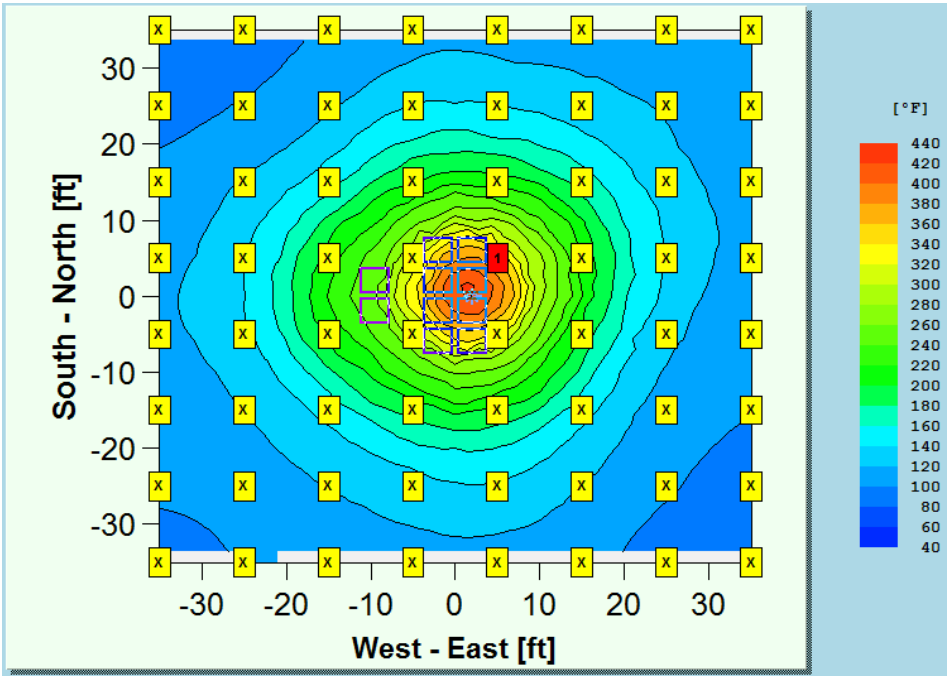

Figure C-8: Ceiling TC contours at first sprinkler operation (1 min 48 s) - Test 14

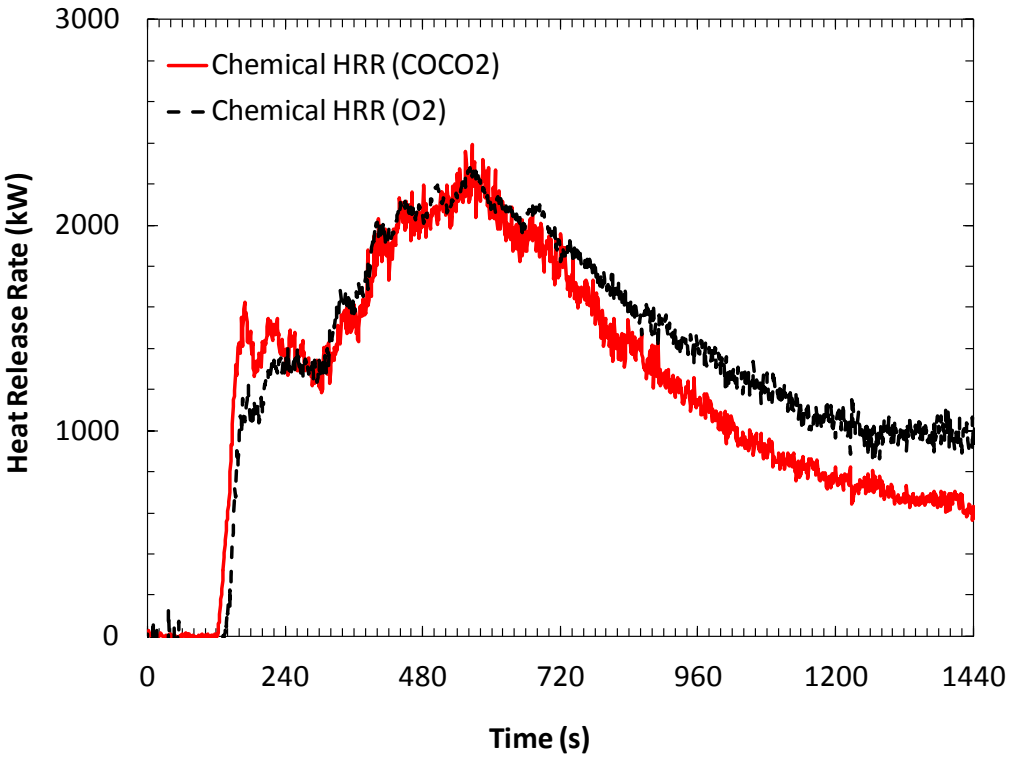

Figure C-9: Chemical heat release rates - Test 14

C.2 TEST 15

The fifteenth test was conducted on January 11, 2013, at 1:30 pm under the South Movable ceiling portion of the Large Burn Lab. Environmental conditions inside the lab were as follows: dry-bulb temperature, 16°C (60°F) and relative humidity, 25%. Weather conditions outside the lab were as follows: dry-bulb temperature, 3°C (38°F) and relative humidity, 64%.

The main fuel array consisted of an open-frame, double-row rack of cartoned unexpanded plastic (CUP) commodity as described in Section 5.2. The array dimensions measure approximately 4.9 m long x 2.3 m wide (16 ft x 7.5 ft) in a 4 x 2 pallet load arrangement. The end pallet of each row consisted of FM Global standard class 2 commodity as described in Section 4.3.1 (except for the noncombustible aluminum covering). A single-row target array contained two pallet loads of the class 2 commodity across a 1.2 m (4 ft) aisle to the west of the main array[a]. Overall the target array measured approximately 2.4 m long x 1.0 m deep (8 ft x 3.25 ft). For each array, a three-pallet-load-high configuration was used, representing storage up to 4.6 m (15 ft) high. The ceiling was set at a height of 7.6 m (25 ft) above the floor. The rack storage arrays were oriented perpendicular to the sprinkler pipes, which run east-west across the ceiling.

The main array was centered among four sprinklers. Ignition was accomplished with two FM Global standard half igniters, offset 0.6 m (2 ft) east in the central transverse flue, located at the rack uprights.

The sprinkler system was comprised of quick-response pendent sprinklers with a K-Factor of 200 L/min/bar$^{1/2}$ (14 gal/min/psi$^{1/2}$) and a 74°C (165°F) rated link installed with the thermal element 0.36 m (14 in.) below the ceiling. A nominal operating pressure of 517 kPa (75 psig) was chosen to provide a discharge of 454 L/min (120 gpm) per sprinkler. The sprinklers were installed on 3 m x 3 m (10 ft x 10 ft) spacing, resulting in a 49 mm/min (1.20 gpm/ft^2) water density at the floor.

[a] No target was located to the east of the main array to improve viewing angles of the ignition area.

Visual observations were made looking at the east aisle face of the main test array, as shown in Figure 5-4 of Section 5.3. The igniters were lit and the test time started at 0 min. During initial growth the fire spread rapidly upward in the central transverse flue and extended 1 m to 1.5 m (3 ft to 5 ft) over the top of the array at approximately 55 s after ignition. By 1 min 30 s, the fire had spread across the underside of the pallets adjacent to ignition and to the east (front) face of the array at the second and third tiers. The four sprinklers surrounding ignition operated from 1 min 38 s to 1 min 41 s. The fire was largely suppressed; however, persistent burning occurred on a small portion of the upper two tiers until test termination by water hose streams at 20 min. A total of four sprinklers operated and the fire was mostly contained to the commodity on either side of the central transverse flue (ignition flue), with minimal damage to the commodity across the longitudinal flue.

Figure C-10 shows images of Test 15 at initial sprinkler operation and during test termination. No additional images are shown before test termination due to obscuration of the array from smoke and sprinkler water.

[1 min 38 s] **[> 20 min]**

Figure C-10: Images of Test 15 at initial sprinkler operation (left) and test termination (right)

Figure C-11 shows images from the FLIR® SC655 long-wave IR (LWIR) infrared camera at initial sprinkler operation and 5 min after ignition. These images indicate that the sprinkler system was effective at suppressing the fire; however, deep-seated burning continued within the commodity surrounding ignition on the upper two tiers. The image at 5 min was selected to coincide with the predicted time of battery involvement from the reduced-commodity tests conducted with Li-ion batteries.

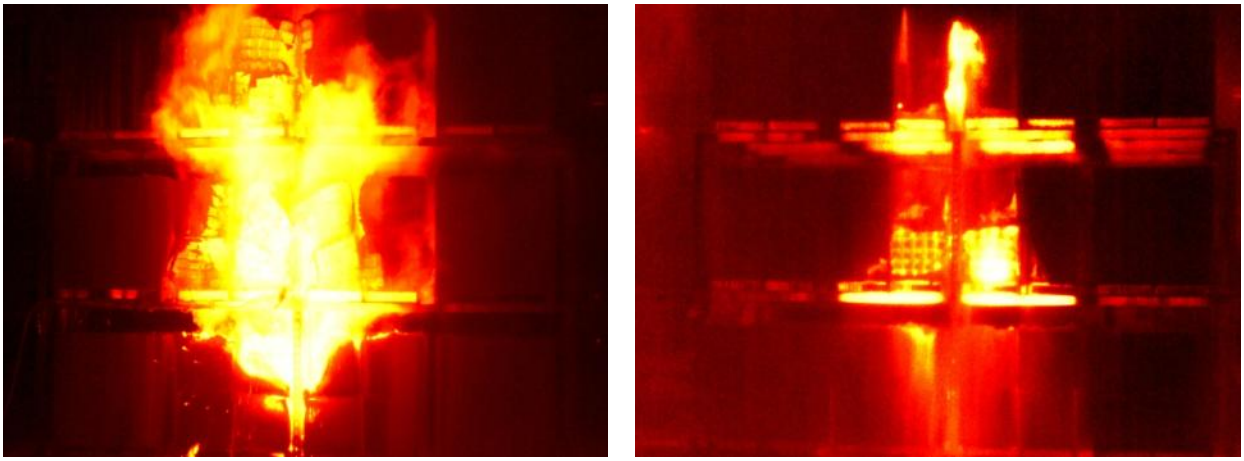

[1 min 38 s] **[5 min]**

Figure C-11: IR images of Test 15 at initial sprinkler operation (left) and 5 min after ignition (right)

A schematic overview of the sprinkler operation sequence and operation times can be found in Figure C-12. As indicated, the four sprinklers surrounding ignition operated from 1 min 38 s to 1 min 41 s. No additional sprinkler operation occurred during this test.

The overall extent of fire damage for Test 15 is represented by the shaded areas in Figure C-13 for the main array. As shown, damage represents visual observation of burning on the outside faces of the commodity. Damage was primarily contained to the commodity on either side of the central transverse flue, surrounding the ignition location. Limited damage across the longitudinal flue also occurred on the second and third tiers. The fire spread remained within the confines of the main array and there was no damage to the target array.

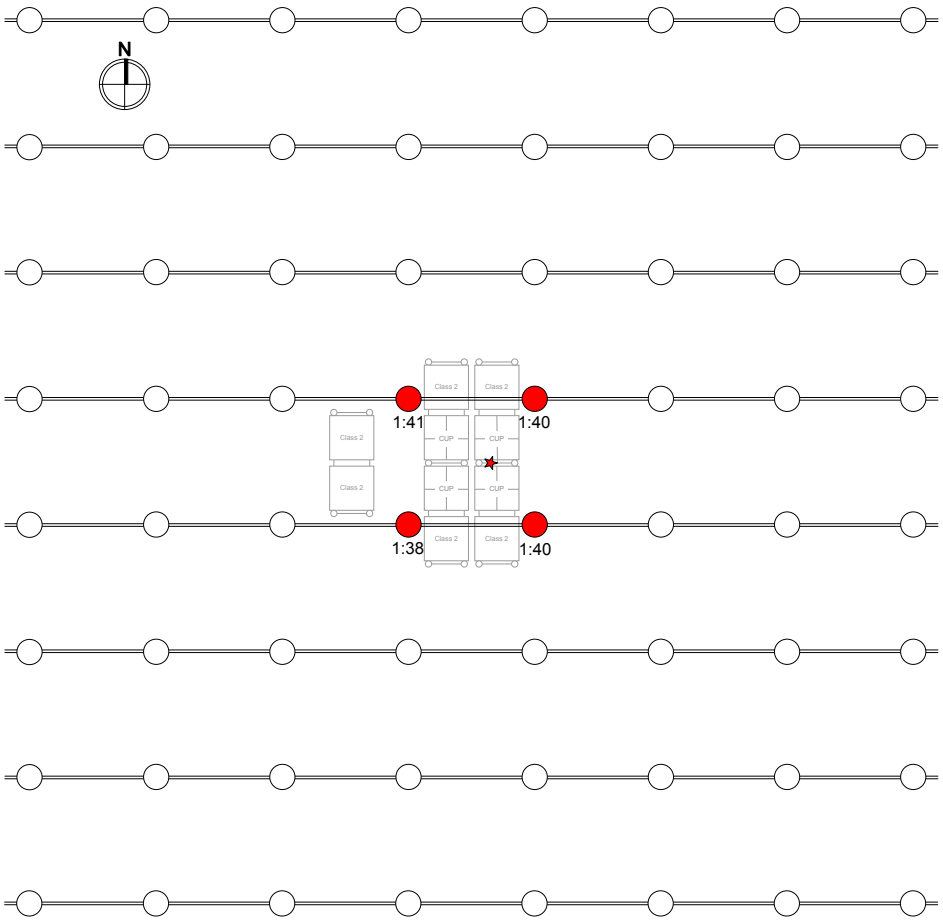

Figure C-12: Plan view of sprinkler operation pattern - Test 15

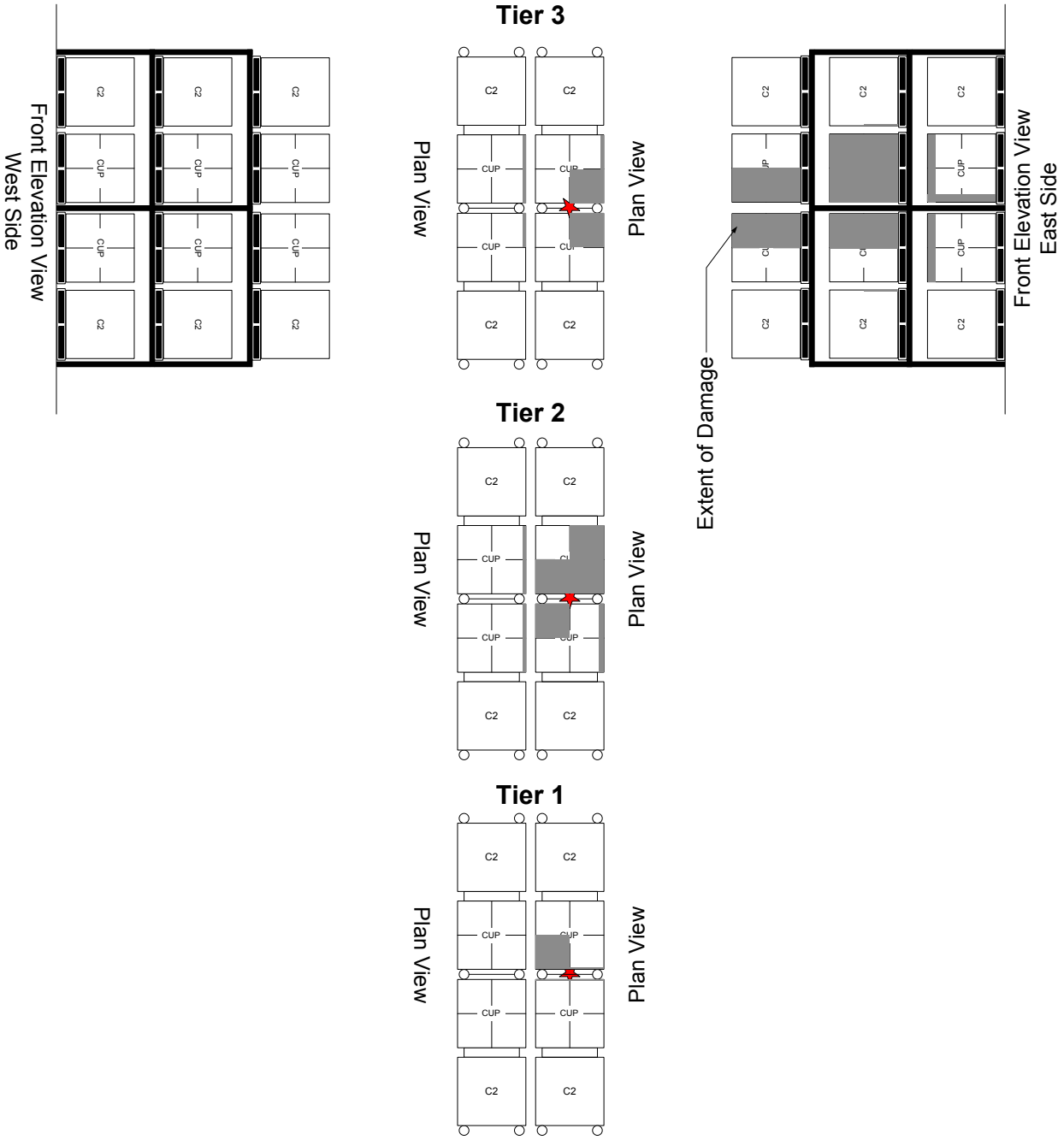

Figure C-13: Extent of damage - Test 15

Figure C-14 (a) through (f) shows various near-ceiling measurements for Test 15. The branch-line water discharge pressure, as shown in Figure C-14 (a), closely matched the target value of 517 kPa (75 psig). To minimize the expected pressure drop due to sprinkler operation, the initial pressure was set higher than the target value. Figure C-14 (b) – (d) show the near-ceiling TC measurements centered over the main array, and at a radial distance of 1.5 m (5 ft) and 3.0 m (10 ft) from center. The TC centered over the main array recorded a peak measurement of 311^{o}C (592^{o}F) at 1 min 40 s, which nominally coincides with first sprinkler operation. The peak steel TC measurement of 41^{o}C (106^{o}F) was recorded at 1 min 48 s. Steel temperatures shown in the graph represent the average of all nine thermocouples located out to 0.3 m (12 in.) in all four directions from the center of the ceiling. The thermocouples located radially 1.5 m (5 ft) and 3.0 m (10 ft) recorded peak TC measurements of 214^{o}C (417^{o}F) to the east and 147^{o}C (297^{o}F) to the west of the ceiling center, respectively, at first sprinkler operation. Figure C-14 (e) and (f) show the near-ceiling gas velocities at 2.1 m (7 ft) and 4.0 m (13 ft), with recorded peak velocities of 5.9 m/s and 4.4 m/s, both to the east of the ceiling center, respectively, at first sprinkler operation.

Figure C-15 (a) and (b) show the measurements from the TCs located within the test commodity, as detailed in Section 5.7. The TCs were adhered to the inside of the commodity cartons, facing the ignition flue. The fire was initiated in the east row of the main array and the TC measurements reached > 700^{o}C (1,290^{o}F) starting at 1 min 5 s after ignition and reached a maximum value of 900^{o}C (1,650^{o}F) by 1 min 49 s. These measurements are consistent with flame temperatures and indicate that the cartons were breached by the flames before the first sprinkler operation occurred at 1 min 38 s. On the west row commodity, the TC measurements were 40^{o}C (104^{o}F) or less, which is consistent with visual observations of minimal fire damage.

Figure C-16 presents the time evolution of the two coordinates of the ceiling gas layer centroid. At first sprinkler operation, 1 min 38 s, the coordinates were 0.4 m (1.3 ft) to the west and 0.2 m (0.7 ft) to the south. For convenience, Figure C-17 presents the corresponding ceiling TC measurement contours, which illustrate the extent of the fire plume at first sprinkler operation. Ceiling gas centroid and contour plots are calculated using the 125 TCs located 152 mm (6 in.) below the ceiling. The combination of the ceiling gas layer centroid and contour plots show that

the highest temperatures were experience directly over ignition (slightly east of the ceiling center). The zero coordinate values at the beginning and end of the test are due to a preset condition of the calculation where a zero value is reported when minimal temperature variations are measured across the entire ceiling.

Figure C-18 presents the chemical heat release rate, based on the generation rates of carbon dioxide and carbon monoxide (HRR-COCO2) and oxygen depletion (HRR-O2), during Test 15. For both measurements, the species concentrations (CO, CO_2, and O_2) were near the lower end of the analyzer ranges, resulting in the minor discrepancy between the subsequent chemical HRR calculations. Note that the heat release rate measurements do not account for lag and smear of the data, which can be significant, due to complex mixing of the gases above the movable ceiling or transport time through the collection ducts. Therefore, time-resolved heat release rates (HRR) cannot be determined directly from the calorimetry data. However, the total energy generated can be calculated by integrating the chemical HRR curve, calculated from mass flow rate and gas analysis data for CO and CO_2. Integration under the data curve is possible up to test termination. After the test is terminated, an exponential bestfit curve of the decay portion of the test data is used to estimate the tail portion of the HRR and integrated to provide total energy released during that period. These two values were added to provide a value for the total energy released during the test. For error analysis, it was assumed that the total energy up to test termination has ± 10% error and the post-test curve fit data have 50% error. Based on the HRR-COCO2 measurements, an estimated 620 ± 125 MJ (590 ± 120 BTU x 10^3) of total energy was estimated for the test. Dividing by the energy content of a pallet load of CUP commodity discussed in Section 5.2, an equivalent of 0.5 pallet loads of CUP commodity was consumed during the test. A similar value was calculated based on the HRR-O2 measurements.

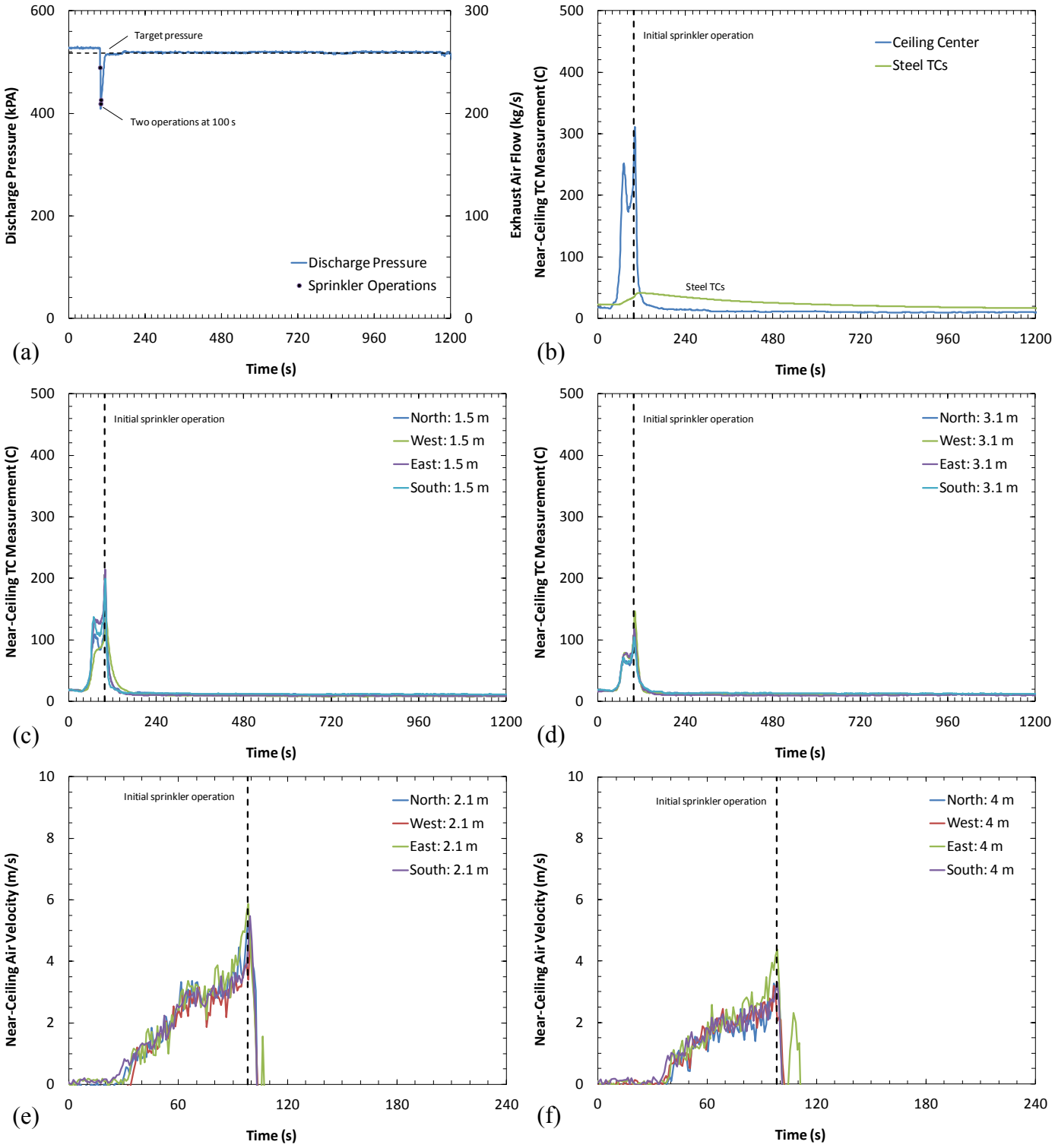

Figure C-14: Various near-ceiling measurements - Test 15

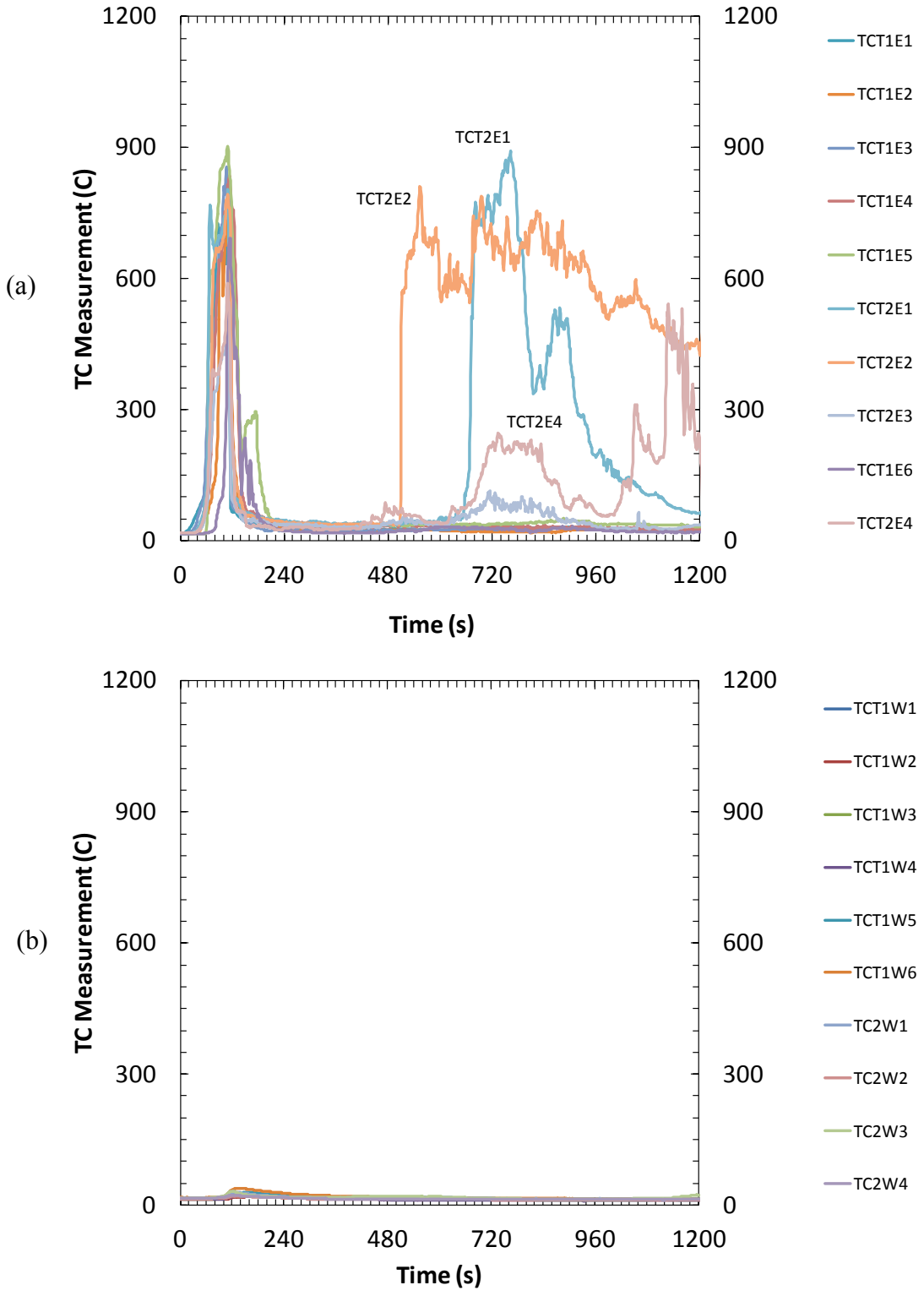

Figure C-15: Measurements from thermocouples within commodity on east (a) and west (b) side of longitudinal flue - Test 15

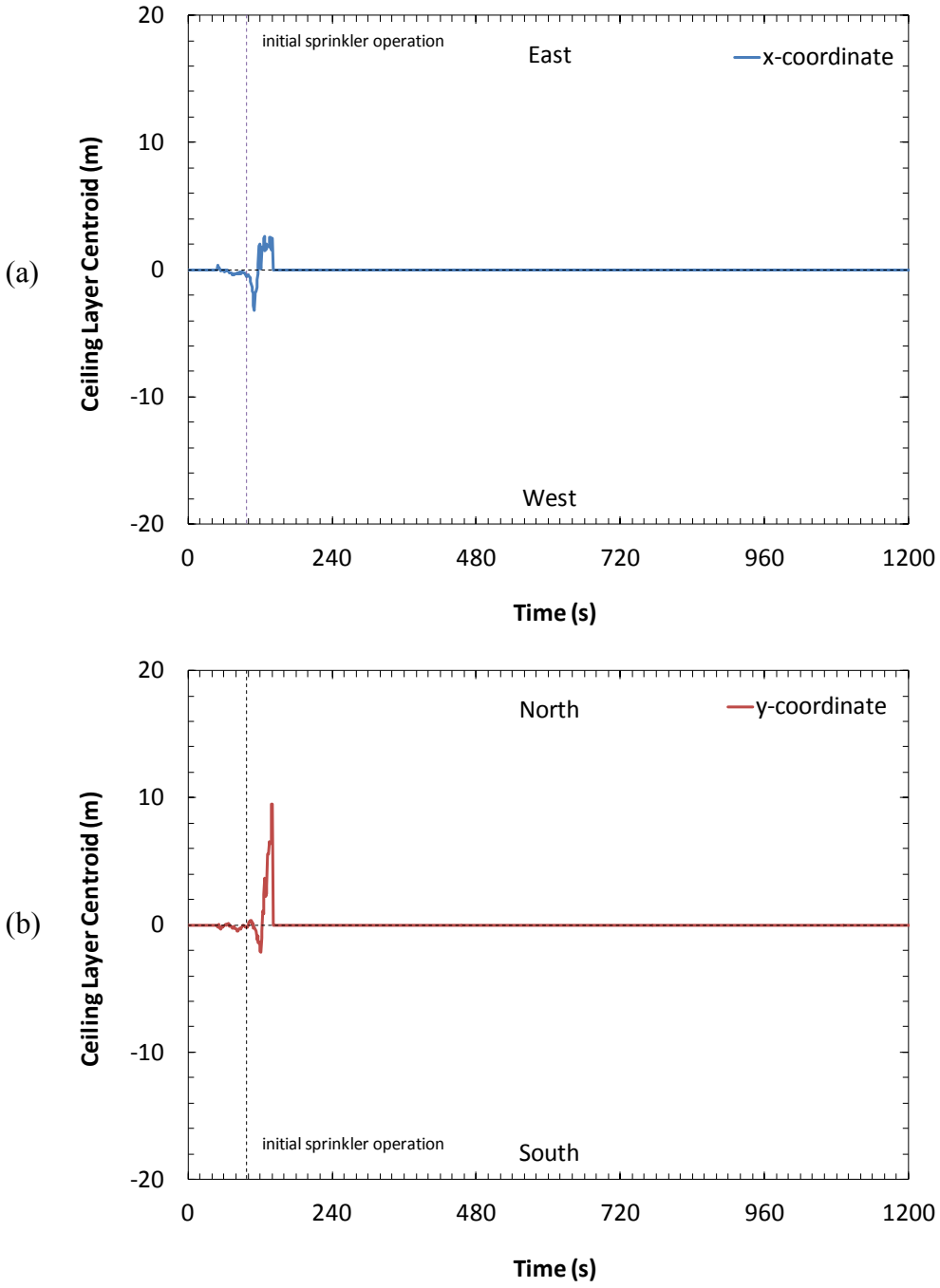

Figure C-16: Time evolution of x- (a) and y-coordinate (b) of ceiling layer centroid - Test 15

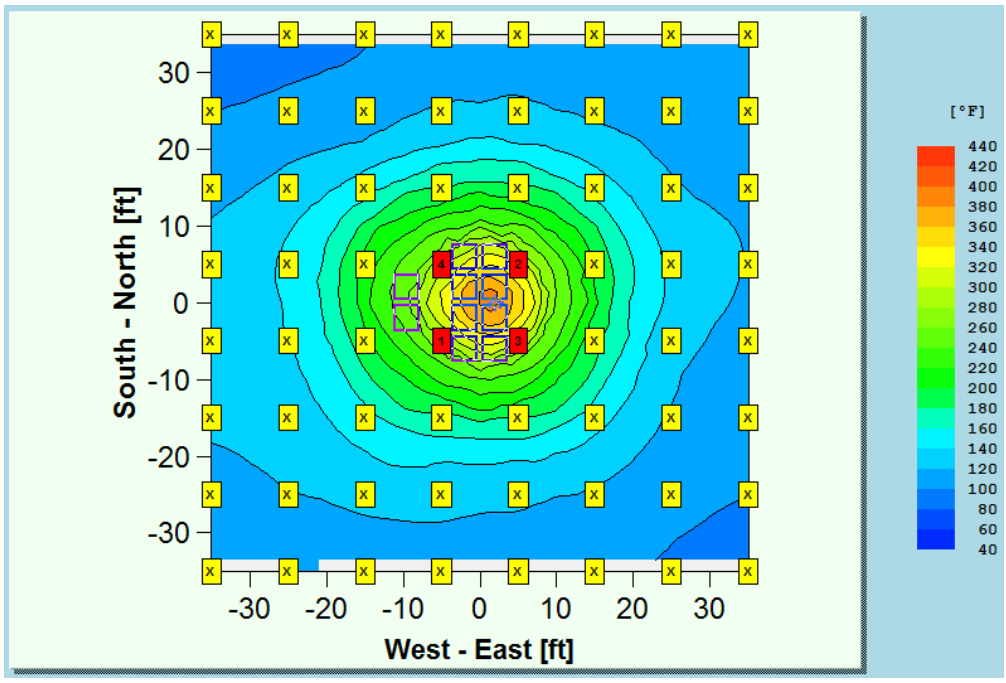

Figure C-17: Ceiling TC contours at final sprinkler operation (all four operations occurred from 1 min 38 s to 1 min 41 s) - Test 15

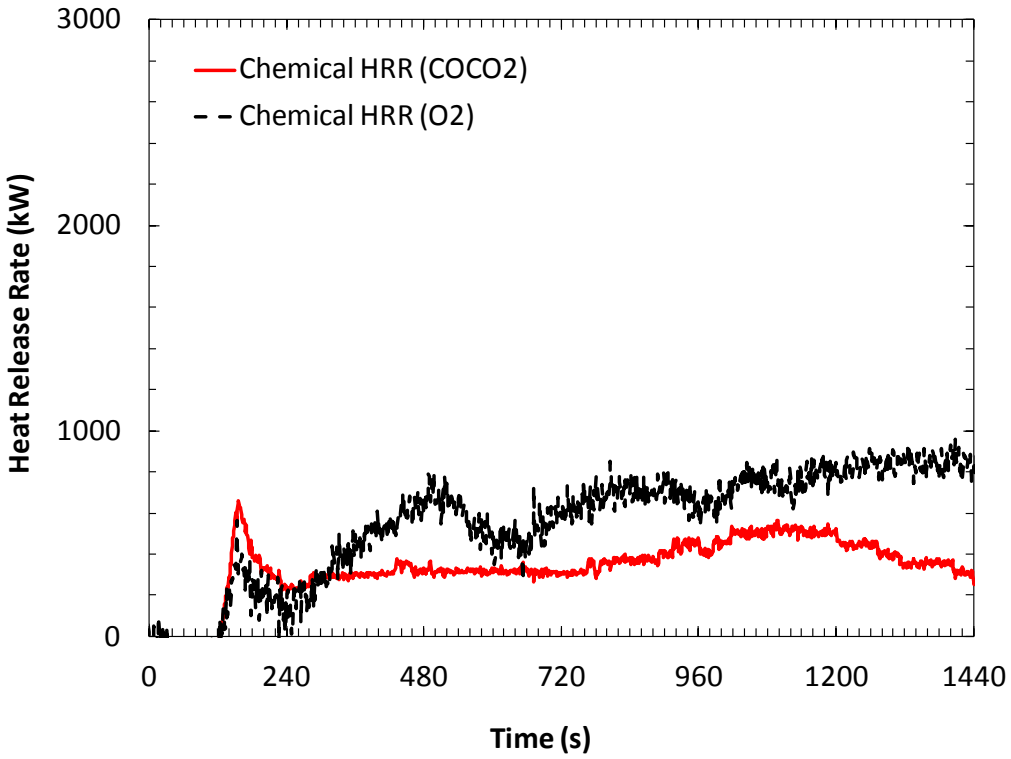

Figure C-18: Chemical heat release rates - Test 15

C.3 TEST CHRONOLOGIES

Test: #14
Date: January, 7 2013
Test Commodity: FM Global standard CUP commodity
Observer: Benjamin Ditch

Time (mm:ss)	Observation
0:00	Ignition; two standard ½ igniters
0:30	Flames at top of first tier
0:52	Flames at top of second tier
1:05	Flames extend 3-5 ft above array; minimal flame spread underneath pallets at any tier
1:12	Flames reach east face of main array, at central transverse flue, on second and third tiers; flames spread halfway across underside of pallets on second and third tiers
1:33	Flame spread; at first tier spread halfway across top of commodity; at second tier has significant burning at front face of array (biased east) and spread across entire underside of pallets (biased east); at third tier significant burning at front face of array and spread three quarters across underside of pallets
1:48	First sprinkler operation: northeast sprinkler surrounding ignition
2:01	Second (and final) sprinkler operation: southwest sprinkler surrounding ignition; significant burning on front face of second and third tiers and on top of first tier
2:30	View of array partially obscured by smoke and steam; fire visible on first and second tiers
5:00	No change; significant burning visible on at least first and second tiers
9:00	Additional flames visible on third tier; view of array still partially obscured
11:00	Fire size at all tiers appears to be reducing; persistent flames still visible
20:00	Test termination by water hose stream; small persistent flames visible at all tiers
25:00	Data collection ended

Test: #15
Date: January 11, 2013
Test Commodity: FM Global standard CUP commodity
Observer: Benjamin Ditch

Time (mm:ss)	Observation
0:00	Ignition; two standard ½ igniters
0:30	Flames at top of first tier
0:47	Flames at top of second tier
0:55	Flames extend 3-5 ft above array; minimal flame spread underneath pallets at any tier
1:30	Flames spread; at first tier spread halfway across top of commodity; at second tier has significant burning at front face of array and spread across entire underside of pallets; at third tier flames halfway across underside of pallets
1:38 – 1:41	Operation of the four sprinklers surrounding ignition
2:00	View of test array partially obscured by smoke and steam; small flames appear persistent at first and third tier
5:00	View of test array improving; small fires persistent at front face of array on second tier and within central transverse flue at third tier; all flames appear to be result of deep seated fires with individual commodity cartons
11:00	Fire spreading slowly at second and third tier
20:00	Test termination by water hose stream; small fires existed at second and third tiers
25:00	Data collection ended

www.fmglobal.com/researchreports

In the United Kingdom:
FM Insurance Company Limited
1 Windsor Dials, Windsor, Berkshire, SL4 1RS
Regulated by the Financial Services Authority.